UNCLASSIFIED

AD NUMBER

AD874891

NEW LIMITATION CHANGE

TO

Approved for public release, distribution unlimited

FROM

Distribution: No Foreign without approval of Director, Defense Atomic Support Agency, Washington, D. C. 20305.

AUTHORITY

DTRA ltr, 3 Nov 99

THIS PAGE IS UNCLASSIFIED

AD874891

DASA 2519-2

Final Report — Part B

June 1970

DDC
RECEIVED
SEP 29 1970
B

PROJECT 617 RADAR READINESS ACHIEVEMENT PROGRAM
Part B — Ionospheric Measurements

By: M. J. BARON T. M. WATT H. F. BATES

STATEMENT #2 UNCLASSIFIED

This document is subject to special export controls and each transmittal to foreign governments or foreign nationals may be made only with prior approval of

Prepared for:

DIRECTOR
DEFENSE ATOMIC SUPPORT AGENCY
WASHINGTON, D.C. 20305

CONTRACT DASA01-67-C-0019

STANFORD RESEARCH INSTITUTE

MENLO PARK, CALIFORNIA

DASA 2519-2

Final Report — Part B

June 1970

PROJECT 617 RADAR READINESS ACHIEVEMENT PROGRAM
Part B — Ionospheric Measurements

By: M. J. BARON T. M. WITT H. F. BATES

Prepared for:

DIRECTOR
DEFENSE ATOMIC SUPPORT AGENCY
WASHINGTON, D.C. 20305

CONTRACT DASA01-67-C-0019

This work sponsored by the Defense Atomic Support Agency under NWER/Subtask HA 048.

SRI Project 6291

Approved by:

DAVID A. JOHNSON, *Director*
Radio Physics Laboratory

RAY L. LEADABRAND, *Executive Director*
Electronics and Radio Sciences Division

Copy No. 32

ACCESSION for
CFSTI WHITE SECTION ☐
DDC BUFF SECTION ☑
UNANNOUNCED ☐
JUSTIFICATION .....
BY .....
DISTRIBUTION/AVAILABILITY CODES
DIST. AVAIL. and/or SPECIAL
2

This document is subject to special export controls and each transmittal to foreign governments or foreign nationals may be made only with prior approval of Director, Defense Atomic Support Agency, Washington, D.C. 20305.

THE BALLAD OF SITE 522

Deep dusk, falling on aluminum struts, and stark
Butler Building white,
What bringeth the children of the farm to greenline
stare and while away this night?
Ionosphere 'tis said, and in its incoherence, doth we
scatter Hertz for some shadow of what might be.
Aided are we by XDS in whose computer's restless guts
whirl countless hysteresis loops
Counting, weighting, autocorrelating, jumping through
the Fourierian hoops.
All this we do, and hoping that when our time is come
to pass beyond ionosphere and sun - -
Lord Rayleigh, Hertz, and Maxwell too, will receive
and say, "Well Done!"

H. D. Olson
8/18/70

ABSTRACT

This report describes the ionospheric studies performed between June 1969 and May 1970 using the DASA Project 617 incoherent-scatter radar. During this time period, significant improvements were made in the radar system to allow nearly real-time processing of the data and to increase the accuracy, time resolution, and altitude extent of the measurements. The 1970 measurements presented here are the first to be made using the new system.

The daytime F-layer over Palo Alto between 1967 and 1969 was studied to determine (1) its seasonal behavior, (2) its day-to-day variations, and (3) its correlation with solar geophysical indices. Continuous 48-hour data runs were made in 1969-1970 and were used to study the ionosphere's diurnal behavior as well as its seasonal behavior during the sunrise and sunset periods. A new type of measurement, the determination of ionospheric vertical velocities, was made for the first time in 1970. Increased upward velocities during the sunrise period were found to exist. Observations of the F-layer during two partial solar eclipses were made and are reported.

ACKNOWLEDGMENTS

The authors wish to acknowledge the valuable assistance of a number of colleagues in performing the experiments described in this report, especially J. Petriceks, R. A. Barnes, H. Olson, and R. I. Presnell. We would also like to thank B. Craig for developing the on-line computer programs, O. de la Beaujardiere for writing the off-line analysis programs, and G. H. Burch for implementing the digital autocorrelator.

CONTENTS

ABSTRACT iii

ACKNOWLEDGMENTS v

LIST OF ILLUSTRATIONS ix

LIST OF TABLES xv

I INTRODUCTION 1

II 1967-1969 DAYTIME F-LAYER TEMPERATURE STUDY 5

III 1969-1970 DIURNAL AND SEASONAL F-LAYER STUDY 25

IV SUNRISE VERTICAL VELOCITY OBSERVATIONS 59

V PARTIAL SOLAR ECLIPSE OBSERVATIONS 73

VI CONCLUSIONS AND RECOMMENDATIONS 91

REFERENCES 95

DISTRIBUTION LIST 99

DD FORM 1473

ILLUSTRATIONS

Figure 1 Contours of Electron Density, Electron and Ion Temperatures over Palo Alto--12 October and 25 October 1967 8

Figure 2 Contours of Electron Density, Electron and Ion Temperatures over Palo Alto--18 June and 21 June 1968 9

Figure 3 Contours of Electron Density, Electron and Ion Temperatures over Palo Alto--1 October and 2 October 1968 10

Figure 4 Contours of Electron Density, Electron and Ion Temperatures over Palo Alto--11 November and 2 December 1968 11

Figure 5 Contours of Electron Density, Electron and Ion Temperatures over Palo Alto--19 December 1968 and 16 January 1969 12

Figure 6 Contours of Electron Density, Electron and Ion Temperatures over Palo Alto--4 February 1969 13

Figure 7 Average Midday Ion and Electron Temperature Profiles over Palo Alto 14

Figure 8 Average Data Plotted vs. the Month of Observation . . 17

Figure 9 Daily Values of the Midday Average Ion Temperature Plotted vs. Daily Values of the 10.7 cm flux, S, Planetary Magnetic Activity, A_p, Sunspot Number, R, and Solar Flux Averaged over the Previous Five Days, S_5 18

Figure 10 Weekly Average of the Midday Ion Temperature Plotted vs. Weekly Averaged Geophysical Indicators . . 19

Figure 11 Weekly Average of the Midday Ion Temperature Plotted vs. 27-Day Averaged Geophysical Indicators . . 19

ILLUSTRATIONS (Continued)

Figure 12 Contours of Electron Density, Electron and Ion Temperatures--20-21 June 1969 28

Figure 13 Contours of Electron Density, Electron and Ion Temperatures--21-22 June 1969 29

Figure 14 Contours of Electron Density, Electron and Ion Temperatures--16-17 July 1969 30

Figure 15 Contours of Electron Density, Electron and Ion Temperatures--17-18 July 1969 31

Figure 16 Contours of Electron Density, Electron and Ion Temperatures--27-28 August 1969 32

Figure 17 Contours of Electron Density, Electron and Ion Temperatures--28-29 August 1969 33

Figure 18 Contours of Electron Density, Electron and Ion Temperatures--18-19 February 1970 34

Figure 19 Contours of Electron Density, Electron and Ion Temperatures--20 February 1970 35

Figure 20 Contours of Electron Density, Electron and Ion Temperatures--18-19 March 1970 36

Figure 21 Contours of Electron Density, Electron and Ion Temperatures--19-20 March 1970 37

Figure 22 Contours of Electron Density, Electron and Ion Temperatures--22-23 April 1970 38

Figure 23 Contours of Electron Density, Electron and Ion Temperatures--23-24 April 1970 39

Figure 24 Contours of Electron Density, Electron and Ion Temperatures--19-20 May 1970 40

Figure 25 Contours of Electron Density, Electron and Ion Temperatures--20-21 May 1970 41

Figure 26 Maximum Electron Density, Height of Maximum Density, and Layer Thickness--20-22 June 1969 43

Figure 27 Maximum Electron Density, Height of Maximum Density, and Layer Thickness--16-18 July 1969 44

Figure 28 Maximum Electron Density, Height of Maximum Density, and Layer Thickness--27-29 August 1969 . . . 45

ILLUSTRATIONS (Continued)

Figure 29 Maximum Electron Density, Height of Maximum Density, and Layer Thickness--18-20 February 1970 . . 46

Figure 30 Maximum Electron Density, Height of Maximum Density, and Layer Thickness--18-20 March 1970 47

Figure 31 Maximum Electron Density, Height of Maximum Density, and Layer Thickness--22-24 April 1970 48

Figure 32 Maximum Electron Density, Height of Maximum Density, and Layer Thickness--19-20 May 1970 49

Figure 33 Seasonal Variation of Sunrise Behavior of T_e, h_{max}, and N_{max} 52

Figure 34 Seasonal Variation of Sunrise Rate of Change of N_{max} 53

Figure 35 Seasonal Variation of Sunset Behavior of T_e and N_{max} 55

Figure 36 Seasonal Behavior of Midday Maximum Electron Density 57

Figure 37 Seasonal Behavior of Diurnal Variations of h_{max} . . . 58

Figure 38 Illustrative Example of a Doppler-Shifted Spectrum--(a) At the Receiver Input; (b) After Band-Limiting and "Aliasing;" (c) After Folding 62

Figure 39 Example of a Folded Spectrum Obtained from Measurements Made at 1130-1144 UT, 23 April 1970 . . . 63

Figure 40 Vertical Drift Velocity vs. Solar Zenith Angle for the 18 February 1970 Sunrise 64

Figure 41 Vertical Drift Velocity vs. Solar Zenith Angle for the 18 March 1970 Sunrise 65

Figure 42 Vertical Drift Velocity vs. Solar Zenith Angle for the 23 April 1970 Sunrise 66

Figure 43 Vertical Drift Velocity vs. Solar Zenith Angle for the 20 May 1970 Sunrise 67

Figure 44 Electron Temperature vs. Solar Zenith Angle for the 20 May 1970 Sunrise 68

ILLUSTRATIONS (Continued)

Figure 45 Electron Density vs. Solar Zenith Angle for the 20 May 1970 Sunrise 69

Figure 46 Vertical Drift Velocity Envelope Limits vs. Time for the Period 0030-2230 GMT, 20 May 1970 70

Figure 47 Percent Obscuration as a Function of Time for the Eclipses of 11 September 1969 and 7 March 1970 and for Altitudes of 0, 300, and 600 km 76

Figure 48 Electron Density Contours as Functions of Altitude and Time for (a) 10 September, (b) 11 September, and (c) 12 September 1969 77

Figure 49 Electron Density Contours as Functions of Altitude and Time for (a) 6 March; (b) 7 March; (c) 8 March 1970 78

Figure 50 Electron Temperature Contours as Functions of Altitude and Time for (a) 10 September; (b) 11 September; (c) 12 September 1969 79

Figure 51 Electron Temperature Contours as Functions of Altitude and Time for (a) 6 March; (b) 7 March; (c) 8 March 1970 80

Figure 52 Ion Temperature Contours as Functions of Altitude and Time for (a) 10 September; (b) 11 September; (c) 12 September 1969 81

Figure 53 Ion Temperature Contours as Functions of Altitude and Time for (a) 6 March; (b) 7 March; (c) 8 March 1970 82

Figure 54 F-Layer Parameters Ne_{max}, h_{max}, and Thickness vs. Time for 10, 11, and 12 September 1969 83

Figure 55 F-Layer Parameters Ne_{max}, h_{max}, and Thickness vs. Time for 6, 7, and 8 March 1970 84

Figure 56 Contours of Constant Percentage of Ne_{max} as Functions of Altitude and Time for 6 March 1970 . . . 86

ILLUSTRATIONS (Concluded)

Figure 57 Contours of Constant Percentage of Ne_{max} as Functions of Altitude and Time for 7 March 1970 . . . 87

Figure 58 Vertical-Drift-Velocity-Envelope Limits vs. Time for the Period 1330-2130, 6 March 1970 89

Figure 59 Vertical-Drift-Velocity-Envelope Limits vs. Time for the Period 1300-2130, 7 March 1970 89

TABLES

Table I DASA Radar Parameters 2

Table II Periods of Observation, 1969-1970 26

I INTRODUCTION

The incoherent-scatter technique has made possible the measurement of ionospheric electron densities and electron and ion temperatures using a single ground-based radar system. Beginning in 1964, Stanford Research Institute designed, constructed, and operated an incoherent-scatter radar for the Defense Atomic Support Agency (DASA) in order to (1) develop the techniques for operating such a radar in an ionospheric environment that has been highly disturbed by a nuclear detonation, (2) improve the radar system, and (3) conduct ionospheric researches on the natural ionosphere.

During the past twelve months, the objectives of this project have been to implement a program of equipmental and operational improvements to the radar. Specifically the project efforts during the last half of 1969 and first quarter of 1970 have been directed toward the following:

(1) Implementing computer programs and procedures to speed up and automate data processing and data analysis.

(2) Implementing a digital autocorrelator to enable spectral analysis to be performed in (nearly) real time.

(3) Conducting ionospheric studies using the incoherent-scatter technique for the purpose of better understanding ionospheric phenomena.

(4) Planning the move of the radar to the auroral zone.

(5) Maintaining a current awareness in the progress of the incoherent-scatter technique so that maximum usefulness of this technique for DASA's purposes will be realized.

This report, Final Report--Part B, describes the results of the work performed to satisfy Objective 3. A separate report, Final Report--Part A, describes the work performed under Objectives 1 and 2. The work performed under Objective 4 resulted in a proposal entitled "DASA Project 617-Radar Relocation," which was submitted to DASA in early March 1970. Objective 5 is applicable to all other objectives of this project and its achievement is evidenced by the improvement and results described in both Part A and in Part B of this Final Report.

The plasma physics theory governing incoherent scattering of radio waves from the ionosphere is well described in the literature[1,2,3*] and will not be repeated here. The details of the radar equipment and the measurement technique used by the Project 617 radar have also been described.[4,5,6,7] Table I below briefly summarizes the radar parameters used for the bulk of the measurements described in this report.

Table I

DASA RADAR PARAMETERS

Transmit frequency	1390 MHz
Peak transmit power	4 MW
Average transmit power	110 kW
Polarization	Circular
Antenna effective aperture	180 m^2
Antenna gain	47.1 dB
System noise temperature	110 $^\circ$K
Pulse length	360 μs
Receiver bandwidth (IF channel)	50 kHz
Receiver bandwidth (video channel)	32 kHz

* References are listed at the end of the report.

Section II of this report presents the results of a two-year study of F-layer temperatures. Data for this study were collected with the Project 617 radar from autumn 1967 to early 1969. The behavior of various daytime F-layer parameters, and correlation of these parameters with several geomagnetic and solar disturbance indices is discussed. The data used for this study were all taken prior to the installation of the new processing system installed late in 1969.

Section III describes the F-layer data collected between June 1969 and May 1970. During this time period, measurements were made in 48-hour continuous blocks, once per month. Between September 1969 and January 1970, the new processing system was being installed at the radar and no data were taken. The results presented for February, March, April, and May 1970, represent data taken and processed using the new system and are of considerably higher quality than the earlier data. Data taken in 1968-1969 are used in combination with the 1969-1970 data to study the seasonal variations of ionospheric parameters.

Section IV of this report describes the results of a new measurement--the determination of vertical drifts in the ionosphere. Vertical velocity determinations have only been practical with our radar since the completion of the new processing system in February 1970. Particular attention in this study is directed toward the sunrise behavior of the vertical motions.

Section V presents the data collected during two partial solar eclipses--one on 11 September 1969, in which the sun was about 70 percent obscured, and one on 7 March 1970, in which the sun was less than 30 percent obscured.

BLANK PAGE

II 1967-1969 DAYTIME F-LAYER TEMPERATURE STUDY

A. Introduction

This section presents the results of a two-year study of the daytime F-layer over Palo Alto, California (37°25'N, 122°10'W), by means of incoherent scatter. Routine biweekly operations were begun in the autumn of 1967, transmitter problems interrupted operations from November 1967 through May 1968. From June 1968 through February 1969, routine triweekly observations were made. All soundings were made at vertical incidence.

A preliminary report based on the reduction of about half of the data was presented by Bates and Baron.[8] The purpose of this section is to present the final results now that the data reduction has been completed.

B. Equipment and Operations

The SRI incoherent-scatter radar is a monostatic pulsed system whose parameters have been given in Table I. For the 1967 to 1969 measurements, the receiving-system noise temperature was about 170°K. An XDS 930 computer is used to record and reduce the data.

For routine observations, the system operated continuously about eight hours per day for five consecutive days. In all, about sixty days of soundings were made. Fifteen minutes of undetected IF signals were analog-recorded once per hour for spectral analysis; approximately 450 hourly density and temperature profiles were obtained. Observations were made on consecutive days to uncover day-to-day variations, since

Preceding page blank

it was felt that not enough was known of this aspect of the behavior of the F-layer.

The method of computing and interpreting spectra to yield temperatures has been described in previous reports.[5,6] The undetected IF signal was range-gated at 50-km intervals between 200 and 550 km and also at about 900 km. Twenty digital samples were taken from each range gate. The autocorrelation function was computed from these samples and Fourier transformation of the autocorrelation function gave the power spectrum. The eight spectra obtained between 200 and 550 km contained the noise spectrum plus the incoherent scatter spectrum, while the spectrum obtained at 900 km contained only noise. Since the noise at the system input is white, the noise spectrum represents a measure of the transfer gain of the system. Incoherent scatter spectra were therefore found by dividing the noise spectrum into the signal-plus-noise spectra to compensate for the non-constant, system transfer gain, and then subtracting unity from each value so obtained to subtract the noise from the signal plus noise. The two halves of each spectrum were added together to form an average half-spectrum.

The electron density was first computed under the assumption of temperature equilibrium. This trial density was then punched on a card together with the peak-to-valley ratio and bandwidth scaled from the computed spectra. Values of electron-to-ion temperature ratio versus ion temperature as functions of peak-to-valley ratio versus half-power bandwidth were stored in the memory of the computer. The computer then determined the ion temperature, electron temperature and corrected electron density; i.e., electron density calculated on the basis of the measured electron-to-ion temperature ratio. The final determination of the temperatures involved an iterative procedure as described in Part A of this report.

We believe that random errors in both the ion and electron temperatures were less than 5 percent. However, it is possible that systematic errors, introduced by the use of analog tape recordings and the manual parts of the data reduction procedures could have amounted to more than 5 percent.

C. Temperature Measurements

Electron- and ion-temperature contours for representative days between the early autumn of 1967 and February of 1969 are shown in Figures 1 through 6 along with the corresponding electron density contour maps. The autumn measurements were characterized by high electron densities, high ion temperatures, and low electron temperatures. As winter progressed, electron densities fell, electron temperatures rose, and ion temperatures fell.

It is difficult, however, to characterize the "average" ionosphere since two consecutive days may exhibit quite different behavior. The 1 and 2 October data shown in Figure 3 is a good example of the day-to-day variability.

To show the behavior of the F-layer at midday, the electron and ion temperatures were averaged over three hours centered on local noon for one day from each observing period; these are plotted in Figure 7. Also plotted in Figure 7 are the height and electron density (in units of 10^6 el/cm^3) at the F-layer maximum. As an aid in comparing the various plots, the line indicating the height of the F-layer maximum extends between 1000° and 1500°K.

The June 21 and July 22 plots present extreme rather than representative cases observed during June and July. As noted in the previous paper[8] the electron densities and temperatures were quite variable from day to day, and these two plots represent the extremes that we observed

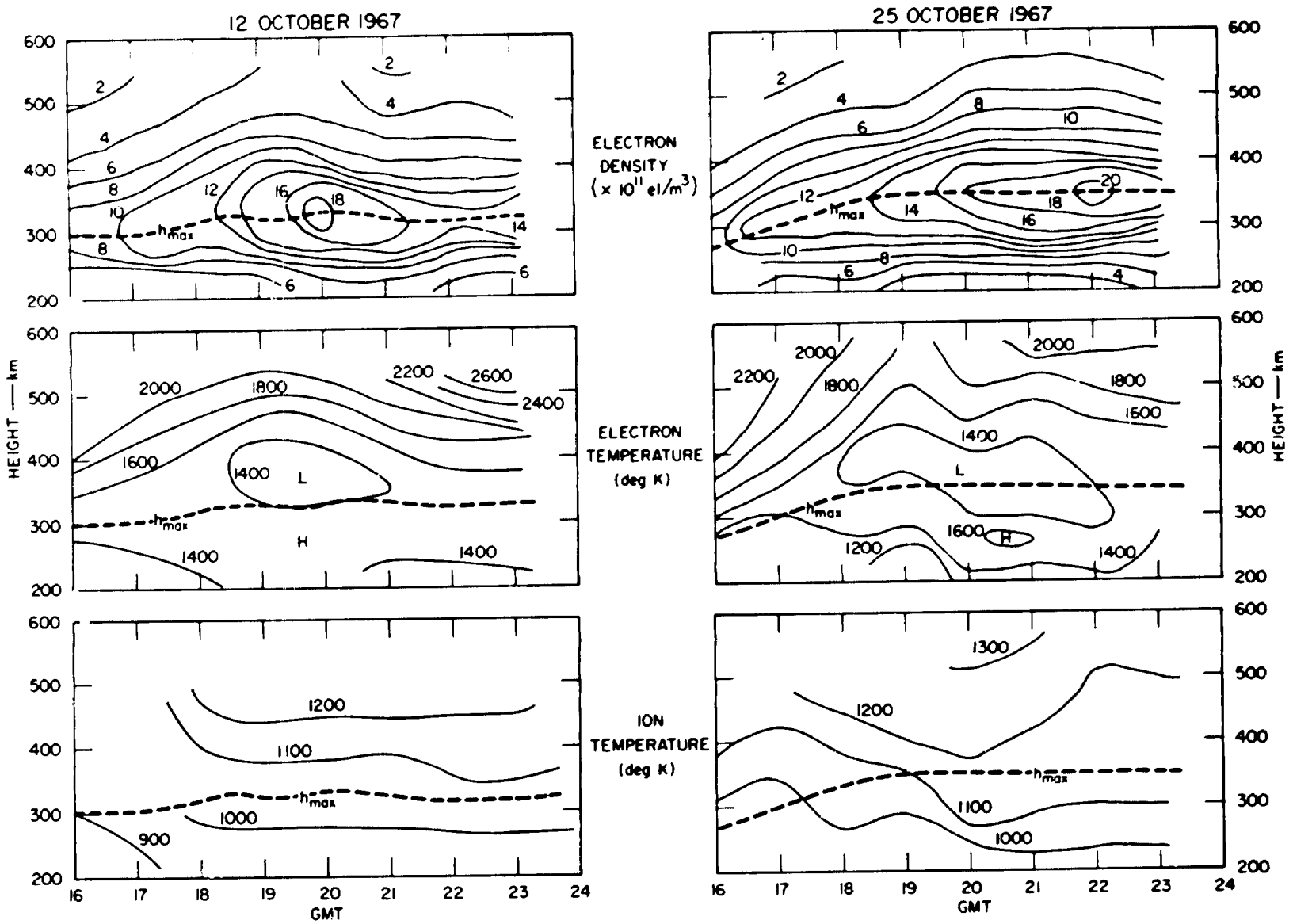

FIGURE 1 CONTOURS OF ELECTRON DENSITY, ELECTRON AND ION TEMPERATURES OVER PALO ALTO—12 OCTOBER AND 25 OCTOBER 1967

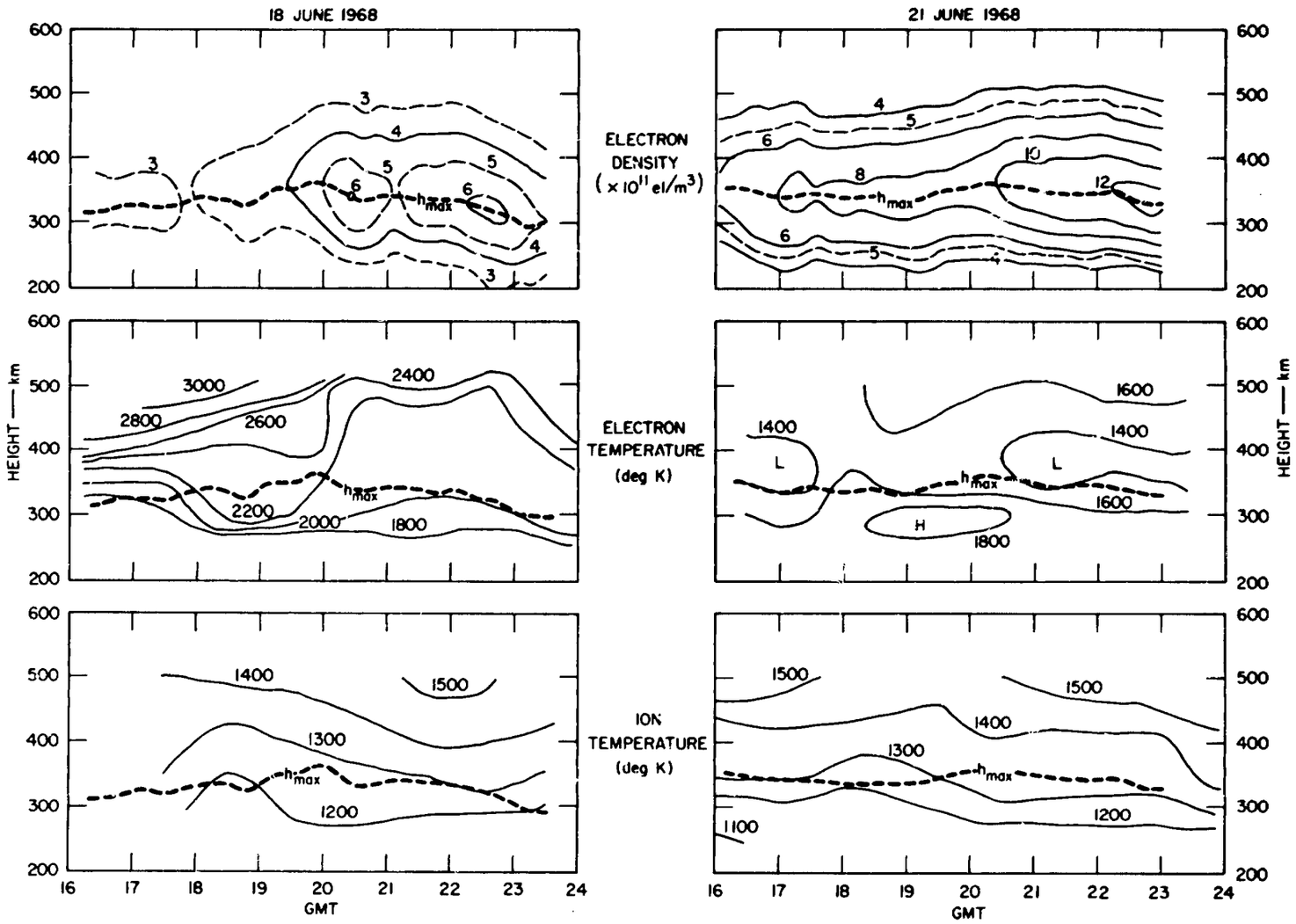

FIGURE 2 CONTOURS OF ELECTRON DENSITY, ELECTRON AND ION TEMPERATURES OVER PALO ALTO--18 JUNE AND 21 JUNE 1968

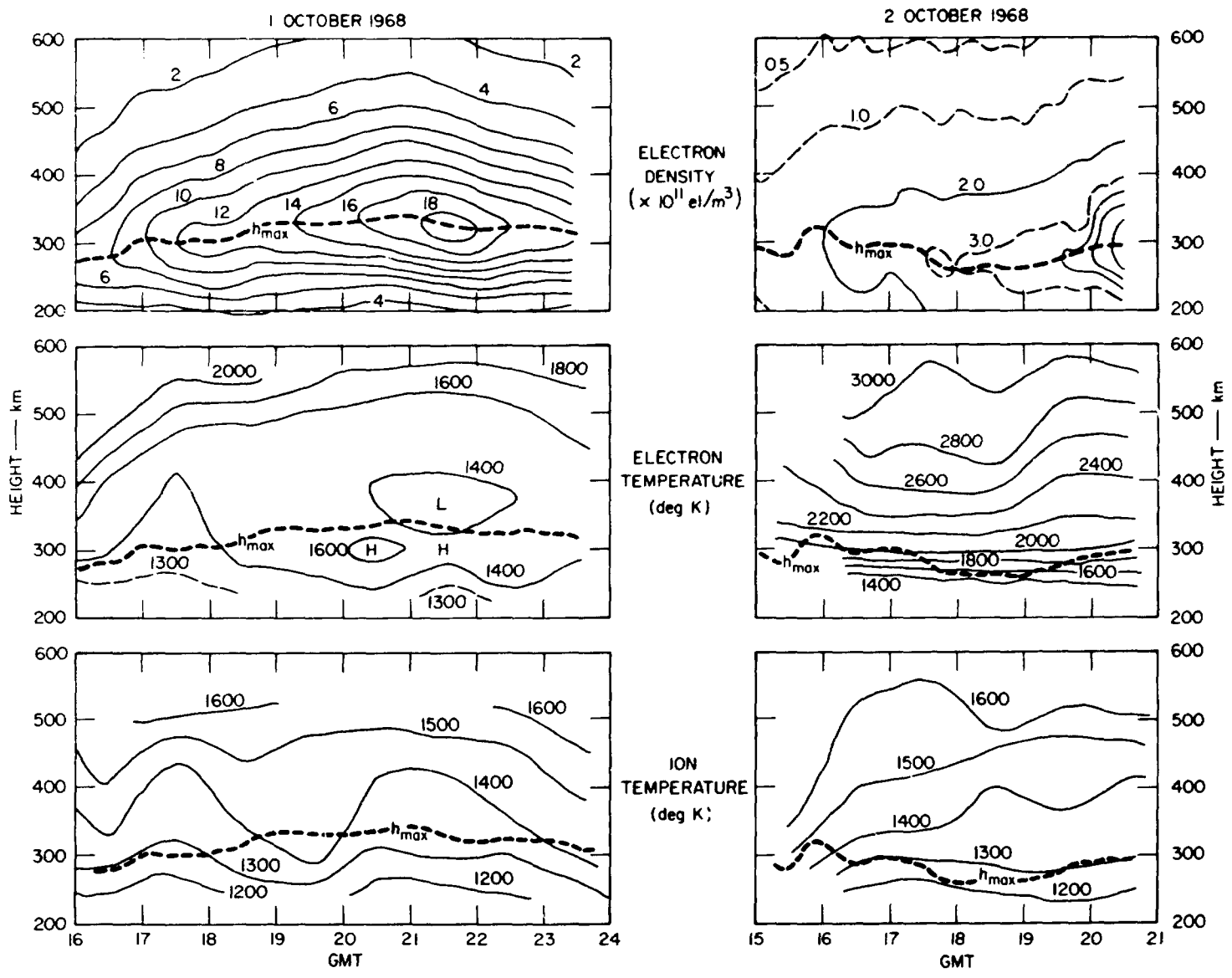

FIGURE 3 CONTOURS OF ELECTRON DENSITY, ELECTRON AND ION TEMPERATURES OVER PALO ALTO—1 OCTOBER AND 2 OCTOBER 1968

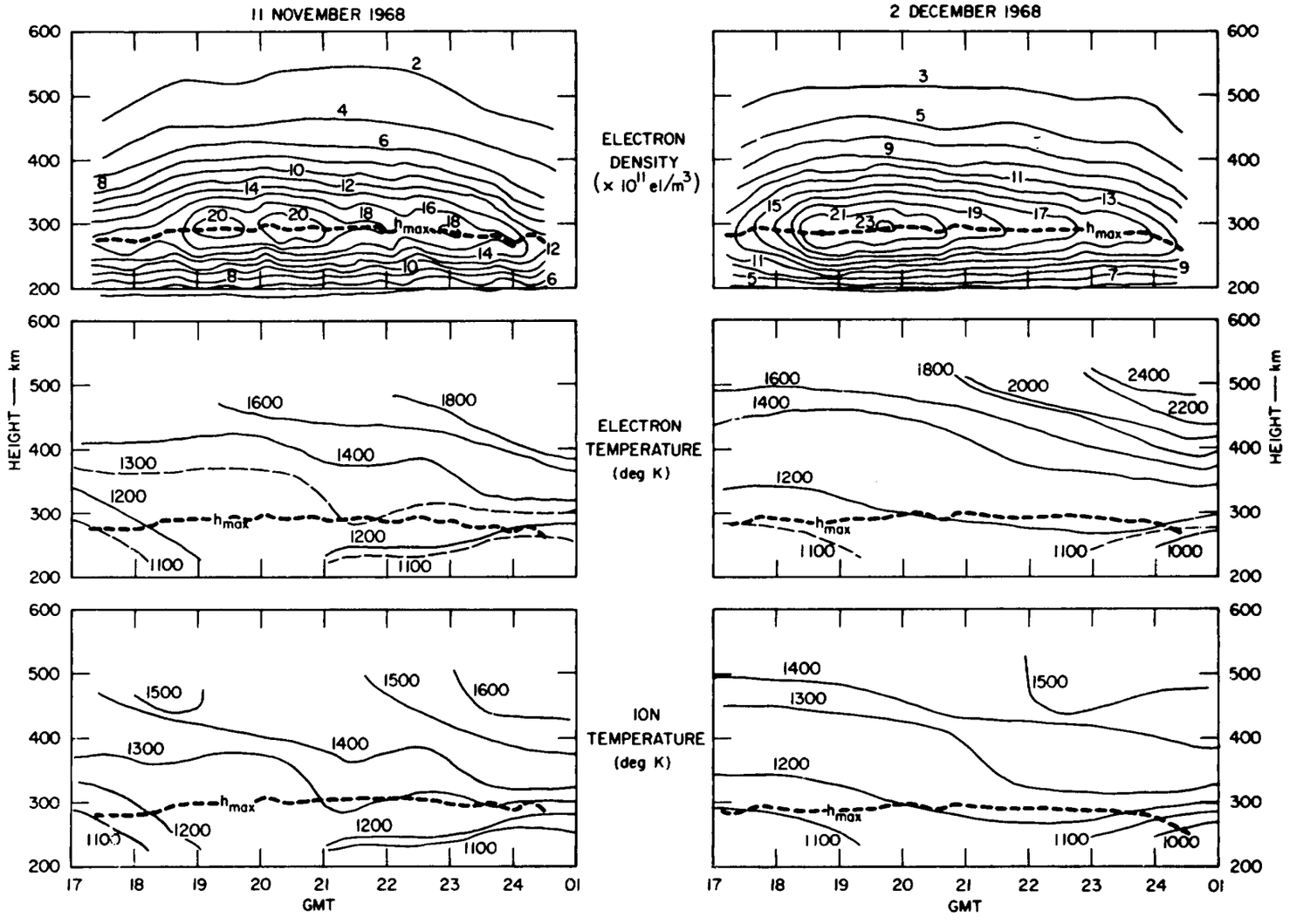

FIGURE 4 CONTOURS OF ELECTRON DENSITY, ELECTRON AND ION TEMPERATURES OVER PALO ALTO—11 NOVEMBER AND 2 DECEMBER 1968

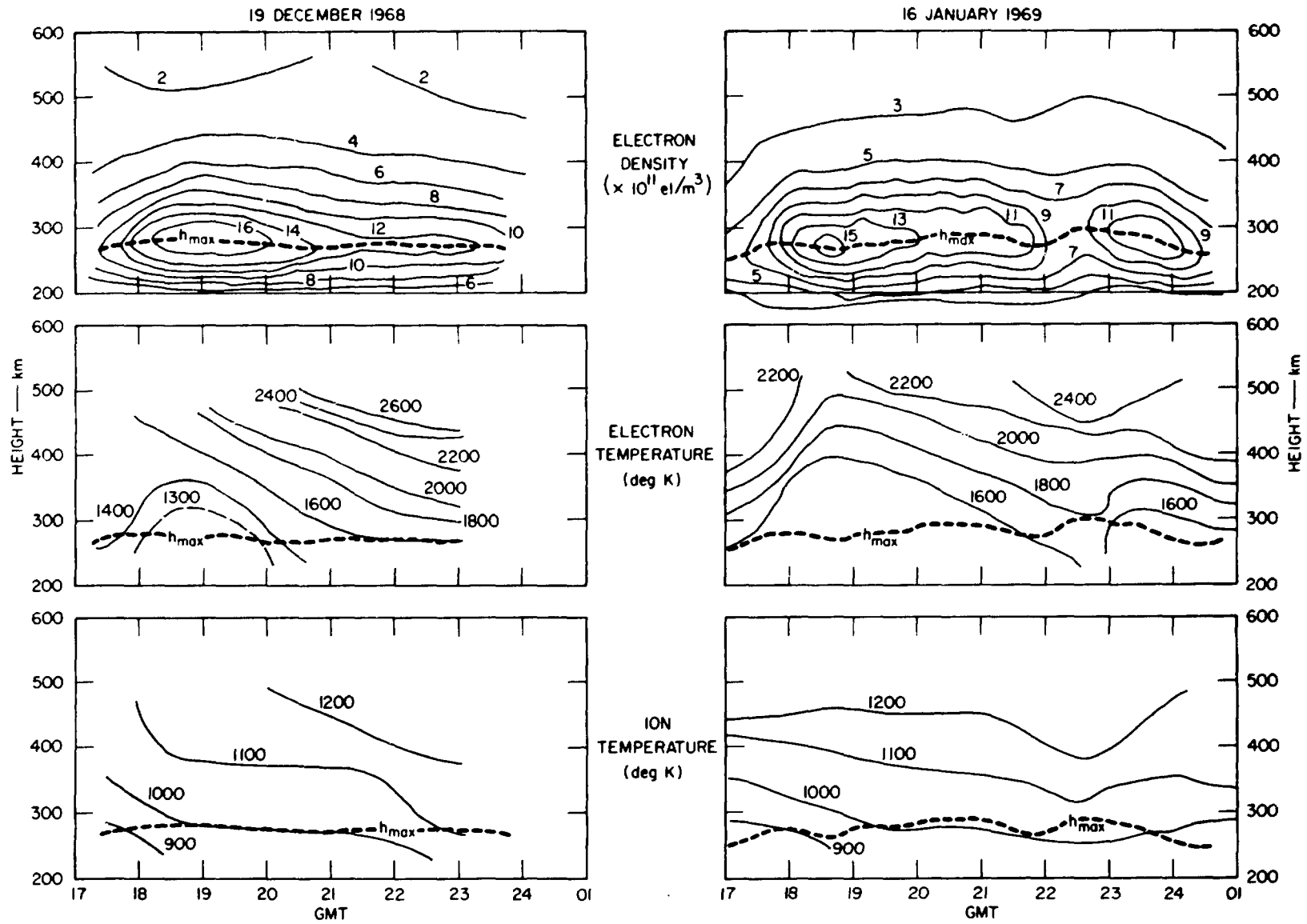

FIGURE 5 CONTOURS OF ELECTRON DENSITY, ELECTRON AND ION TEMPERATURES OVER PALO ALTO—— 19 DECEMBER 1968 AND 16 JANUARY 1969

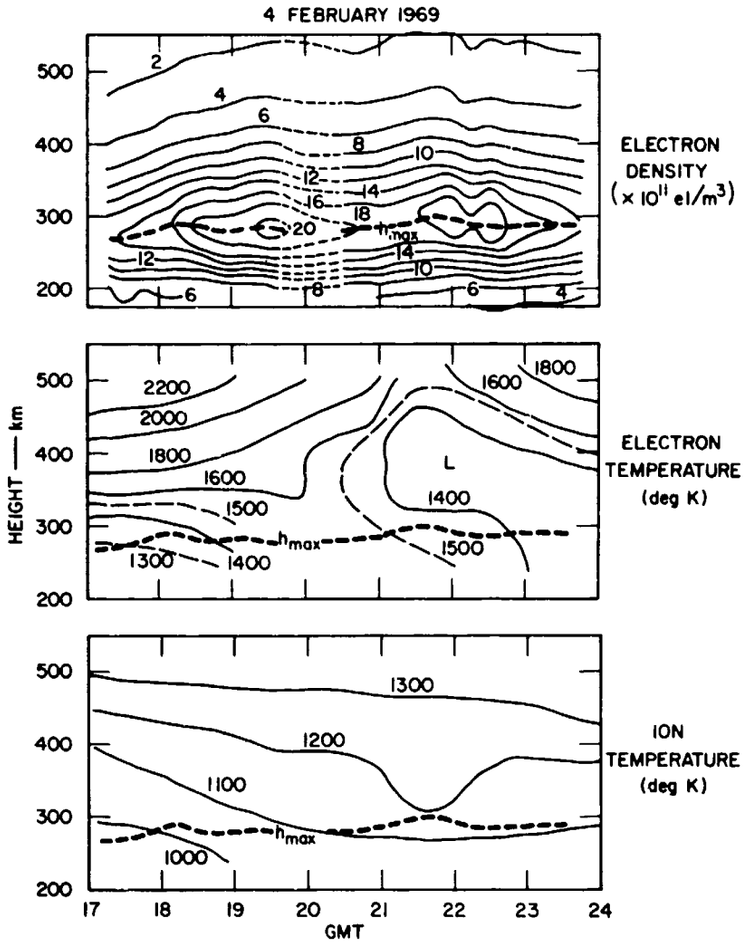

FIGURE 6 CONTOURS OF ELECTRON DENSITY, ELECTRON AND ION TEMPERATURES OVER PALO ALTO--4 FEBRUARY 1969

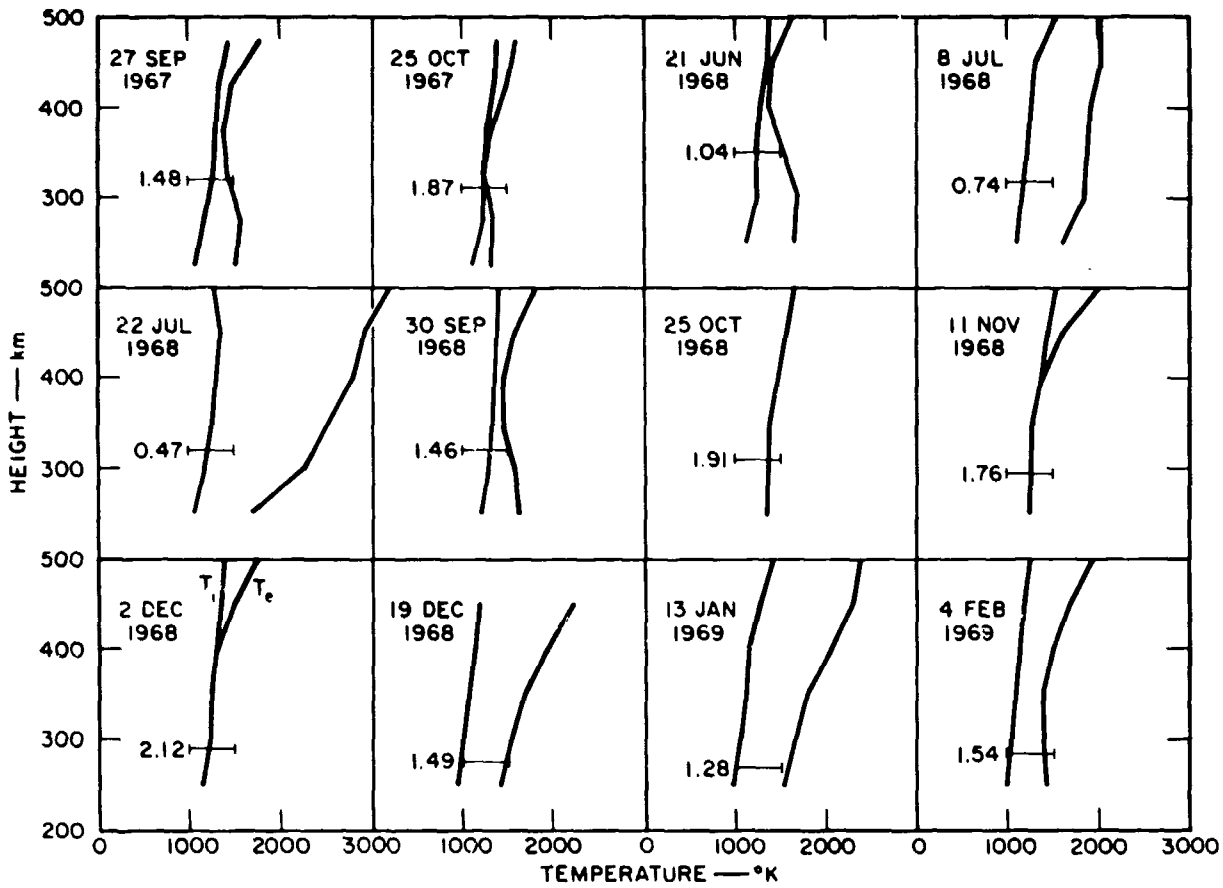

FIGURE 7 AVERAGE MIDDAY ION AND ELECTRON TEMPERATURE PROFILES OVER PALO ALTO

in these variations. The July 8 data represent the average behavior observed in the June-July 1968 soundings. Only isolated soundings were made in August and September 1968 because of minor equipmental problems; these show some decrease in electron temperature and an increase in electron density from those observed in June and July.

By October of both years, near thermal equilibrium existed between ions and electrons in the midday F-layer. From late October through early December 1968, thermal equilibrium existed between ions and electrons throughout most of the midday F-layer between 250 and 500 km. The winter 1968-1969 soundings were characterized by increased electron temperatures, low ion temperatures, and decreased electron densities from the soundings in late autumn 1968.

The height of the F-layer maximum tended to be high in the summer and low in the winter, and the converse was true for the electron density of the maximum. The electron-temperature profiles changed grossly from summer through winter 1968. Some of the variations can be explained, and others cannot. First, let us consider the June 21 and July 22 electron-temperature profiles (Figure 7). While they appear to be quite different, the differences in the profiles can be explained rather simply as the result of the inverse relationship between the electron density and electron temperature which has been reported by many authors.[8,9,10,11,12]

General sense can be made from the experimental records in Figure 7 when the profiles are considered in this light. Consider first the increase in electron temperature near 250 km in the summer and its absence during the late autumn and winter. In the summer, the F-layer maximum at noon was near 325 km, and the electron density at 250 km was considerably lower than that at the maximum. Thus, the summer and autumn increase in electron temperature near 250 km is explainable as the consequence of the increase in electron temperature accompanying the decrease in electron density below the F-layer maximum; this effect is discussed by Geisler and Bowhill.[13] In the winter, however, the F-layer maximum was near 275 km, so that the electron density at 250 km was only slightly smaller than that at the maximum. Hence, a noticeable increase in electron temperature would not be expected at 250 km in the late autumn and winter, but rather the increase may have existed lower where ground clutter prevented its detection. As Geisler and Bowhill discuss, however, the exponentially increasing atmospheric density tends to produce thermal equilibrium between ions and electrons below 200 km; thus, there may have been no appreciable increase in the winter electron temperature over Palo Alto below the F-layer maximum.

The existence of approximate thermal equilibrium between ions and electrons at all altitudes measured during the late autumn of 1968 was a somewhat surprising result. Electron densities were high during this period, but other factors, such as a seasonal variation, may also have been involved. At this time we have too few data to form a conclusion.

D. Correlation of Ion Temperature with Geophysical Indicators

When ion-temperature profiles obtained throughout one day at Palo Alto are compared, the profiles usually agree from hour to hour to within approximately $\pm 50^{\circ}$K. Therefore, this finding suggests that although individual values may have large discrepancies, on the average the values found are within 50°K of the true value.

Figure 8 shows the average ion temperature plotted vs. month; the average ion temperature was found by averaging the values from 300 and 350 km over the hours 1000 through 1400 local time for each series of measurements, usually one week in length. Unfortunately, the measurements extend neither through the spring equinox nor midsummer, but the data suggest a minimum near summer and winter solstices and a maximum near the autumnal equinox.

Near 300 km, the ion temperature should be close to the neutral temperature. Thus, since various disturbances are believed to be accompanied by changes in the neutral temperature, the average ion temperatures were compared in Figure 8 with the 10.7-cm solar flux $\bar{S}$ received at Ottawa, sunspot number $\bar{R}$, and the planetary magnetic activity index $\bar{A}_p$. Each of these indicators was averaged over the same days for which the ion temperatures were averaged. Little close correspondence is evident between ion-temperature variations and the disturbance indicators.

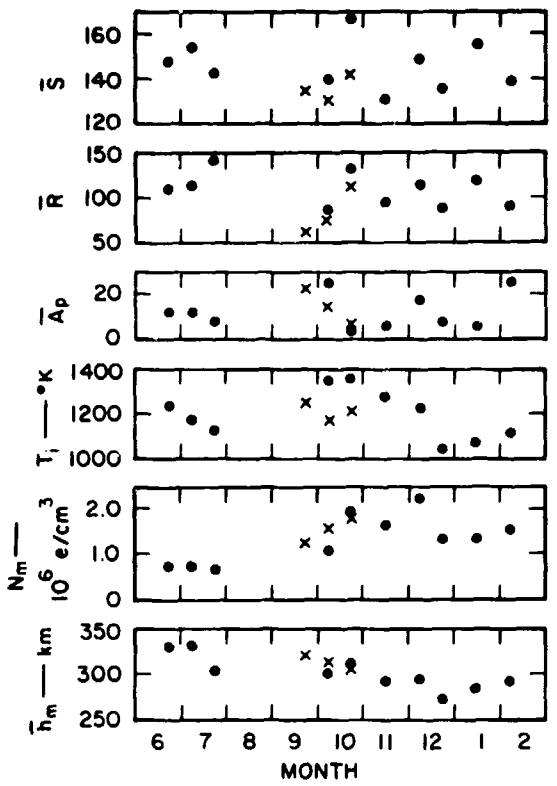

FIGURE 8 AVERAGE DATA PLOTTED vs. THE MONTH OF OBSERVATION

Scatter diagrams between ion temperature and disturbance indicators were constructed to show any possible correspondence between data. The daily value of the ion temperature averaged over 300- and 350-km heights from 1000 to 1400 local time is plotted vs. the daily values of the disturbance indicators in Figures 9(a), 9(b), and 9(c). Little correspondence is evident.

Under the assumption that ionospheric temperatures might respond slowly to increasing energy input from the sun, ion temperatures for each day are compared with the average solar flux received during the previous five days in Figure 9(d). Again, little correspondence is evident.

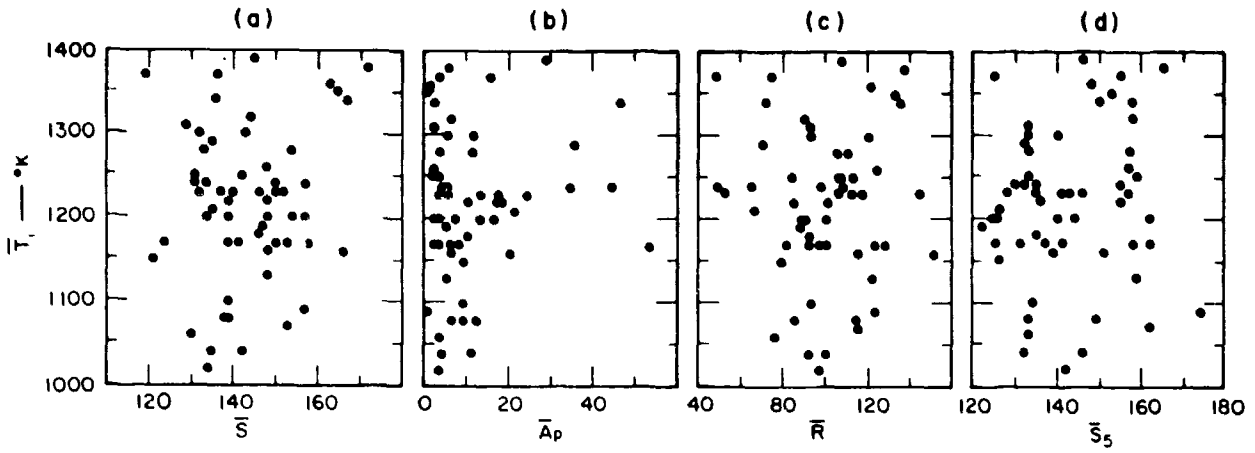

FIGURE 9 DAILY VALUES OF THE MIDDAY AVERAGE ION TEMPERATURE PLOTTED vs. DAILY VALUES OF THE 10.7 cm FLUX, S, PLANETARY MAGNETIC ACTIVITY, A_p, SUNSPOT NUMBER, R, AND SOLAR FLUX AVERAGED OVER THE PREVIOUS FIVE DAYS, S_5

Next, the daily data were averaged over each series of observations and plotted. These data are shown in Figure 10; with the possible exception of planetary magnetic activity, the average data show little common variation.

Finally, the average ion temperature found for each series of observations is compared in Figure 11 to the disturbance indicators, averaged over the twenty-seven days before the series of observations. Again, there is little common trend apparent in the data.

The scatter plots did not reveal any marked correspondence between variations in the various sets of data. During the plotting, some of the data gave the impression that changes in the sense of one variable were accompanied systematically by changes in the sense of the other. To check this possibility, the sense of the change in each set of data was correlated as follows: whenever there was an increase from one day to the next, the value +1 was assigned, while a decrease was assigned the value -1. These sets of data were then cross-correlated, resulting in correlation coefficients of 0.2 or less. Since that value is an upper limit on the magnitude of the correlation coefficient between the

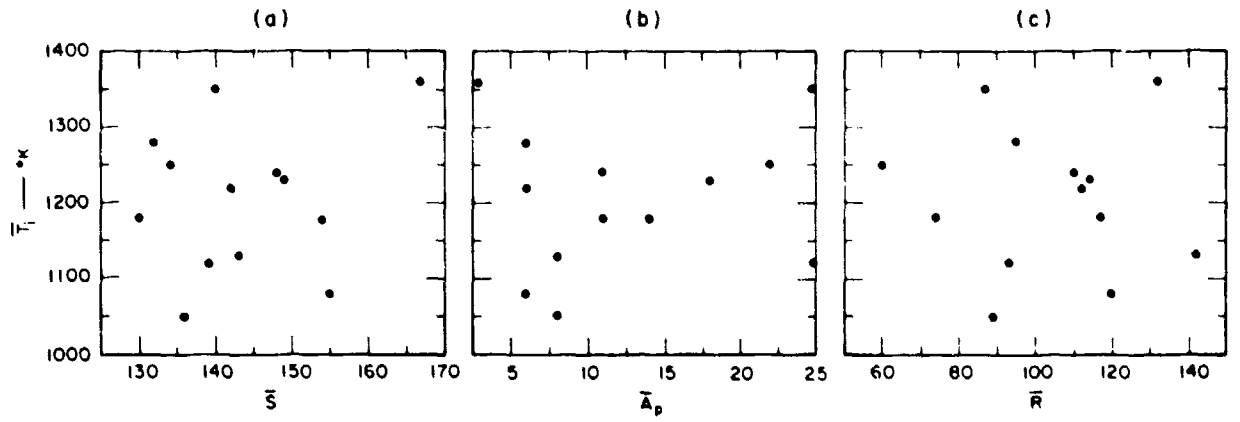

FIGURE 10 WEEKLY AVERAGE OF THE MIDDAY ION TEMPERATURE PLOTTED vs. WEEKLY AVERAGED GEOPHYSICAL INDICATORS

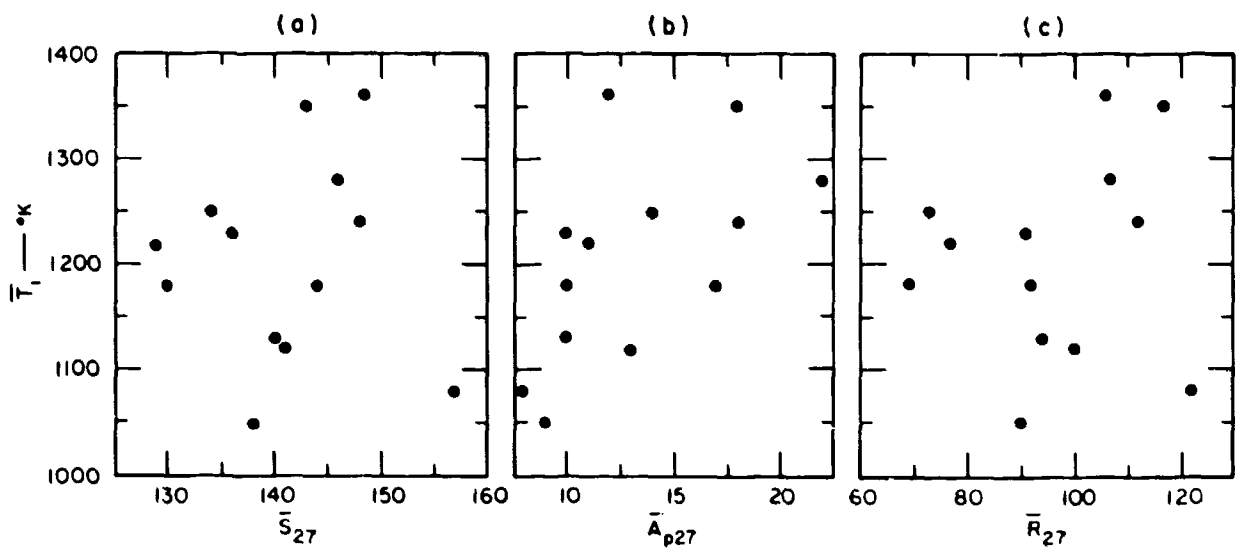

FIGURE 11 WEEKLY AVERAGE OF THE MIDDAY ION TEMPERATURE PLOTTED vs. 27-DAY AVERAGED GEOPHYSICAL INDICATORS

original sets of data, the actual correlation coefficient between ion temperature and sunspot number, 10.7-cm solar flux, or magnetic activity is less, further confirming our conclusion that changes in the data do not correlate strongly.

Figures 8 through 11 show that there was little correlation between changes in the ion temperature found at Palo Alto at the F-layer maximum, and changes in the geophysical disturbance indicators for sunspot number, magnetic activity, and 10.7-cm solar flux. In particular, no correspondence is apparent between daily values, between values averaged for a week, or between average ion temperatures and the geophysical indicators averaged over the 27 days before the Thomson scatter observations. This lack of correlation may be real; however, it may also be due to systematic errors caused by the manual portions of the data reduction procedure. During the two-year period over which measurements were made, changes in data processing may have introduced biases into the results that masked any real correlation.

E. Height of F-Layer Maximum

The height of the F-layer maximum generally dropped from near the 400-km level before sunrise to the 300-km level an hour after sunrise, the time when the height reached its minimum value. As the day progressed, the height of the maximum typically increased until midday, after which it occasionally dropped slightly. The average midday summer height was higher than the winter height, as shown in Figure 8.

The height of the F-layer maximum varied considerably from day to day, but no correspondence was found between height changes and the various disturbance indicators. When the sense of the change in each variable was cross-correlated as described in the previous section, the correlation coefficients were again found to be less than 0.2,

indicating little correlation between the height of the F-layer maximum and solar 10.7-cm activity, sunspot number, or magnetic activity.

Changes in sense of the height of the F-layer maximum did not correlate with similar changes in the ion temperature; the correlation coefficient was -0.1. There appeared to be a tendency for a decrease in layer height to be accompanied by an increase in ion temperature, but the low correlation coefficient showed that any possible negative correlation was weak.

F. Summary of Results

The height of the F-layer maximum over Palo Alto showed an average decrease of roughly 50 km from summer to winter in 1968-1969. This effect is also seen in the 1969-1970 data discussed in the next section of this report. Observations at Millstone Hill in 1964 showed no seasonal variation,[14] and it is not known whether the decrease observed at Palo Alto was seasonal or was caused by some other agent.

No correspondence was found between the various solar-geophysical indicators and the ion temperature at a height of 300 to 350 km. In particular, we could not confirm the result reported[15] from Arecibo that the midday average of the ion temperature showed a strong correlation with the solar 10.7-cm flux averaged over twenty-seven days; the Palo Alto results showed almost a random correspondence between the two sets of data. As mentioned previously, however, this lack of correlation in our results may be a consequence of possible systematic errors in the data processing.

A basic result of the work at Palo Alto was the large day-to-day variation in height, electron density, and ion temperature of the F-layer maximum. No correspondence was found between these parameters, or between them and the solar-geophysical indicators. In particular, no

correspondence was found between these F-layer parameters and planetary magnetic activity--a disturbance indicator generally thought to correlate with F-layer changes. Other investigators[16] have found that the onset of a sudden-commencement magnetic storm was accompanied by changes in F-layer electron density. The results, however, were reported to be variable and dependent on the time and location of the observation.

For the data reported here, the time after storm onset was not taken into account, and this factor may explain why the Palo Alto results apparently do not agree with those obtained elsewhere. An examination of individual cases, however, does not expose any strong correspondence. During the two years of operations, only two sudden-commencement magnetic storms began during a sounding period. On June 25, 1968, a small sudden-commencement magnetic storm began during the early part of the sounding period. The F-layer electron density was higher on June 25 than during operations the previous week; it decreased by one-third on June 26, and increased again on June 27. The height of the F-layer maximum dropped steadily and ion temperatures decreased during this period.

Another sudden-commencement storm began on July 9 just before midnight. Little change occurred in electron density between July 9 and 10, while the height of the maximum and the ion temperature increased.

No pattern is evident between these two observations. Perhaps the data available are insufficient to form detailed conclusions, but if a strong relationship exists, it should have been evident in the data. Since no such correspondence is apparent, we can only conclude that no strong relationship exists between magnetic disturbances and F-layer parameters over Palo Alto. Possibly a better correspondence would be found if enough data were available so that the data could be separated as to type of magnetic storm and analyzed carefully with respect to storm time.

This great day-to-day variability indicates that morphology studies utilizing incoherent scatter should be based upon a week's data, rather than on one or two days' data taken every few weeks. Such a program is expensive to implement, but the presence of large day-to-day variations may make results of shorter-term observations unrepresentative of average behavior.

BLANK PAGE

III 1969-1970 DIURNAL AND SEASONAL F-LAYER STUDY

A. Introduction

During the time period June 1969 to May 1970 synoptic measurements of the ionosphere were made. The radar was operated generally for a 48-hour continuous period once each month except for those months in which the new computer equipments and the digital autocorrelator were being installed. Table II shows the dates and times of operation during the 1969-70 contract period.

Also shown in Table II are the following geophysical disturbance indicators: sunspot number, R_z, and planetary magnetic activity indices, A_p and Σk_p. To the left of the date, the letters, Q, QQ, or D sometimes appear. These indicate that the indicated date has been designated: (a) one of the five (QQ) or ten (Q and QQ) magnetically quietest days of the month; of (b) one of the five (D) most disturbed days of the months.

Our observing days were, in general, days of low geomagnetic activity. The only exceptions are the three disturbed days in March during which eclipse measurements were made and the first day of the August 48-hour run.

The 1969 data were taken using the old system, in which analog tape recordings were made once per hour. These recordings of the receiver IF signal were then played back for spectral analysis. From the spectra, ion and electron temperatures were deduced and these temperatures were then used to correct the power profile data. The power profiles were recorded separately on digital tape and a large amount of manual data reduction was necessary to relate the two (spectral and power profile)

Preceding page blank

Table II

PERIODS OF OBSERVATION, 1960-1970

	Date	Time (GMT)	R_z	Σk_p	A_p	Purpose
	6/20/69	0700-2400	97	18-	10	
	6/21/69	0000-2400	84	11-	5	Synoptic Study
QQ	6/22/69	0000-0700	56	4-	2	
	7/16/69	0700-2400	75	18+	10	
Q	7/17/69	0000-2400	78	8	4	Synoptic Study
Q	7/18/69	0000-0700	73	6+	3	
D	8/27/69	0700-2400	104	24+	21	
	8/28/69	0000-2400	117	12-	6	Synoptic Study
QQ	8/29/69	0000-0700	143	7+	4	
	9/10/69	1700-2300	51	14+	8	Eclipse Background
	9/11/69	1645-2225	67	16+	8	Partial Solar Eclipse
Q	9/12/69	1630-2100	73	9+	4	Eclipse Background
	2/18/70	0800-2400	143	18	9	
	2/19/70	0000-0440	120	9	4	
	2/19/70	1715-1830	120	9	4	Synoptic Study
	2/19/70	2315-2400	120	9	4	
Q	2/20/70	0000-2400	125	6-	3	
D	3/06/70	1300-2200	100	29-	25	Eclipse Background
D	3/07/70	1235-2200	108	37	42	Partial Solar Eclipse
D	3/08/70	1320-1715	116	53-	149	Eclipse Background
	3/18/70	0800-2400	41	13-	6	
	3/19/70	0000-2400	48	11-	5	Synoptic Study
Q	3/20/70	0000-0800	93	9	4	
D	4/22/70	0800-2400	57	28	41	
	4/23/70	0000-2400	67	23-	14	Synoptic Study
	4/24/70	0000-0800	90	24+	16	
	5/19/70	0700-2400	179	13-	6	Synoptic Study
	5/20/70	0000-2300	149	22	13	

measurements to yield electron densities and electron and ion temperatures. Thus the 1969 data use 15-minute integration periods spaced at hourly intervals, except during the sunrise periods when analog data were recorded at half-hour intervals.

The 1970 data were taken after the installation of the new spectral-analysis and data-processing system described in Part A of this final report.[7] Time resolution for this data is equal to the integration time, which was generally 15 minutes, except during some nighttime periods where 30-minute integrations were used to improve the signal-to-noise ratios.

The 1970 data have better time resolution and greater accuracy, and extend over a wider altitude regime than the 1969 and earlier data.

B. Measurement Results

Figures 12 through 25 show the results of the synoptic measurements in the form of contour maps of the ionospheric parameters, electron density, electron temperature, and ion temperature. Each figure contains three contour maps, one for each of the above parameters, covering a 24-hour period centered roughly around local solar noon. This presentation clearly shows the diurnal variations. The times at which the local solar zenith angle reaches 90, 100, and 110 degrees (both during sunrise and sunset) are indicated on the contour maps along with the time and zenith angle at solar transit. Also shown on each contour map is h_{max}, the height of the F-layer maximum.

The 1969 data, essentially all summertime data, show great variability from day to day. Electron densities on successive days change by 50 to 100 percent. Large day-to-day differences in electron temperature are also seen--differences that are related to the density changes. As seen in earlier data (c.f., Figure IV-2 of Ref. 5), when the electron

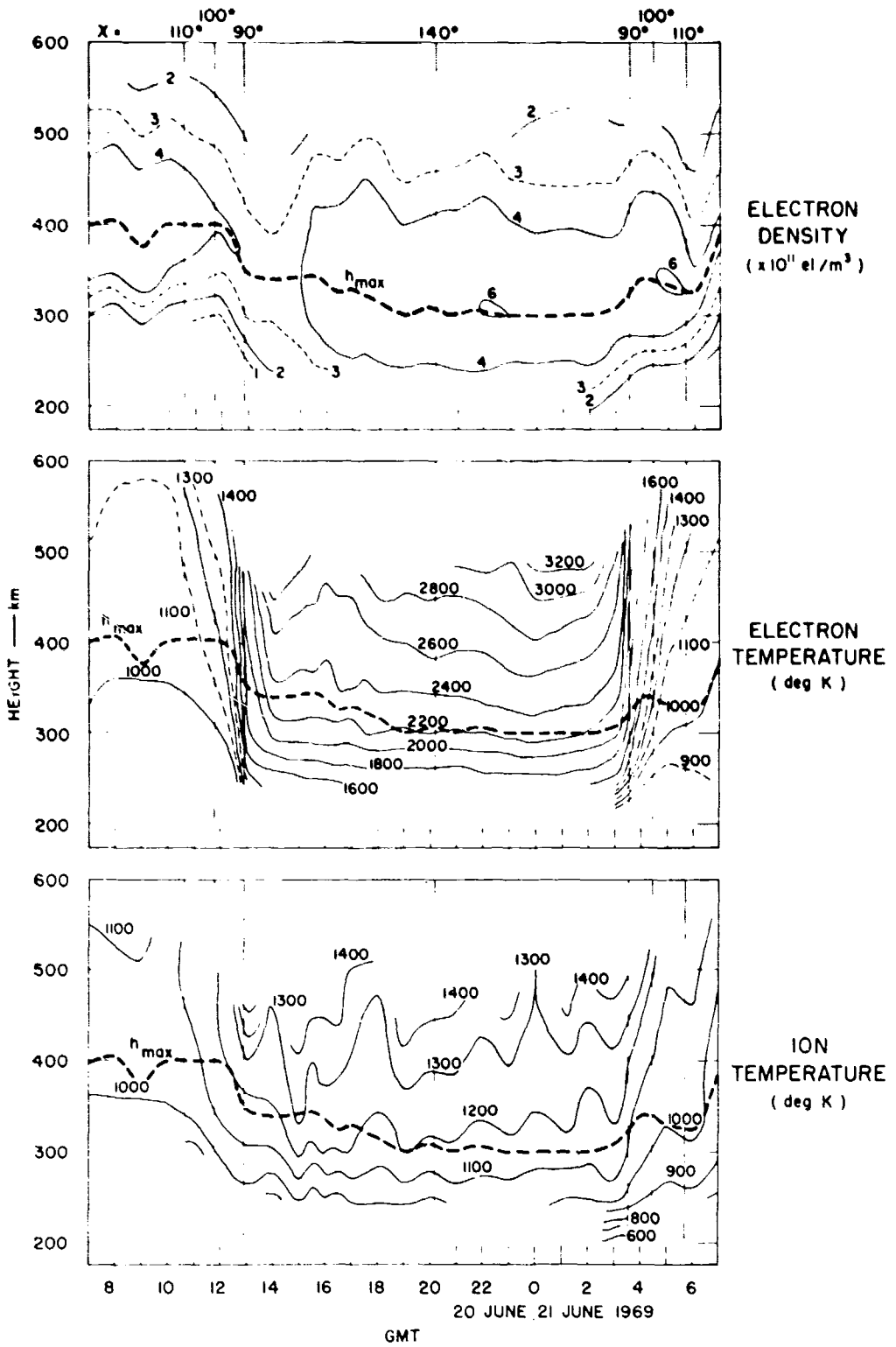

FIGURE 12 CONTOURS OF ELECTRON DENSITY, ELECTRON AND ION TEMPERATURES--20-21 JUNE 1969

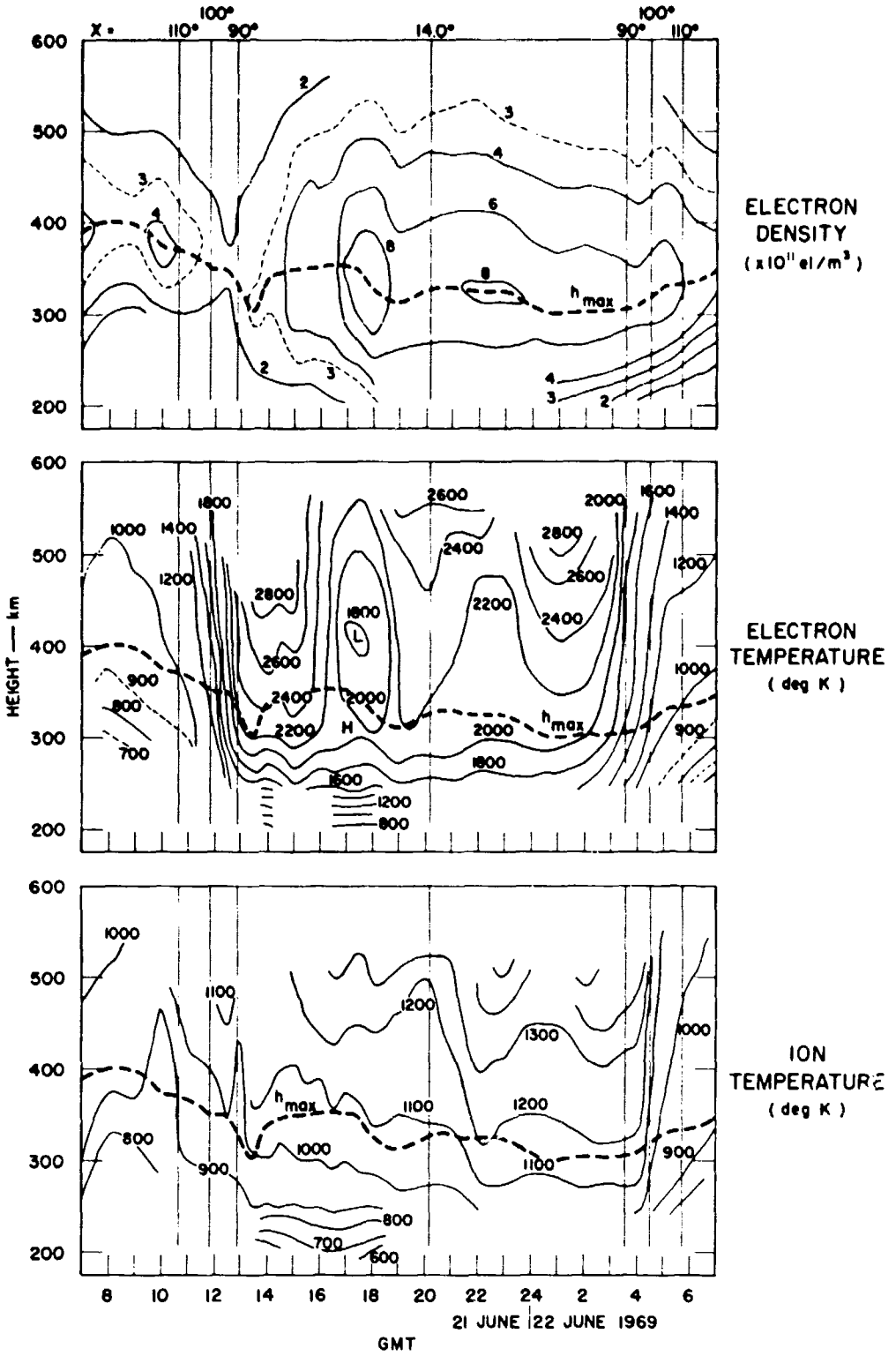

FIGURE 13 CONTOURS OF ELECTRON DENSITY, ELECTRON AND ION TEMPERATURES—— 21-22 JUNE 1969

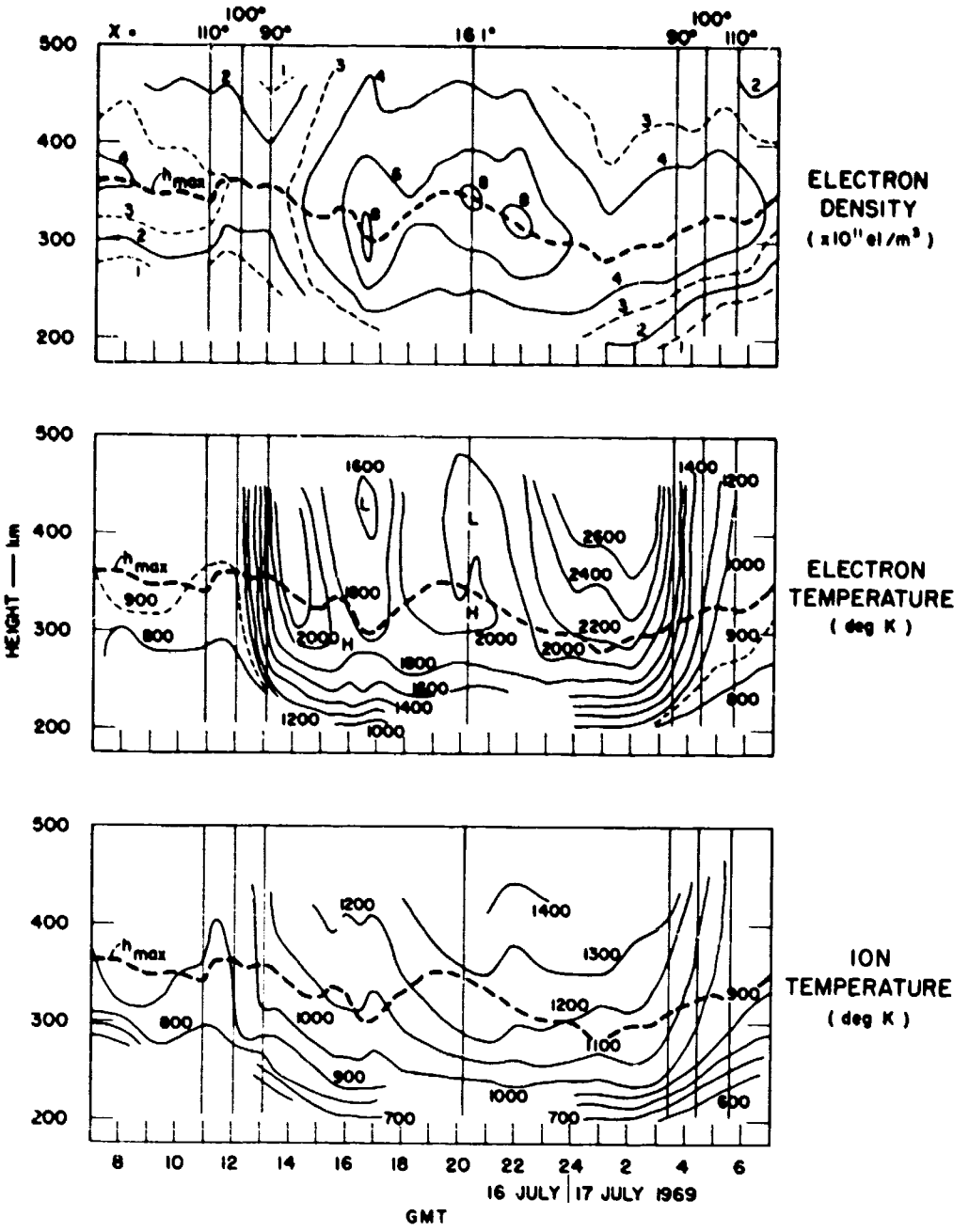

FIGURE 14 CONTOURS OF ELECTRON DENSITY, ELECTRON AND ION TEMPERATURES—— 16-17 JULY 1969

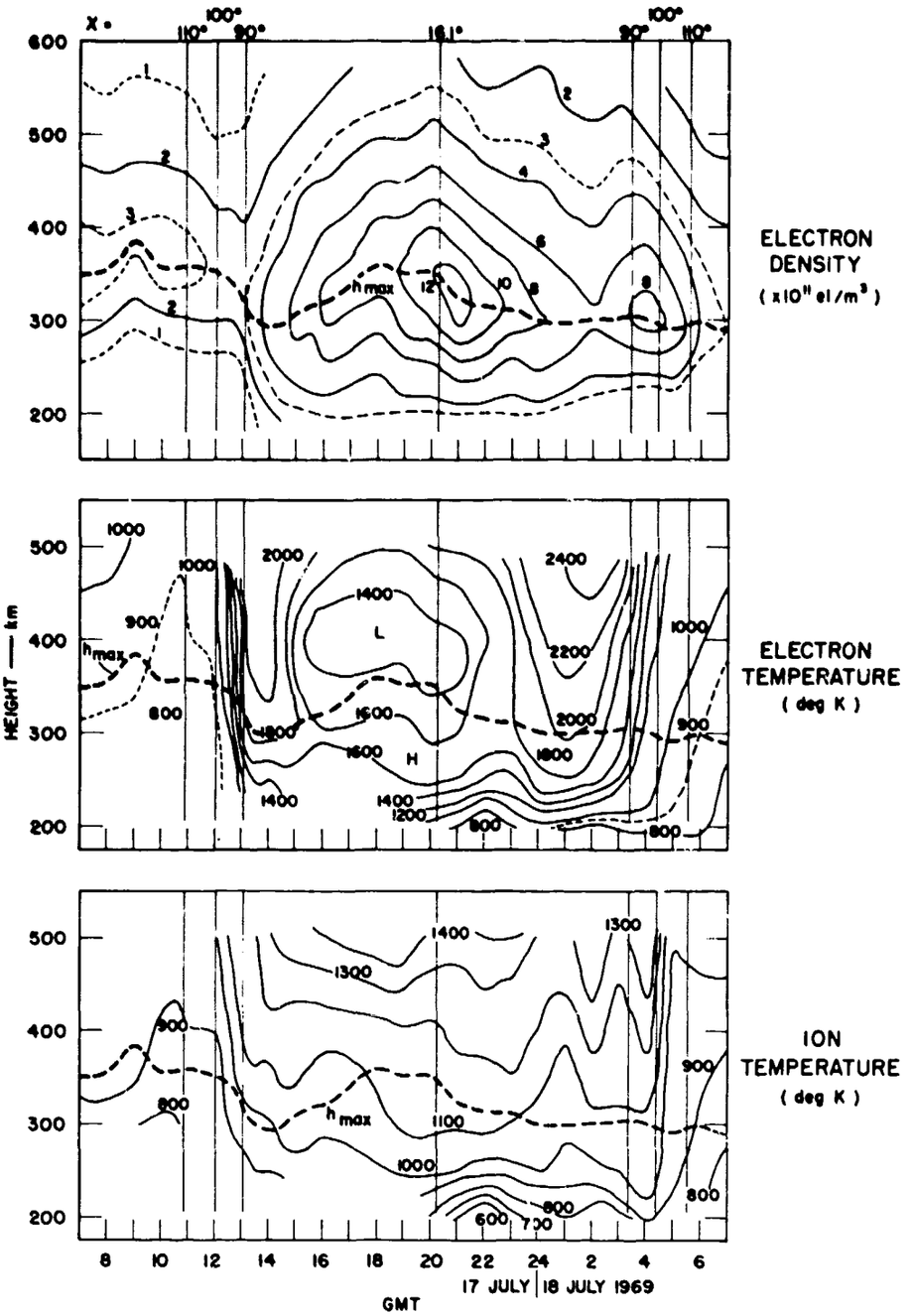

FIGURE 15 CONTOURS OF ELECTRON DENSITY, ELECTRON AND ION TEMPERATURES--17-18 JULY 1969

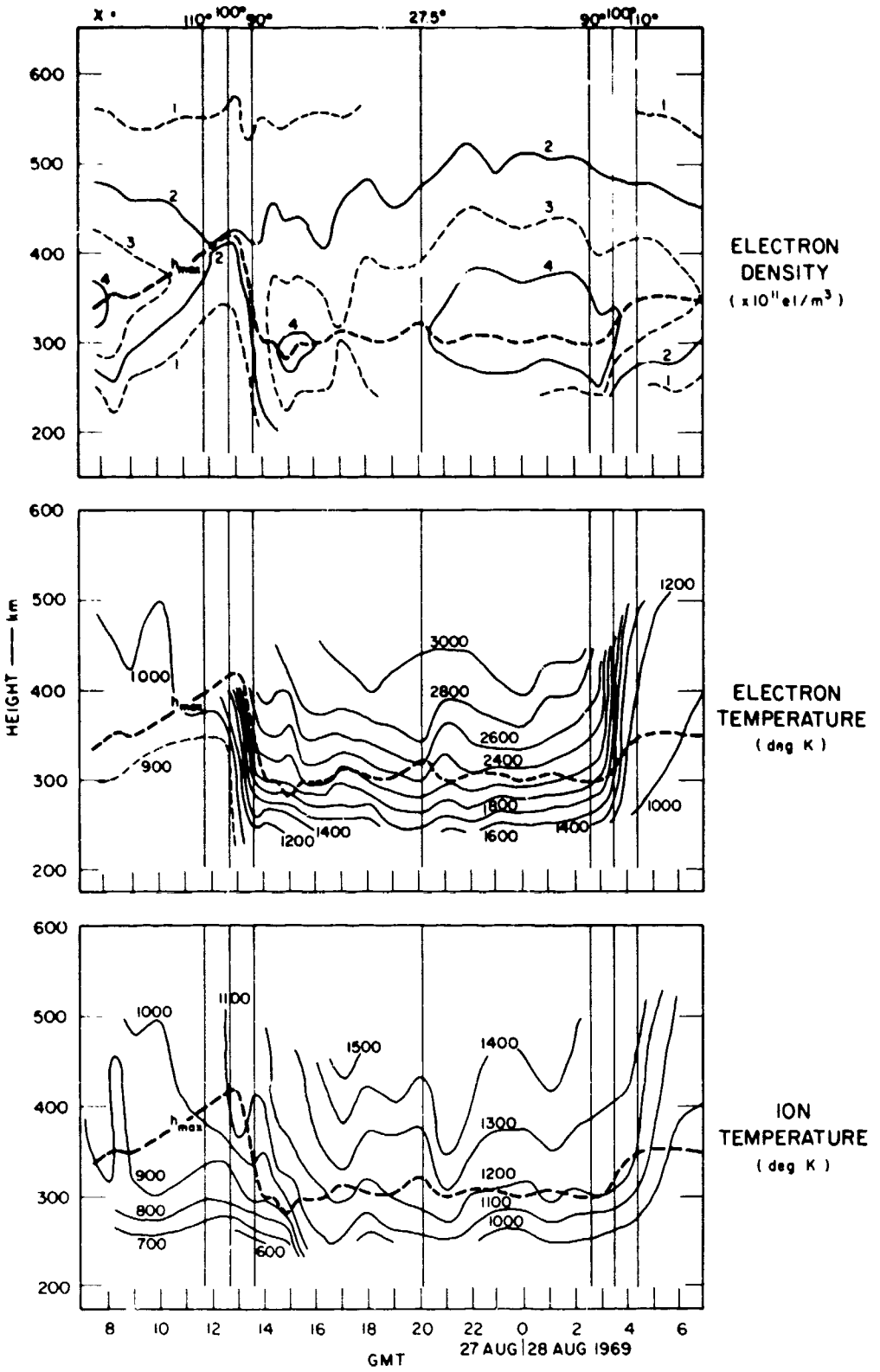

FIGURE 16 CONTOURS OF ELECTRON DENSITY, ELECTRON AND ION TEMPERATURES—— 27-28 AUGUST 1969

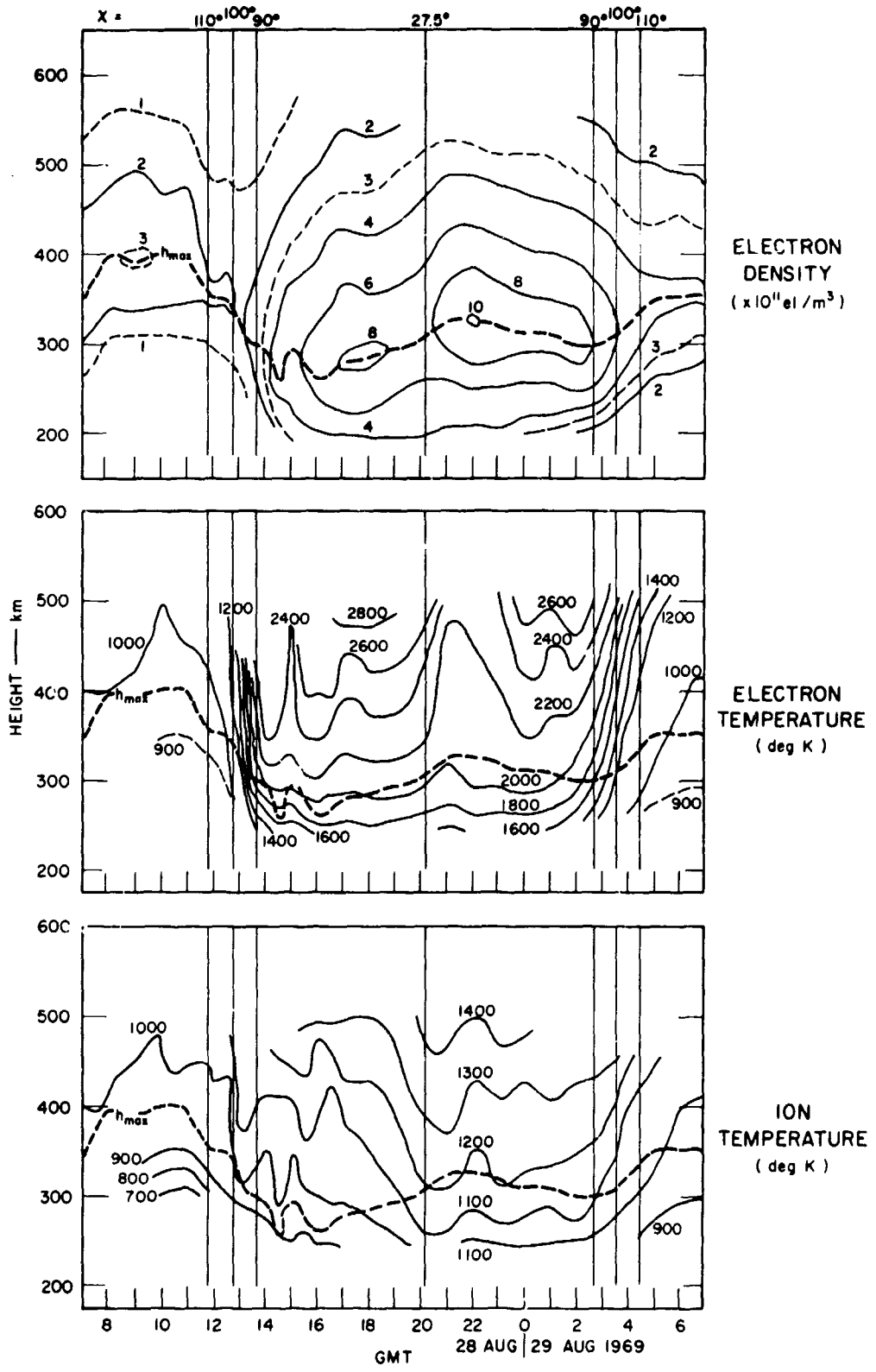

FIGURE 17 CONTOURS OF ELECTRON DENSITY, ELECTRON AND ION TEMPERATURES—— 28-29 AUGUST 1969

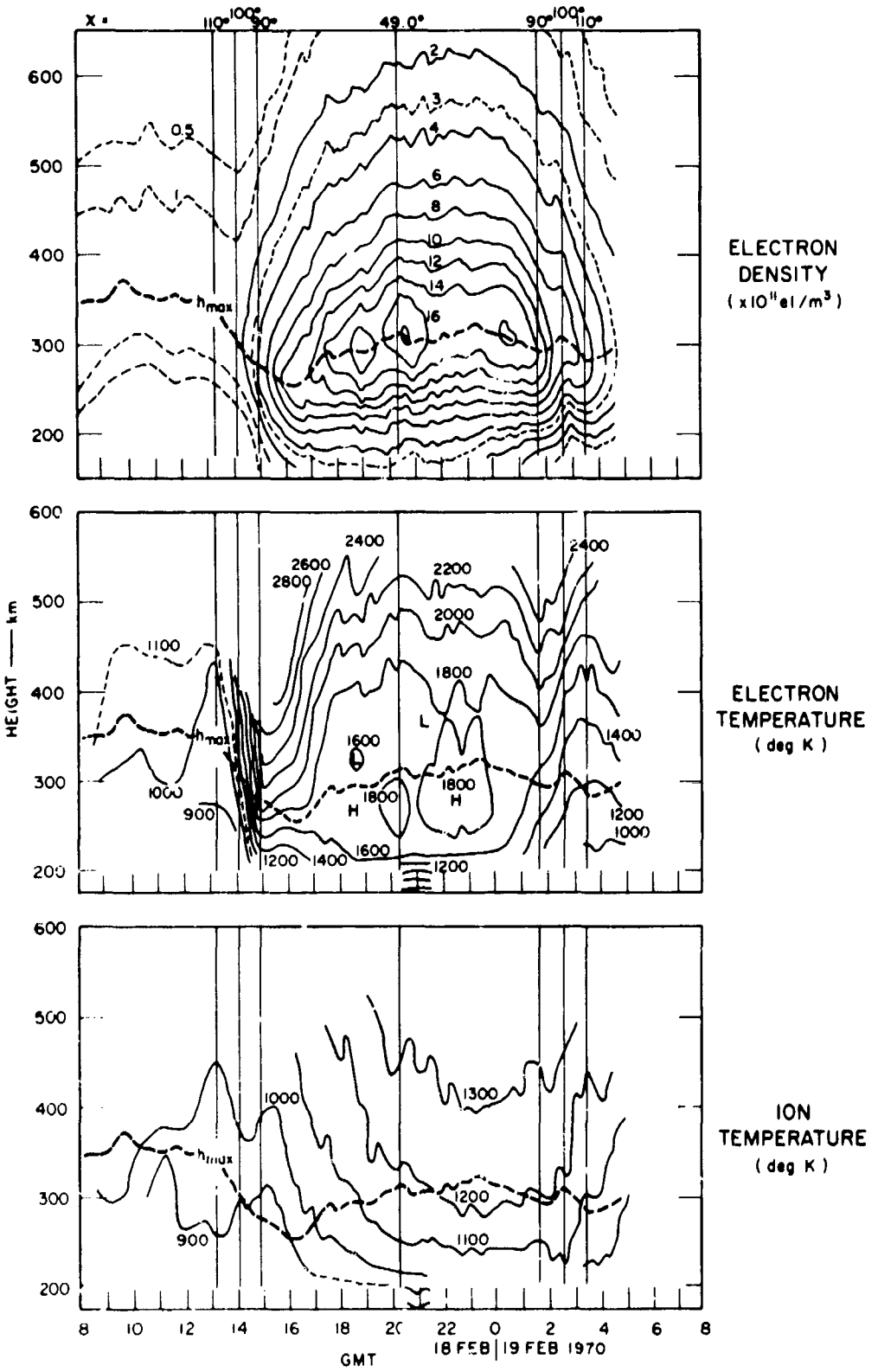

FIGURE 18 CONTOURS OF ELECTRON DENSITY, ELECTRON AND ION TEMPERATURES—— 18-19 FEBRUARY 1970

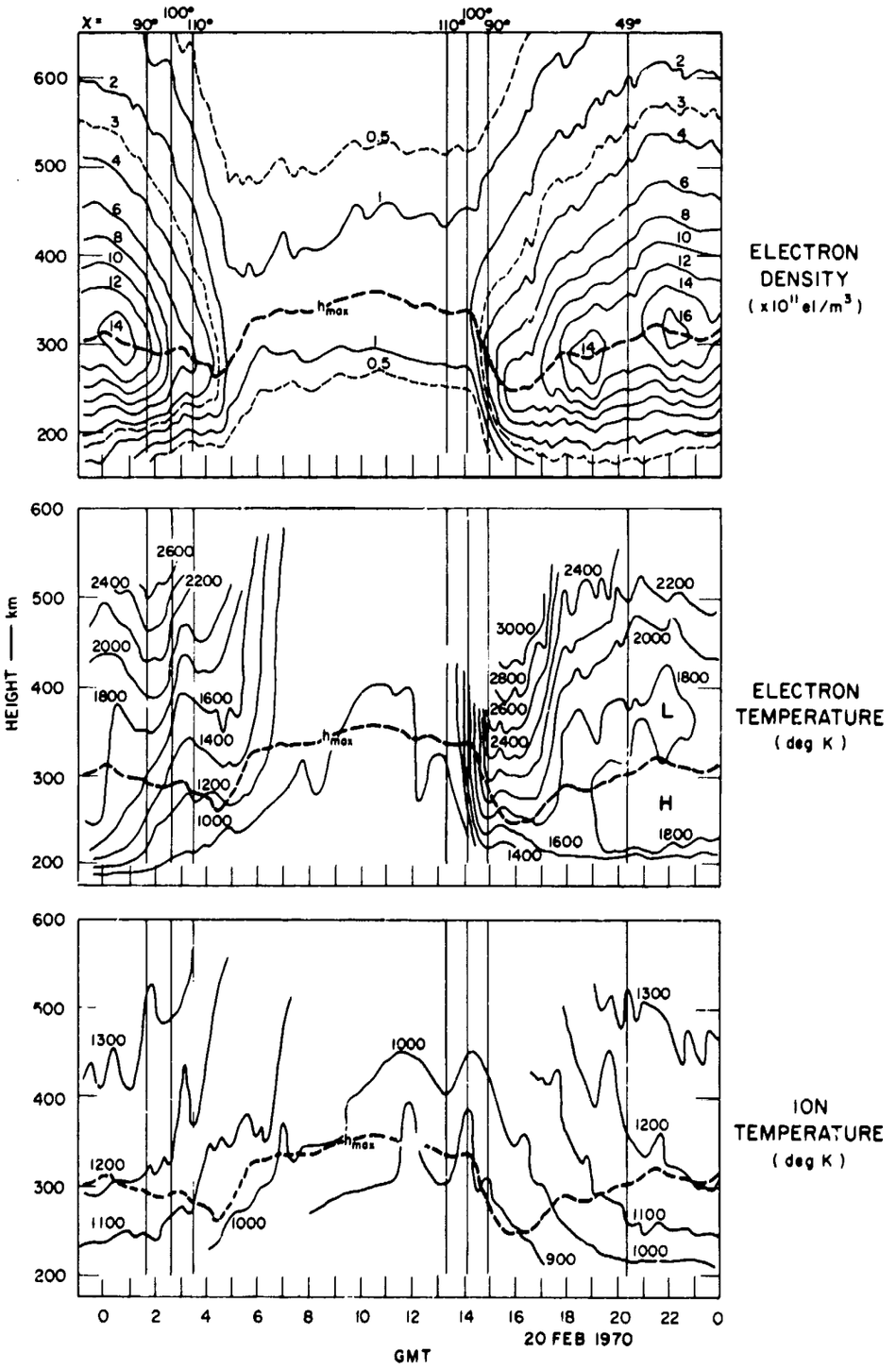

FIGURE 19 CONTOURS OF ELECTRON DENSITY, ELECTRON AND ION TEMPERATURES—— 20 FEBRUARY 1970

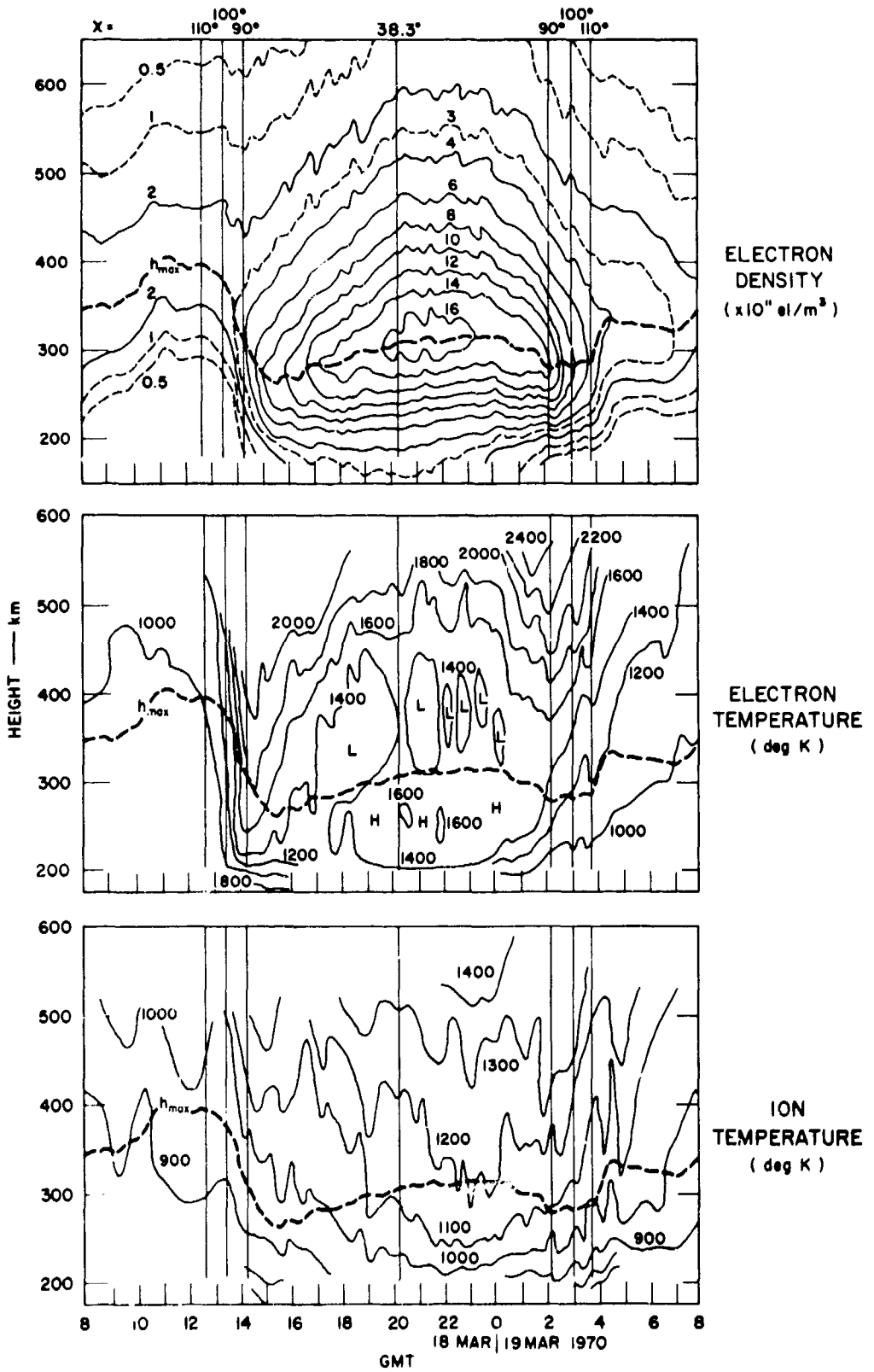

FIGURE 20 CONTOURS OF ELECTRON DENSITY, ELECTRON AND ION TEMPERATURES—18-19 MARCH 1970

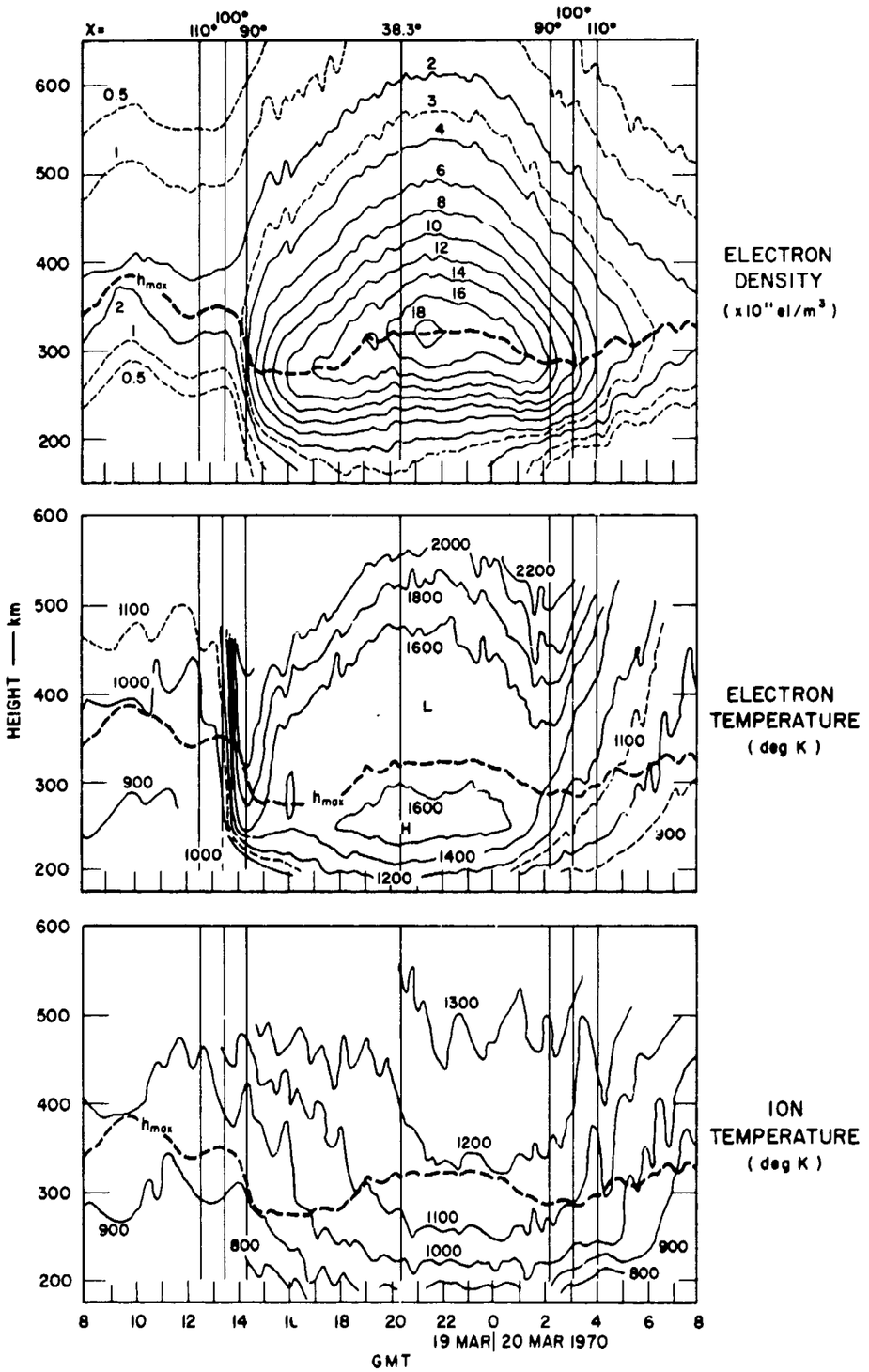

FIGURE 21 CONTOURS OF ELECTRON DENSITY, ELECTRON AND ION TEMPERATURES--19-20 MARCH 1970

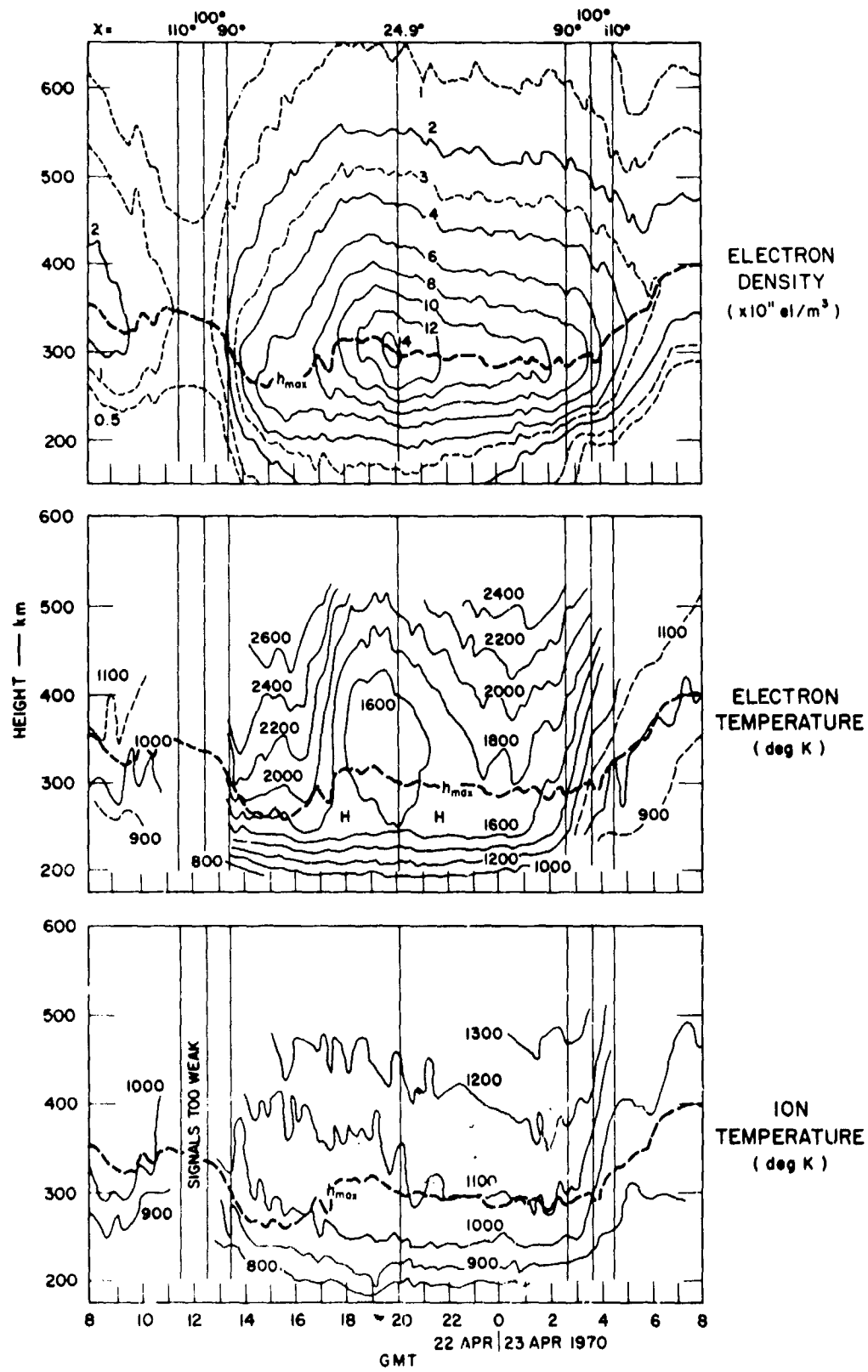

FIGURE 22 CONTOURS OF ELECTRON DENSITY, ELECTRON AND ION TEMPERATURES--- 22-23 APRIL 1970

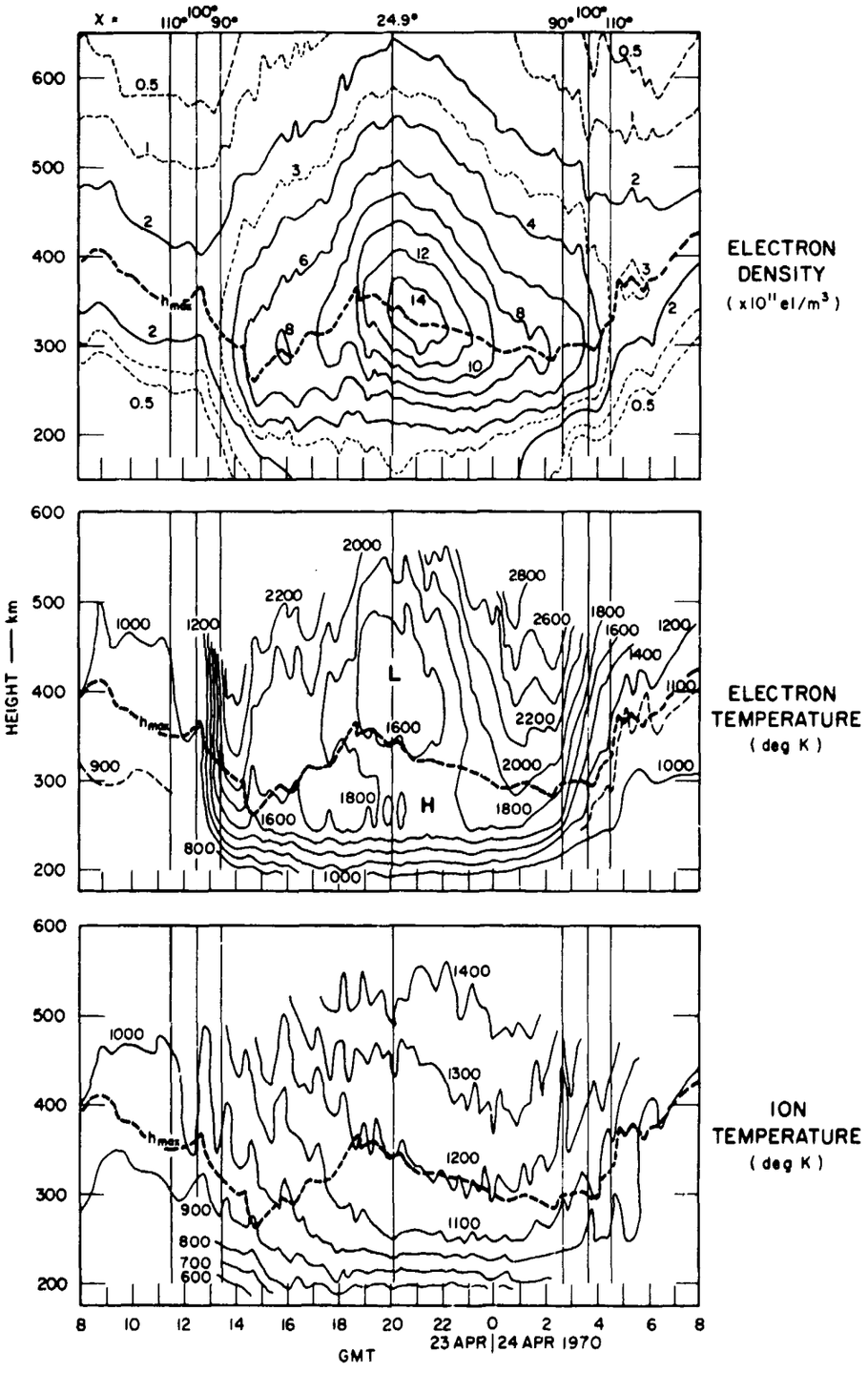

FIGURE 23 CONTOURS OF ELECTRON DENSITY, ELECTRON AND ION TEMPERATURES--- 23-24 APRIL 1970

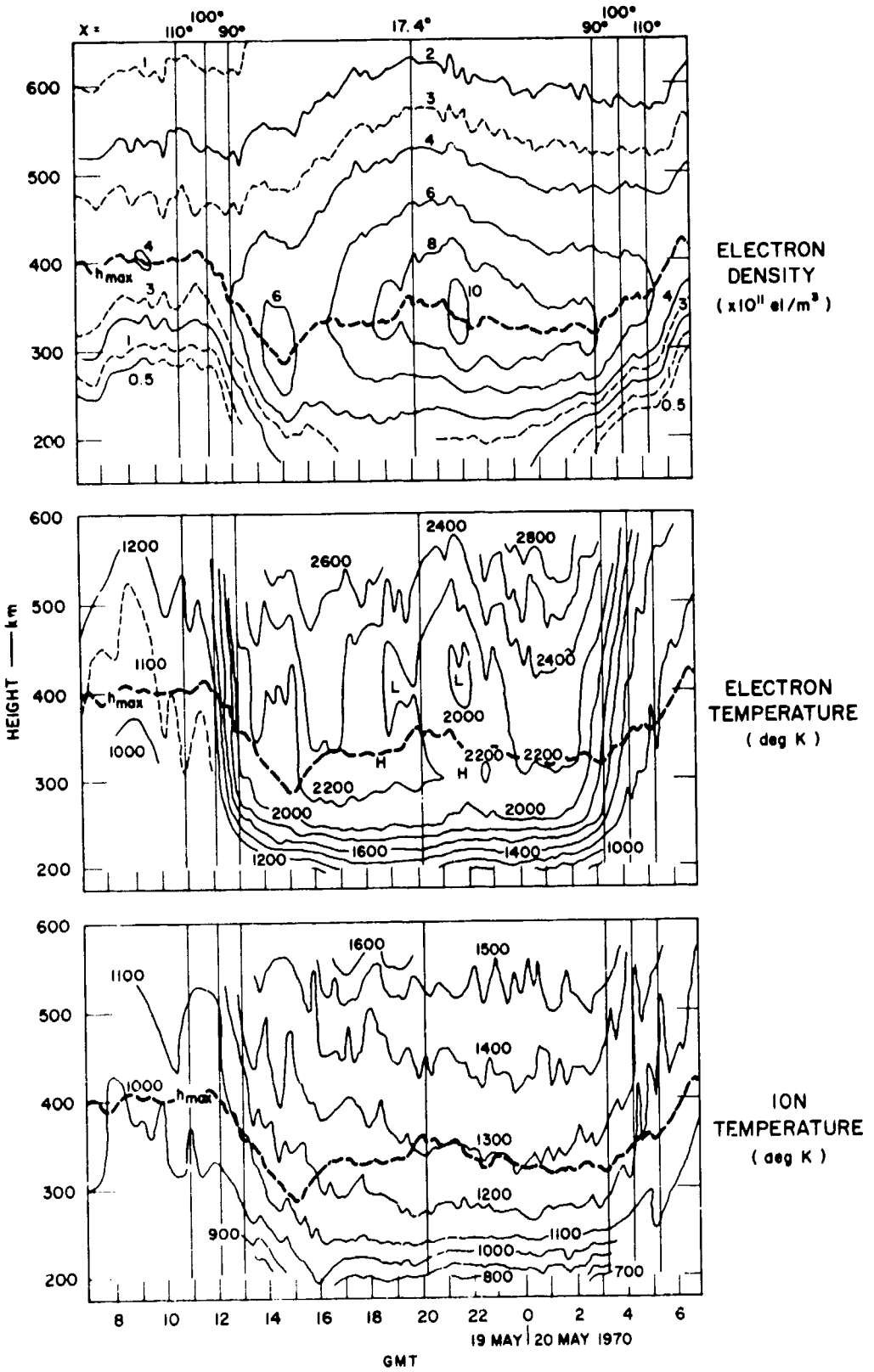

FIGURE 24 CONTOURS OF ELECTRON DENSITY, ELECTRON AND ION TEMPERATURES—— 19-20 MAY 1970

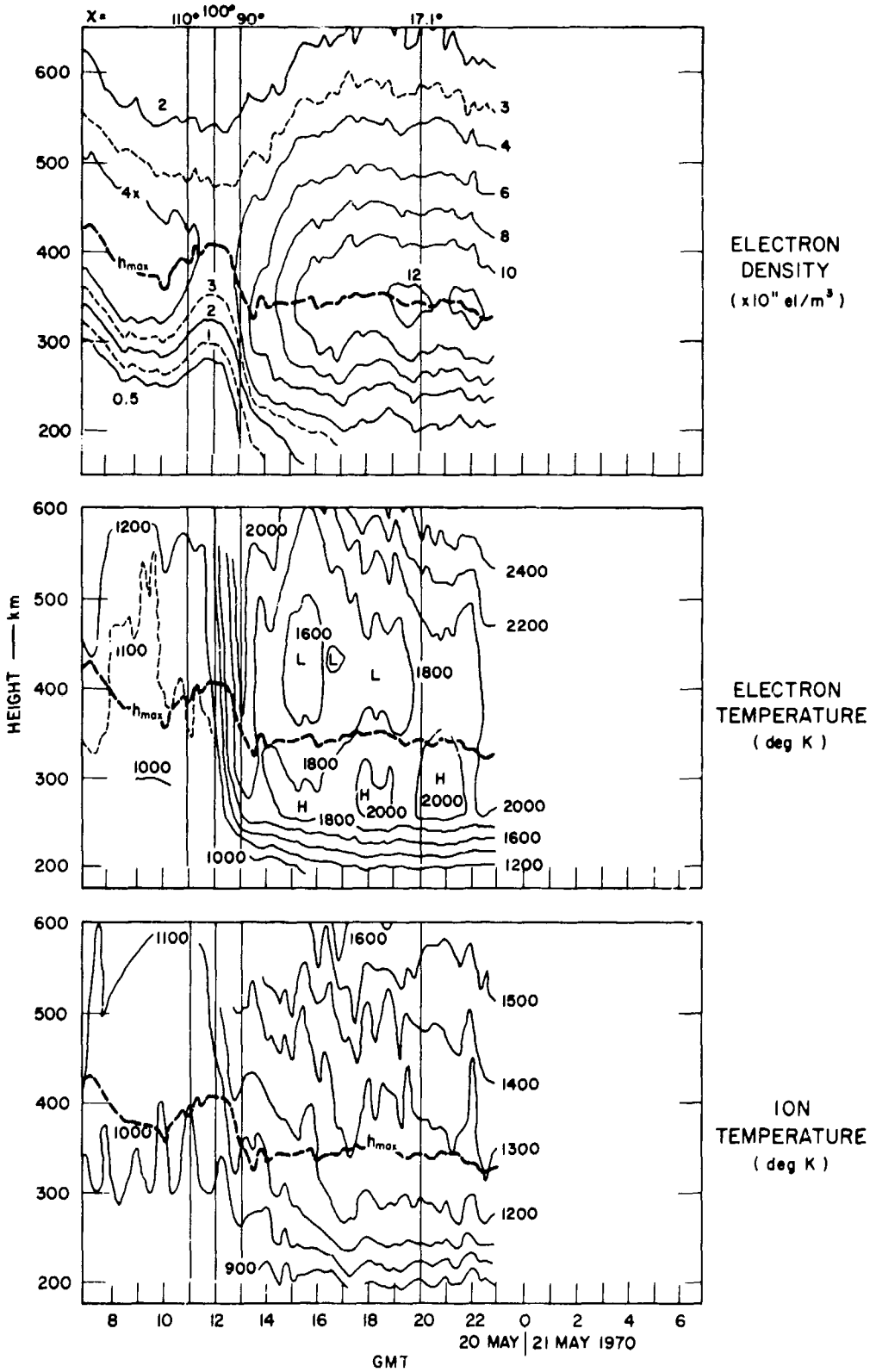

FIGURE 25 CONTOURS OF ELECTRON DENSITY, ELECTRON AND ION TEMPERATURES—20–21 MAY 1970

density is increased, the thermal contact between electrons and ions is improved and the rate at which electrons transfer heat to ions through Coulomb collisions is much greater. Thus at altitudes and times at which the electron density is high, the electron temperature approaches the ion temperature. However, during the daylight hours when the electron density is low the electron temperature is much higher than the ion temperature. This inverse relationship between electron density and temperature does not hold, of course, at night when the solar heat source is not present. During the night at our location the ions and electrons are at very nearly equal temperatures for all months of the year.

In Figures 26 through 32, the following ionospheric parameters have been scaled and plotted as a function of time of day for each of the seven 48-hour runs:

(1) The maximum electron density in the F-layer (N_{max})

(2) The height of the maximum electron density (h_{max})

(3) The upper and lower half-thickness of the F layer.

The N_{max} plots present a simple picture of increases and decreases in ionization due to electron production, loss, and redistribution.

The height of the maximum electron density is an indicator of apparent vertical ionospheric motions. However, it should be remembered that these motions are only apparent and may not be real. For example, the sunrise decrease in h_{max}, which occurs at all seasons, is not a consequence of ionization being displaced downward, but is a consequence of increased production at lower altitudes and an upward transport of ionization above the layer maximum. The vertical drift measurements discussed in detail in Section IV, show clearly an upward drift of ionization during the sunrise period.

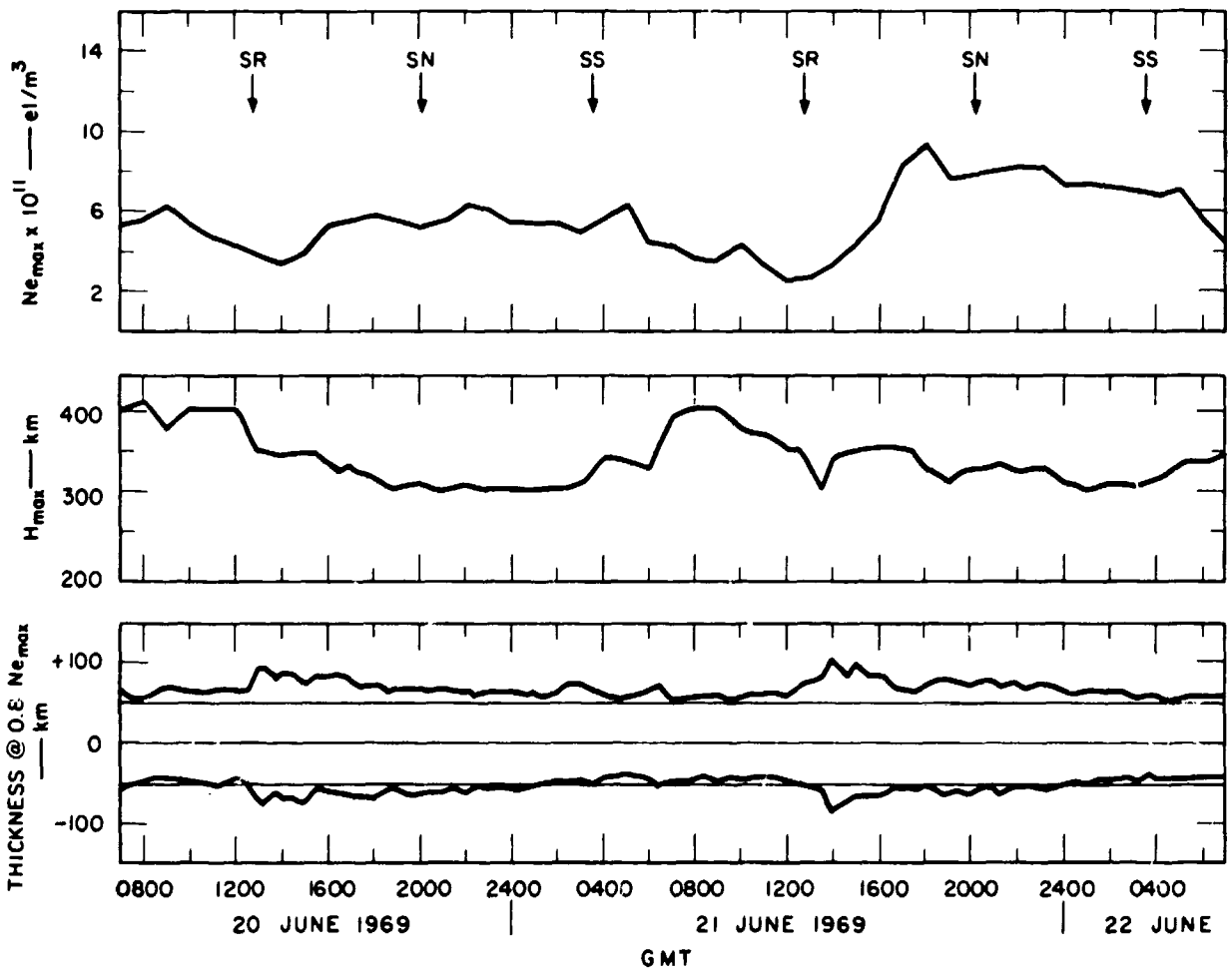

FIGURE 26 MAXIMUM ELECTRON DENSITY, HEIGHT OF MAXIMUM DENSITY, AND LAYER THICKNESS--20-22 JUNE 1969

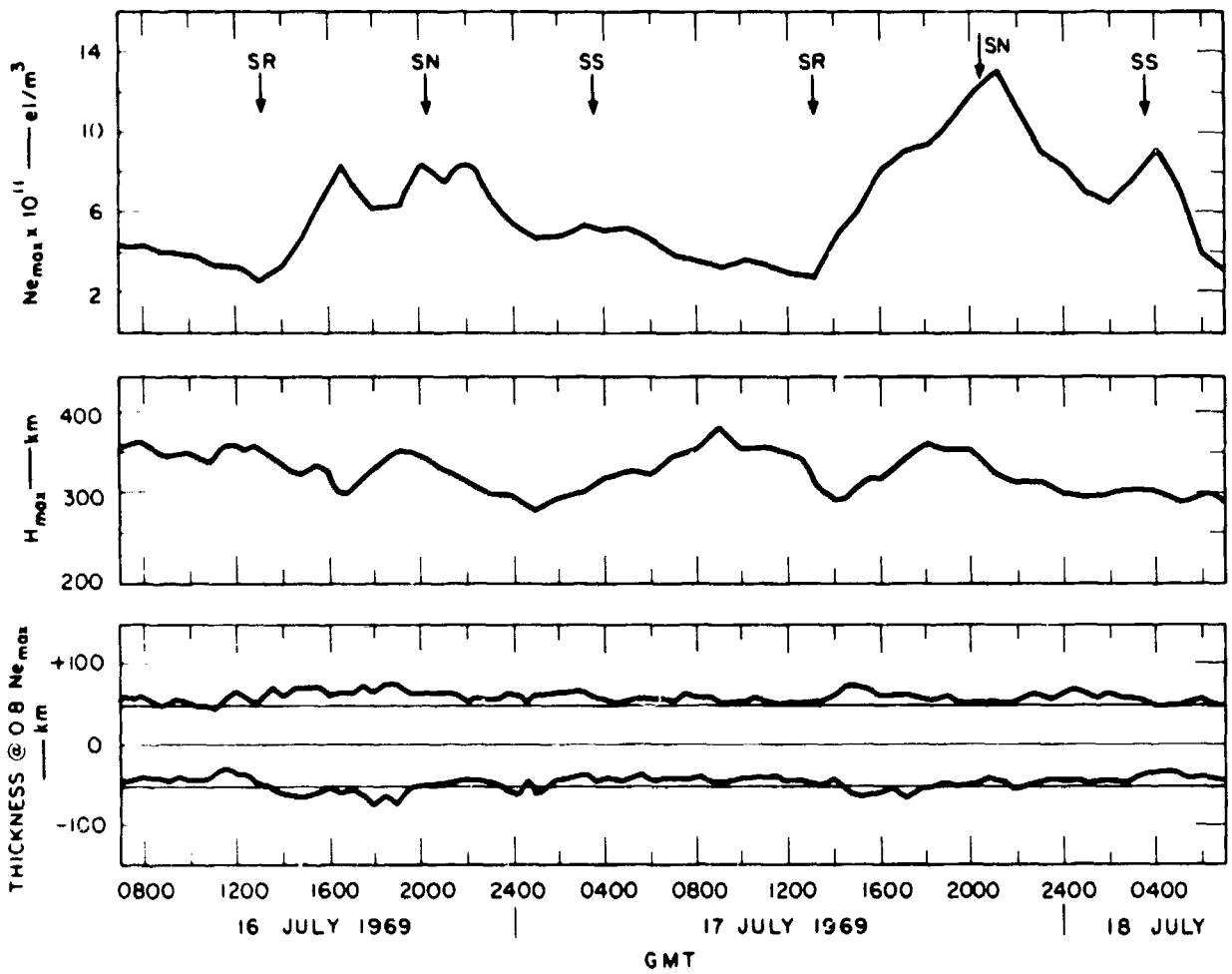

FIGURE 27 MAXIMUM ELECTRON DENSITY, HEIGHT OF MAXIMUM DENSITY, AND LAYER THICKNESS--16-18 JULY 1969

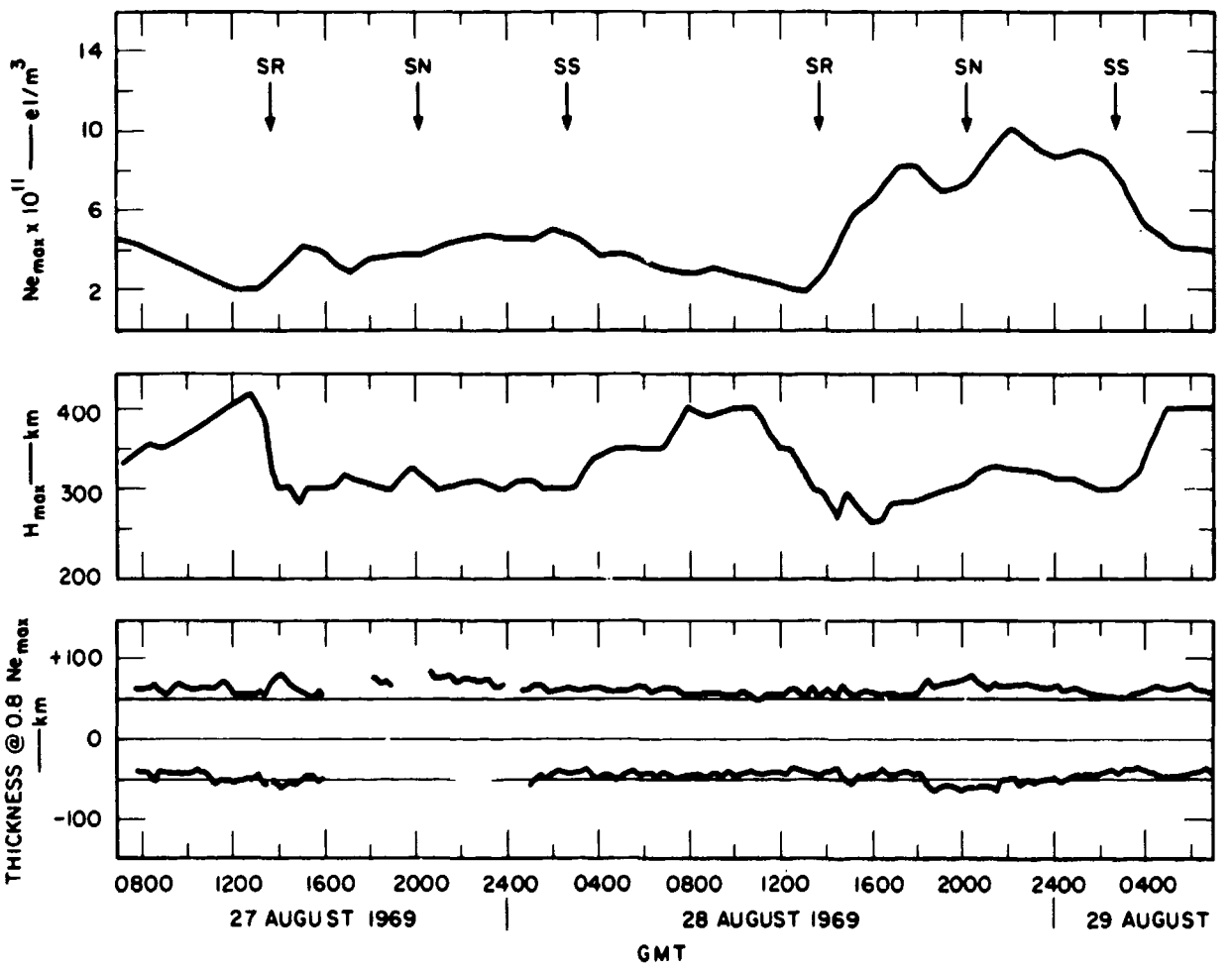

FIGURE 28 MAXIMUM ELECTRON DENSITY, HEIGHT OF MAXIMUM DENSITY, AND LAYER THICKNESS--27-29 AUGUST 1969

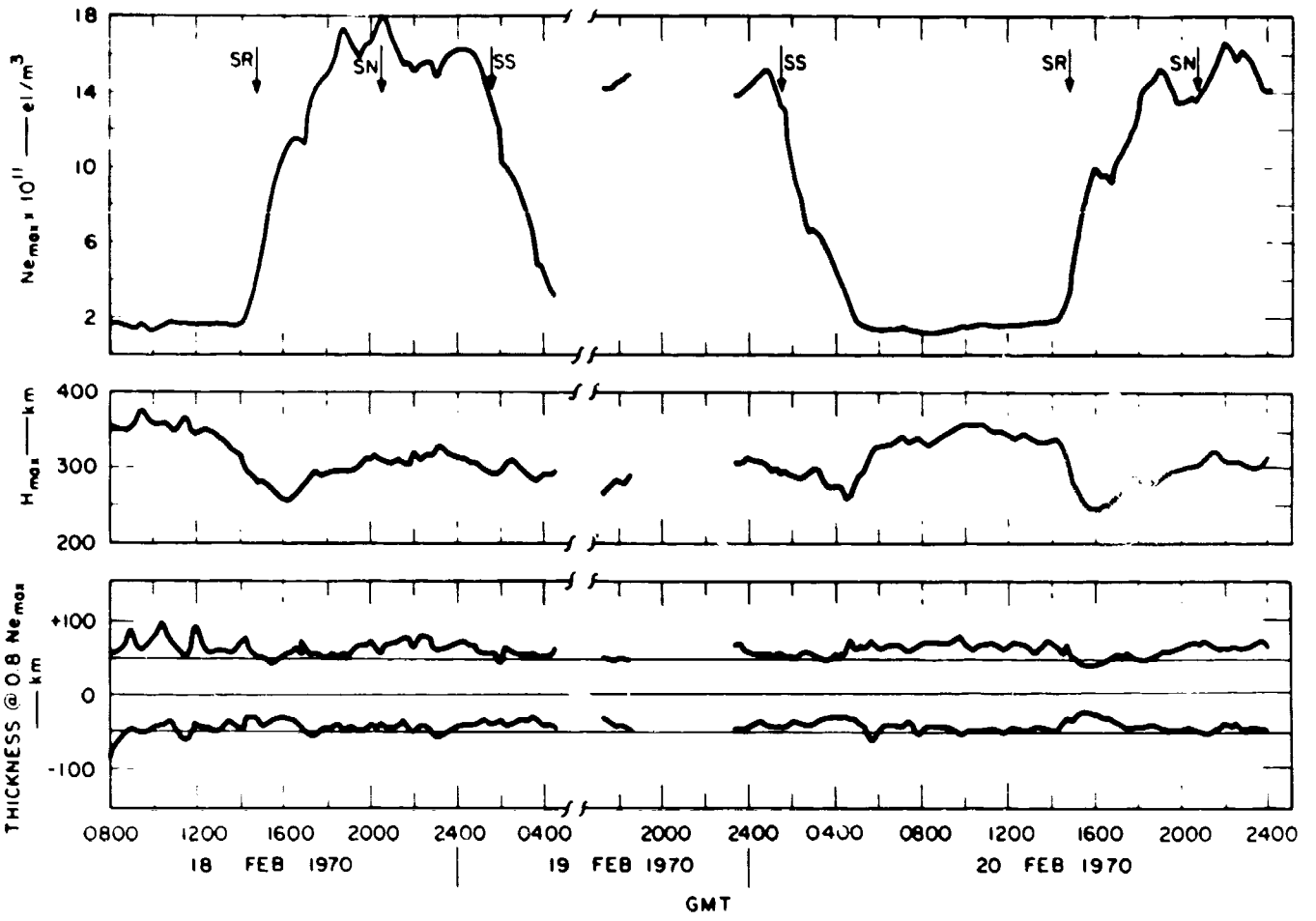

FIGURE 29 MAXIMUM ELECTRON DENSITY, HEIGHT OF MAXIMUM DENSITY, AND LAYER THICKNESS--18-20 FEBRUARY 1970

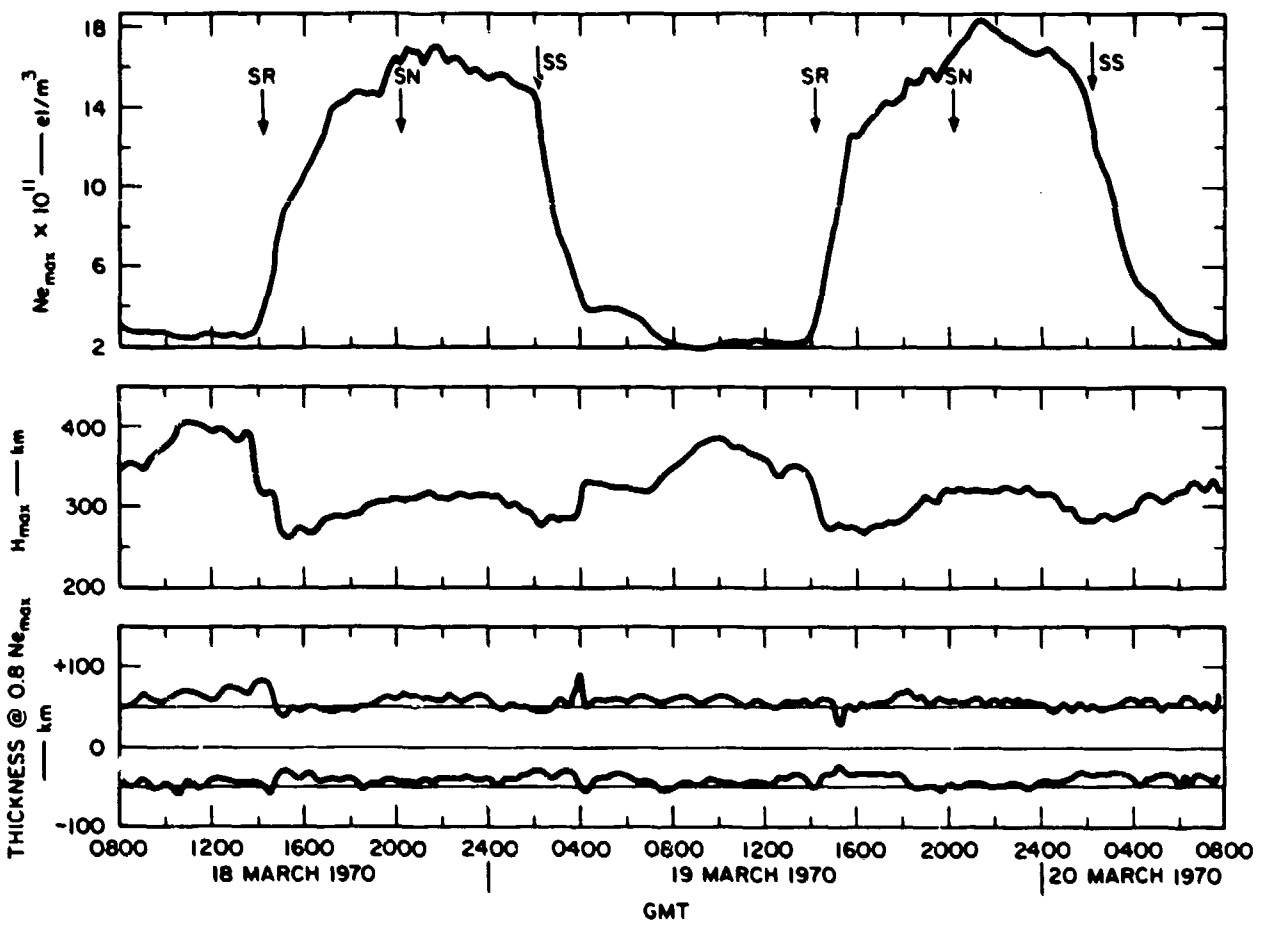

FIGURE 30 MAXIMUM ELECTRON DENSITY, HEIGHT OF MAXIMUM DENSITY, AND LAYER THICKNESS--18-20 MARCH 1970

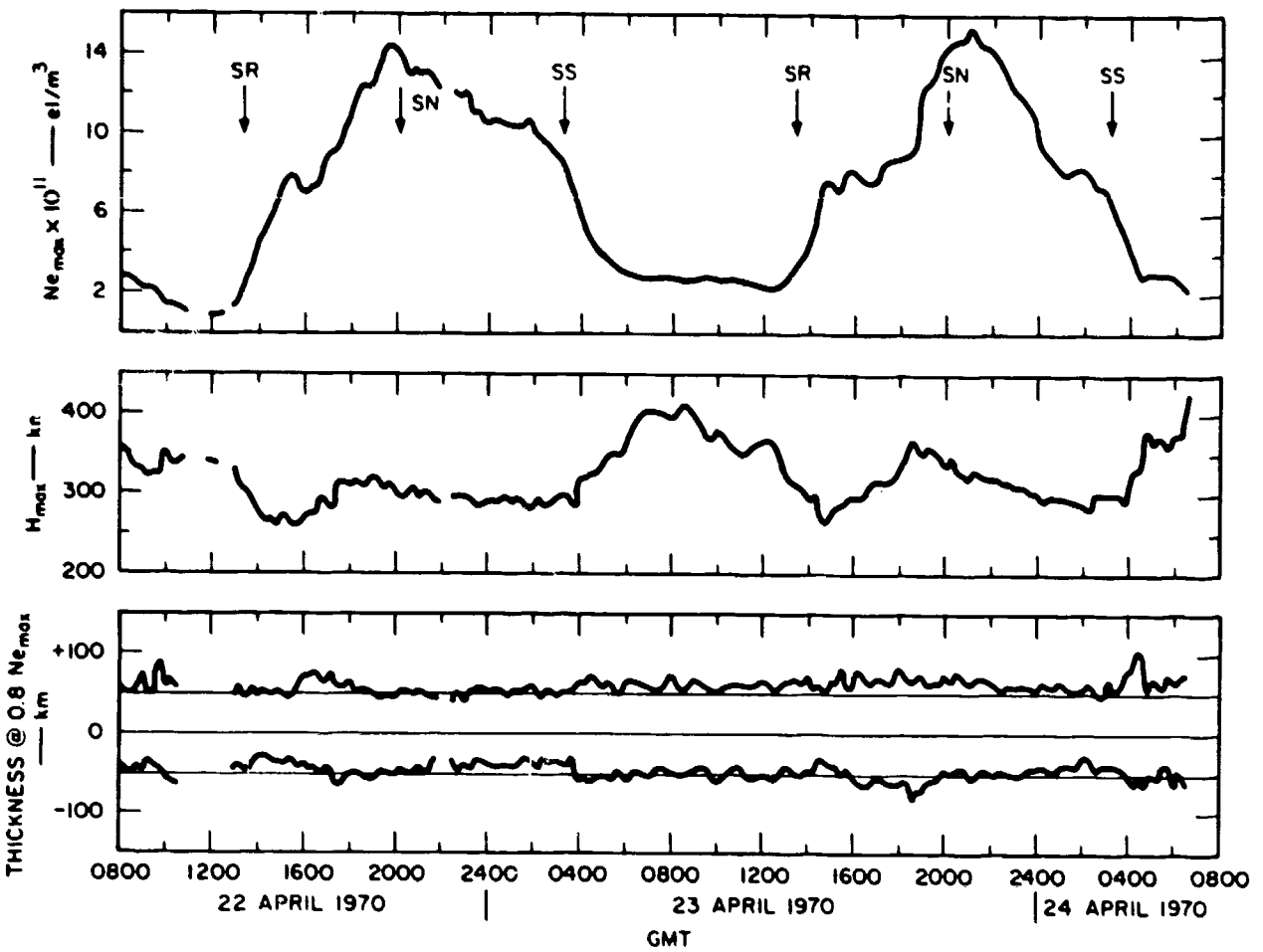

FIGURE 31 MAXIMUM ELECTRON DENSITY, HEIGHT OF MAXIMUM DENSITY, AND LAYER THICKNESS--22-24 APRIL 1970

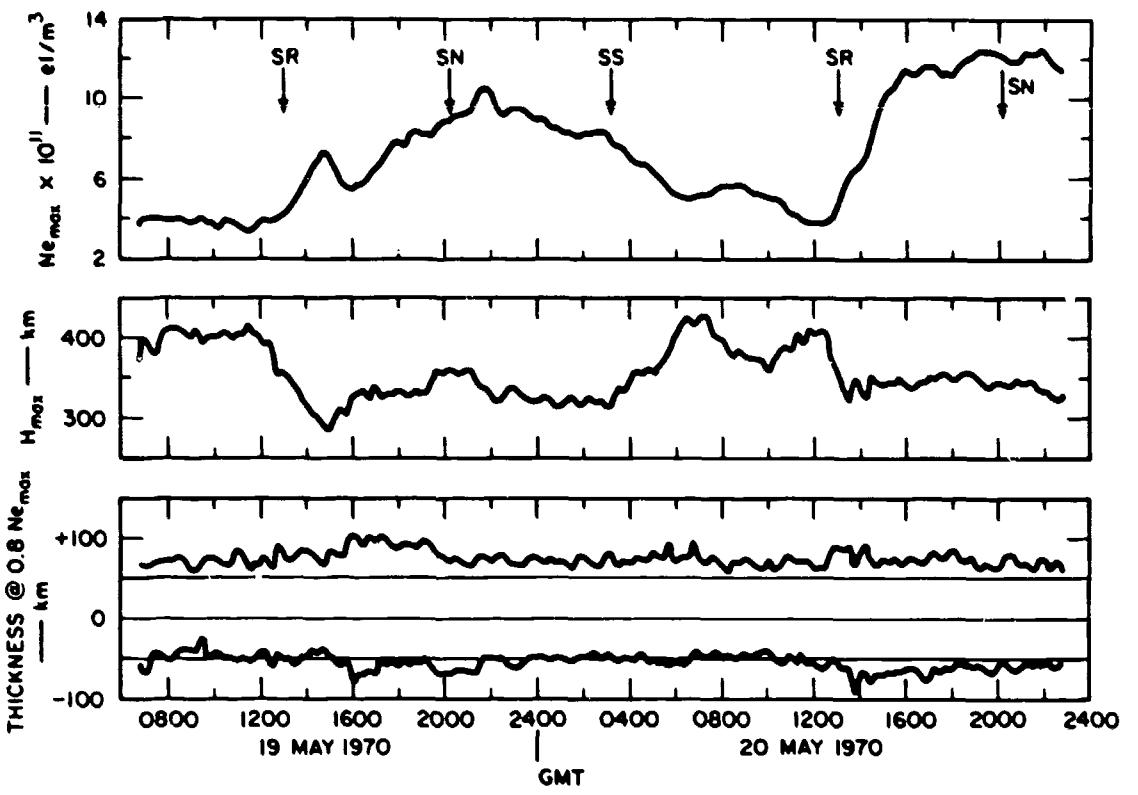

FIGURE 32 MAXIMUM ELECTRON DENSITY, HEIGHT OF MAXIMUM DENSITY, AND LAYER THICKNESS--19-20 MAY 1970

The upper and lower half-thicknesses are measured at the altitudes where the electron density is 80 percent of its peak value. The value of 80 percent was used in order to facilitate comparisons with the 1968-69 data, which was scaled at the 80-percent level. This thickness parameter is an indicator of layer shape--i.e., whether the F layer was "thin" or "fat," whether it is symmetrical above and below the peak, and whether or not the shape changes with time of day and season.

The times of sunrise (SR), and sunset (SS) indicated on Figures 26-32 are the times at which the solar zenith angle is 90°; solar noon (SN) is the time at which the sun is at its maximum elevation.

C. Discussion

The general behavior of the ionosphere has been discussed in previous reports.[5,6] The data for 1969-1970 improve upon the accuracy and time resolution of the measurement and also provide greater altitude coverage. In addition, this year's data are better suited for studying diurnal variations since operations extended over continuous 48-hour periods.

In this report we will concentrate our discussion on seasonal behavior and on aspects of the ionosphere's behavior that we have not previously reported, making use of two years of data. Included are: (1) A study of the sunrise behavior as a function of solar zenith angle and season; (2) a study of the sunset behavior as a function of solar zenith angle and season; (3) an extension of last year's study of the seasonal behavior of N_{max}; (4) layer height variations.

1. Sunrise Behavior

The sunrise behavior of the ionosphere is characterized by three events: an increase in electron temperature, a decrease in the height of the maximum electron density, and an increase in the electron density.

As the solar zenith angle, χ, approaches approximately 103°, a rather abrupt increase in electron temperature, T_e, is seen. During the night the electron temperature is essentially equal to the ion temperature. As the sun rises and χ decreases from 105° to 90°, the electron temperature approximately doubles. The solar zenith angle at which the rise in electron temperature begins is independent of season, being 103 ±3° for all the 1969-1970 data. This is shown by the solid line of Figure 33.

Shortly after T_e begins to rise, the height of the maximum electron density begins to fall. This drop in h_{max} is not a consequence of ionization physically moving downward, but instead is due to increased production at lower altitudes and increased upward diffusion at altitudes above the layer maximum. These two effects combine to cause the decrease in h_{max}. The solar zenith angle at which h_{max} begins to fall does seem to depend on season, as shown by the dashed line in Figure 33, occurring earlier (larger χ) in the winter and early spring, and later (smaller χ) in the late spring and summer.

Following the decrease in h_{max} by 5 ± 3 degree of solar zenith angle, the maximum electron density N_{max} begins to increase. The zenith angle at which this increase takes place seems to depend on season, in the same way as the h_{max} variation--i.e., the increase in N_{max} is earlier in winter and later in summer.

The rate at which the initial increase in density takes place depends on season. Figure 34 is a plot of the post-sunrise rate of change of N_{max} as a function of season and includes data from 1968 through 1970. During the winter the density increase is rapid, with N_{max} increasing at a rate of 4 to 6 $\times 10^{11}$ el/m^3 per hour. During the summer the rate of change of N_{max} is a much more gradual--of the order of 0.8 to 2 $\times 10^{11}$ el/m^3 per hour.

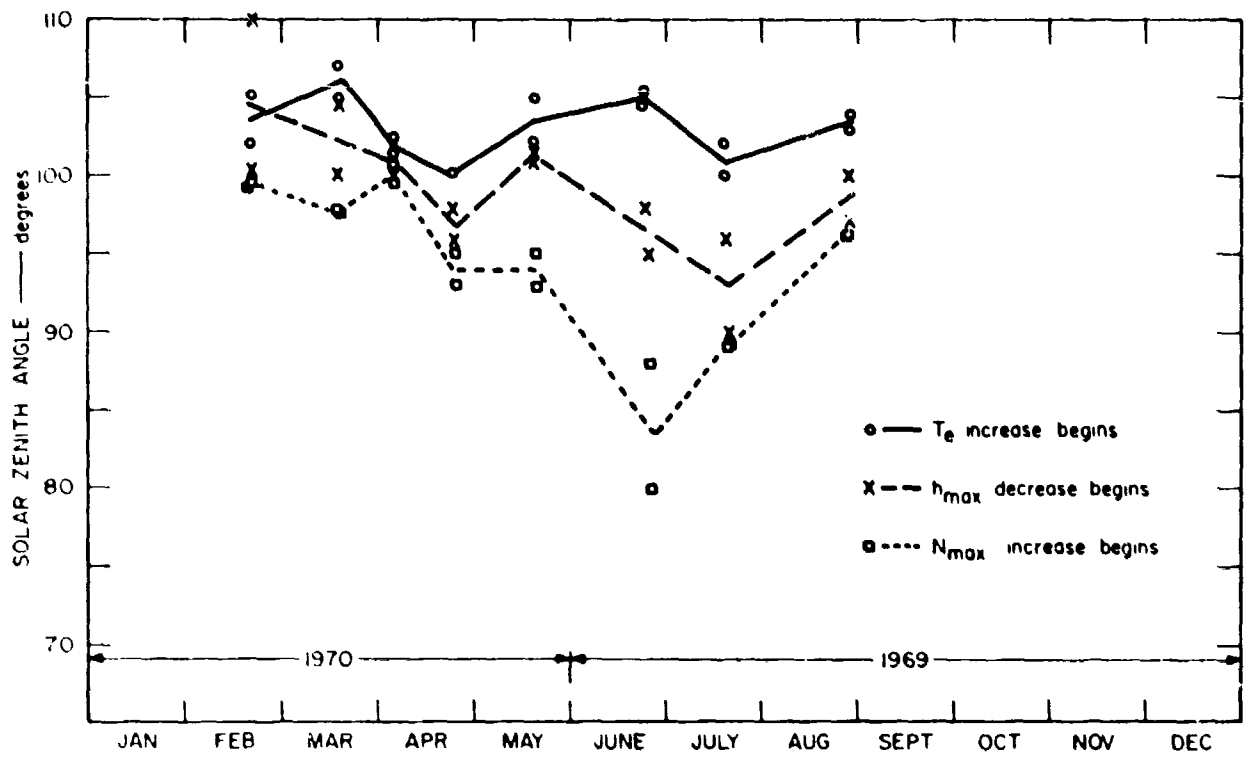

FIGURE 33 SEASONAL VARIATION OF SUNRISE BEHAVIOR OF T_e, h_{max}, AND N_{max}

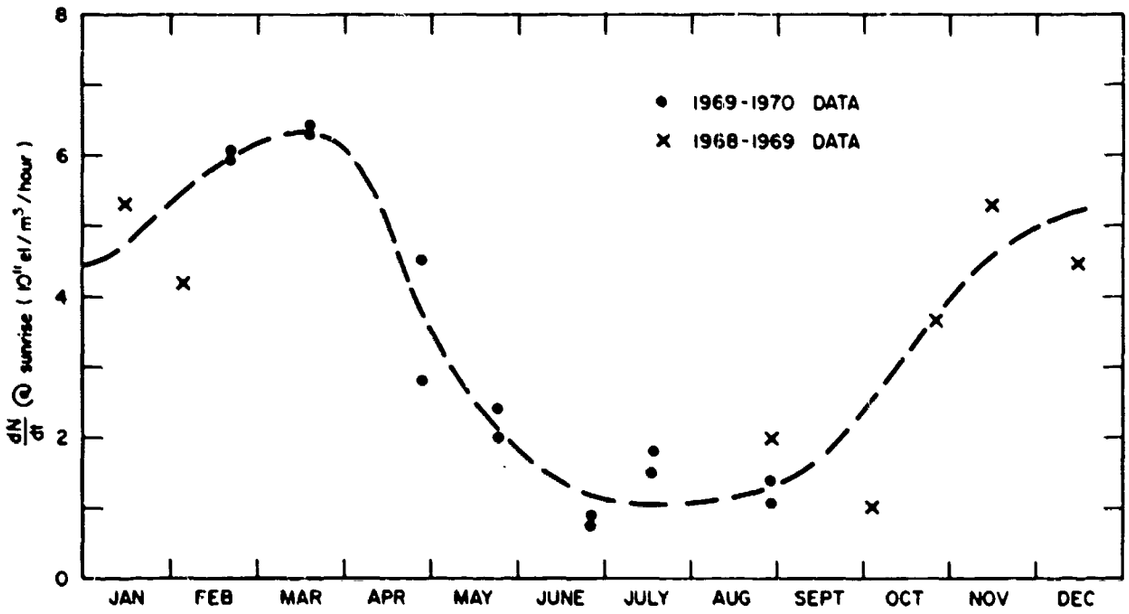

FIGURE 34 SEASONAL VARIATION OF SUNRISE RATE OF CHANGE OF N_{max}

Another interesting seasonal aspect of the sunrise behavior can be seen by inspecting the layer thickness plots. During the winter, the layer becomes thinner during the sunrise period, while during the summer it becomes thicker. This result, in combination with the seasonal differences in $d N_{max}/dt$, implies that the amount of electrons produced after sunrise may not be grossly different in summer and winter. Instead, their spatial distribution is different. During the winter the electrons concentrate near h_{max}, producing a relatively thin F layer with a high peak density, while during the summer the electrons are distributed over a greater altitude regime and form a thicker layer with a smaller peak density.

2. Sunset Behavior

The sunset behavior of the ionosphere is characterized by a rather abrupt decrease in electron temperatures, which generally precedes a decrease in electron density. A general increase in h_{max} is also evident in the data for all months.

Sunset effects are not as rapid as sunrise effects. The sunset decreases in electron temperature and density occur at slower rates than the sunrise increases.

During the winter, the density and temperature begin to decrease at nearly the same solar zenith angle ($80^\circ < \chi < 90^\circ$). Sometimes the density decrease occurs first; sometimes the temperature decrease occurs first. However, during the summer months the temperature decrease begins well before the density decrease. The electron temperature begins to fall when $\chi \approx 85^\circ$, while the density does not decrease until after the sun is well below the horizon ($\chi > 105^\circ$). These effects are shown in Figure 35, in which the solar zenith angles to which N_{max} and T_e begin to decrease are plotted as a function of month.

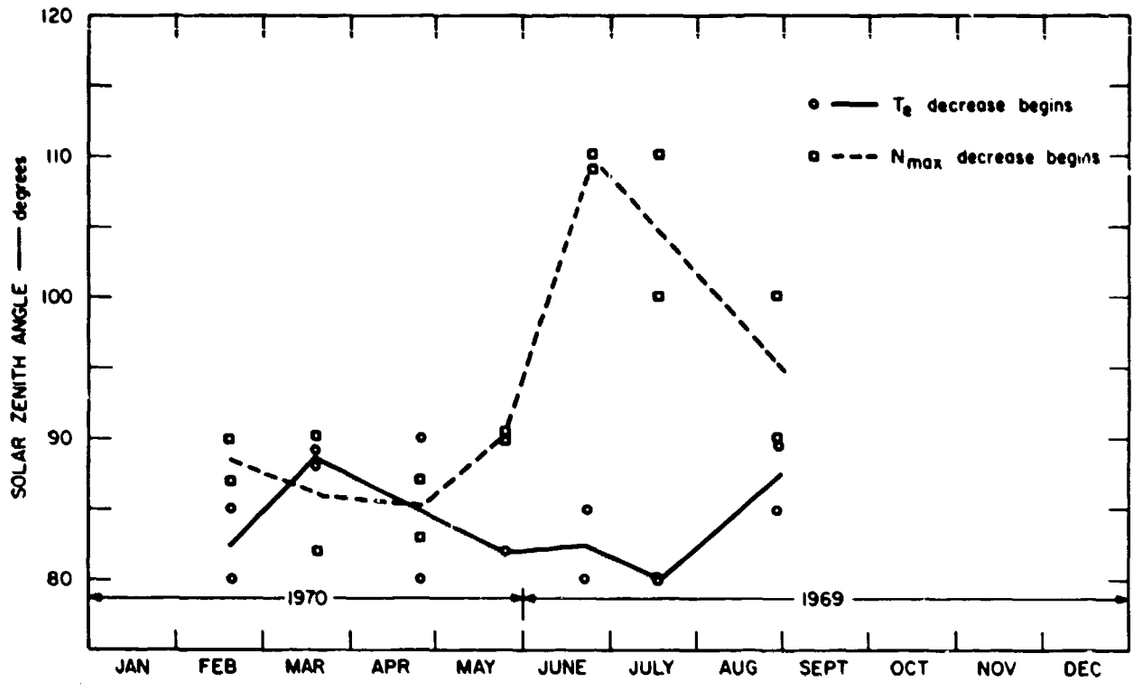

FIGURE 35 SEASONAL VARIATION OF SUNSET BEHAVIOR OF T_e AND N_{max}

For all seasons the layer becomes thinner during the sunset period. This is due to the rapid recombination on the bottomside that reduces the lower half-thickness, and to the reduced electron temperatures above the layer maximum that lead to (1) a smaller scale height and (2) a contraction of the layer as it cools.

3. Seasonal Variation of N_{max}

The seasonal variation of N_{max} is shown in Figure 36. Data from 1968-1970 have been used and the maximum observed electron density for each day's observation has been plotted as a function of month of year. The inclusion of the 1969-70 data has confirmed the conclusion reported earlier,[6] that N_{max} is greatest in the winter and near the equinoxes, and smallest during the summer. There is approximately a 2-1/2-to-1 difference between winter and summer maximum densities.

4. Layer Height Variations

During the course of a 24-hour period the height of the layer maximum changes by a large amount (90 to 170 km). Typically the layer is highest around local midnight and lowest shortly after sunrise. In order to determine whether any systematic seasonal behavior of h_{max} exists, Figure 37 was constructed using data from the past two years. In this figure a vertical line has been drawn between the lowest and highest altitudes that h_{max} achieved during each full day of observation. Thus the length of the line indicates the magnitude of the diurnal variation of h_{max}, and the end points indicate the extremes of h_{max}. From Figure 37 it can be seen that the greatest diurnal variation occurs during the equinoxes, and the smallest variations ($<$ 100 km) during the solstices. Also, h_{max} is generally higher in summer than in winter.

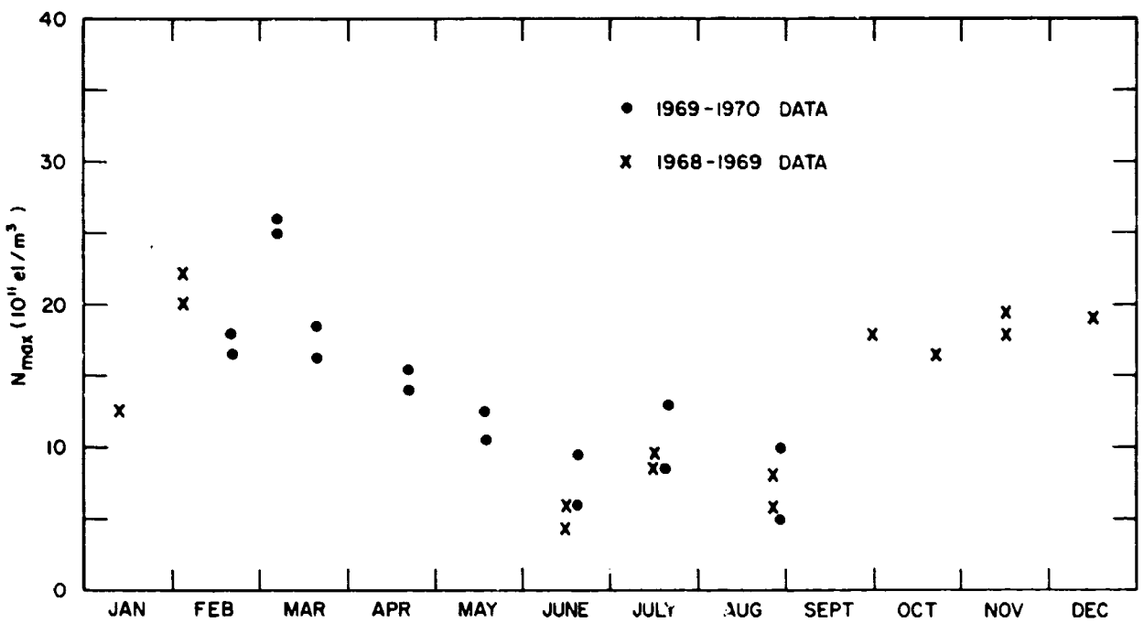

FIGURE 36 SEASONAL BEHAVIOR OF MIDDAY MAXIMUM ELECTRON DENSITY

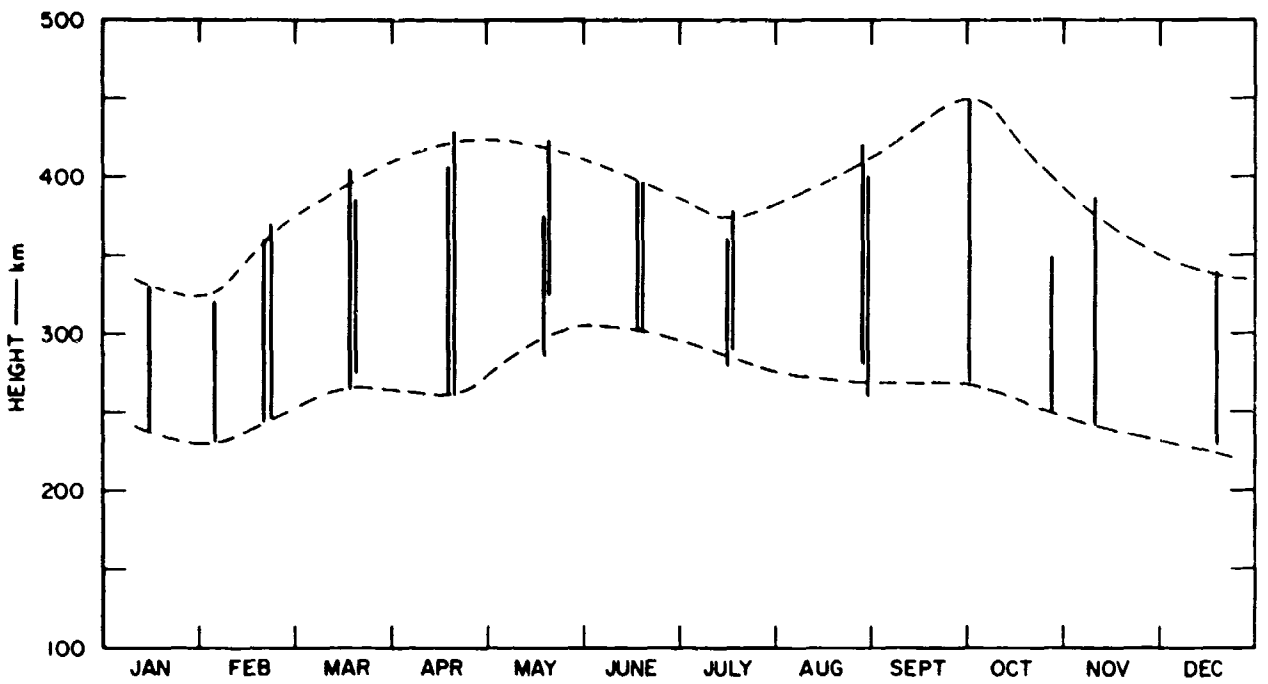

FIGURE 37 SEASONAL BEHAVIOR OF DIURNAL VARIATIONS OF h_{max}

IV SUNRISE VERTICAL VELOCITY OBSERVATIONS

A. Introduction

The Stanford Thomson-scatter radar has been used to examine vertical drift velocities in the upper F-region during the sunrise period.

The sunrise behavior of the ionosphere, especially the region above about 300 km altitude, has been effectively studied only recently. Carlson[17] has reported sunrise observations below 450 km using the Thomson-scatter system at Arecibo; both summer and winter observations were reported, and considerable attention was paid to conjugate effects. Evans[18] has reported the results of observations of sunrise phenomena made during February and March 1967 by the Thomson-scatter system at Millstone Hill. In order to maximize the detail of temporal variations, that study was confined to consideration of a height interval from 350 to 400 km. Da Rosa[19] has theoretically considered the sunrise behavior of electron temperature at all ionospheric altitudes below 1000 km. Carru et al.[10] have reported the results of vertical drift measurements using the bistatic Thomson-scatter system at St. Santin. The measurements were averaged over the altitude range 200 to 400 km and were obtained over the full diurnal cycle. More recently, Evans et al.[20] have observed diurnal F-region drifts over Millstone Hill between 450 and 900 km, and in particular have observed large upward drifts (about 100 m/s) at 600 km during sunrise, and this sunrise effect has also been reported by Watt[21] using the Alouette I topside sounder. Evans[22] has given a very good review of drift measurement techniques using Thomson scatter radar.

It is reasonable to expect transient motion of the ionosphere during sunrise. The rapid increase in solar EUV flux during the sunrise period gives rise to correspondingly rapid increases in both ambient electron temperature and electron density. The increase of either temperature or number density of a plasma should cause pressure gradients to build up, and these in turn should result in a flux of particles away from the high-pressure region. In the middle and upper F-region and at mid-latitudes, the relatively low collision frequency and large dip angle of the geomagnetic field should result in largely vertical flow, provided electric fields can be ignored. It is with this reasoning that attempts have been made here to determine whether or not a systematic vertical flux can be associated with the onset of sunrise in the ionosphere.

Examination of data obtained at Stanford between February and May 1970 has indicated that the best frequency spectra, in terms of drift-velocity interpretation, are obtained at altitudes nominally less than 450 km. Although the Stanford radar regularly provides electron density and electron and ion temperature data above 500 km altitude, it should be pointed out that during the sunrise period, electron density and hence signal power is at its lowest value of the day. Several analysis techniques have been considered that show promise of extending the altitude range from its present limit.

B. Measurement Techniques

At any point in the ionosphere there is a spectrum of velocities associated with the fluctuations of the plasma particle densities. In the presence of any illuminating electromagnetic wave, this velocity spectrum will cause, via Doppler shifts, a spectral broadening of the backscattered signal. In the case of a monochromatic (CW) radar signal,

the received signal spectrum will directly represent the fluctuation spectrum of the plasma. In the case of a pulsed radar, the received signal spectrum will depend on both the fluctuation spectrum of the plasma and the frequency spectrum of the transmitted pulse.

If there is any bulk motion of the plasma with a component along the range vector of the radar, this component of motion will give rise to a Doppler shift in the received signal spectrum. For a vertically pointing radar, the relationship between Doppler shift and vertical velocity is given as

$$\Delta f = -2v/\lambda \tag{1}$$

where Δf is Doppler shift in Hz, v is vertical drift velocity in m/s assumed positive upwards, and λ is carrier wavelength in meters. Figure 38(a) illustrates a typical signal spectrum with an exaggerated negative Doppler indicating an upward drift velocity.

Through mixing and sampling, the received signal is processed such that the original spectrum is frequency-limited to a total width of 50 kHz, reversed, and centered at 25 kHz, and this spectrum is normally plotted by computer for study. Figure 38(b) illustrates such a spectrum for the same conditions as Figure 38(a).

As a convenience for the study of Doppler shifts the spectrum illustrated in Figure 38(b) is folded about 25 kHz and then shifted downward 25 kHz as shown in Figure 38(c). To a first approximation the total frequency difference between the spectrum halves is just twice the Doppler shift--that is, if Δf_s is the scaled frequency difference, then

$$\Delta f_s = 2\Delta f = -4v/\lambda \tag{2}$$

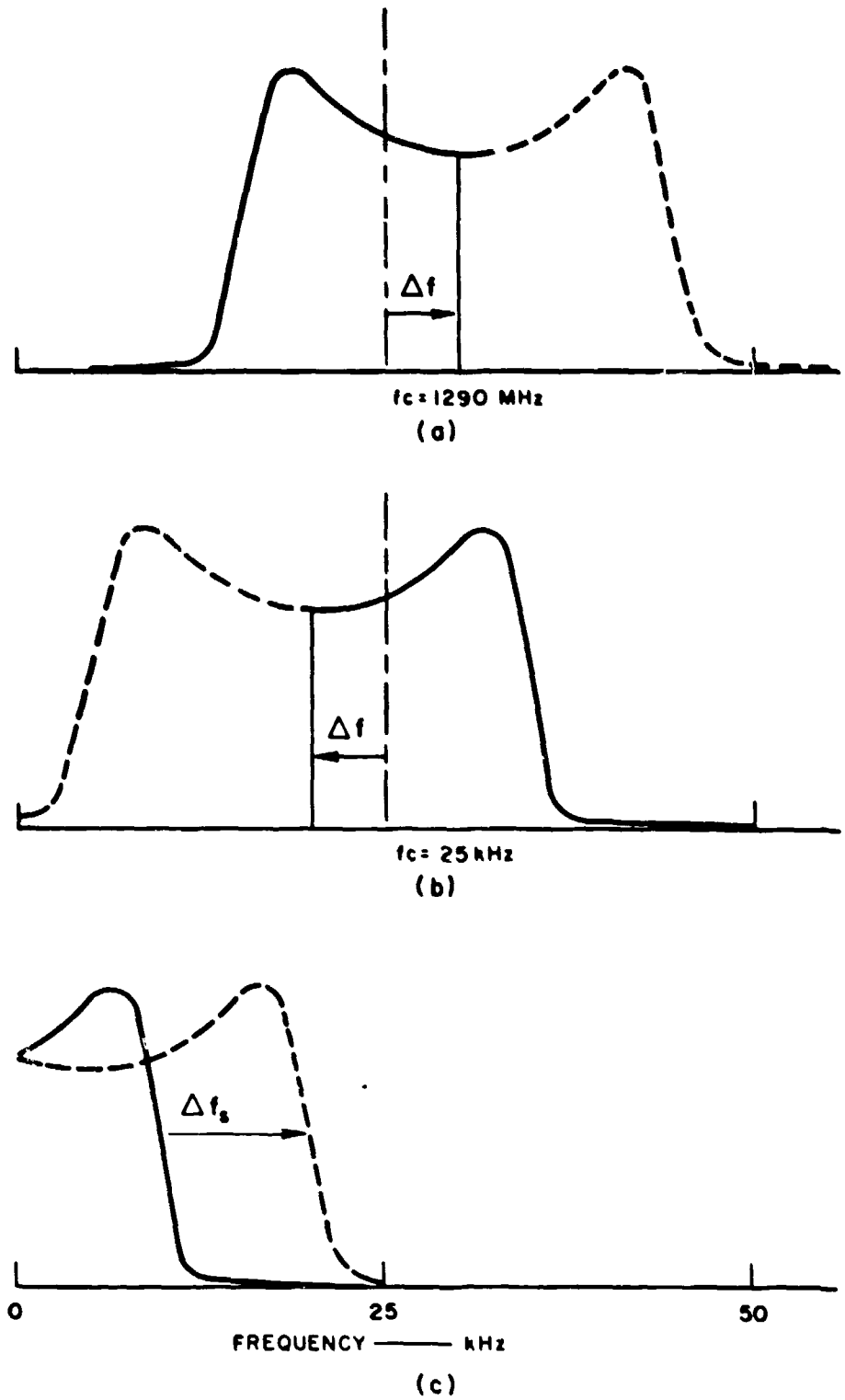

FIGURE 38 ILLUSTRATIVE EXAMPLE OF A DOPPLER-SHIFTED SPECTRUM--
(a) At the Receiver Input; (b) After Band-Limiting and "Aliasing";
(c) After Folding

$$v = \frac{-\Delta f_s(c)}{4f} \quad . \tag{3}$$

For an operating frequency of 1290 MHz, Equation (3) becomes

$$v = 0.5814\ \Delta f_s \ \text{m/s} \quad . \tag{4}$$

In order to be consistent, the shift, or frequency difference, is measured between the limbs of a folded spectrum at an amplitude level of -3 dB, or 50% of the peak amplitude of the entire spectrum. This level is illustrated in Figure 38(c). Under these conditions it is a simple task to automate the computation of drift velocities and, in fact, the velocities illustrated were all computed without the need for any formal spectrum plots such as shown in Figure 38(a), (b), and (c). Figure 39 illustrates a real example of a folded spectrum for measurements made at 1130-1144 UT, 23 April 1970.

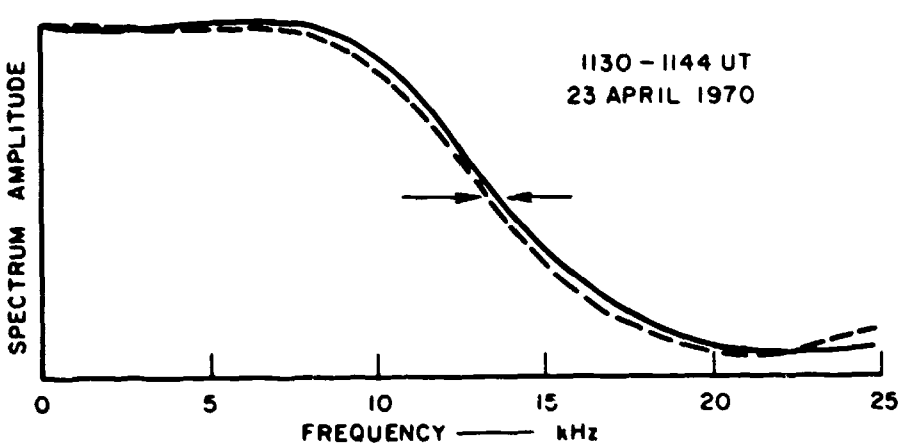

FIGURE 39 EXAMPLE OF A FOLDED SPECTRUM OBTAINED FROM MEASUREMENTS MADE AT 1130-1144 UT, 23 APRIL 1970

C. Observed Velocities

Figures 40-46 illustrate representative results obtained. Each figure represents the sunrise results of a single day and each curve is labeled according to the altitude at which it was obtained. The results for May represent 48-km averages centered at the indicated altitudes; all other results are 37.5-km averages.

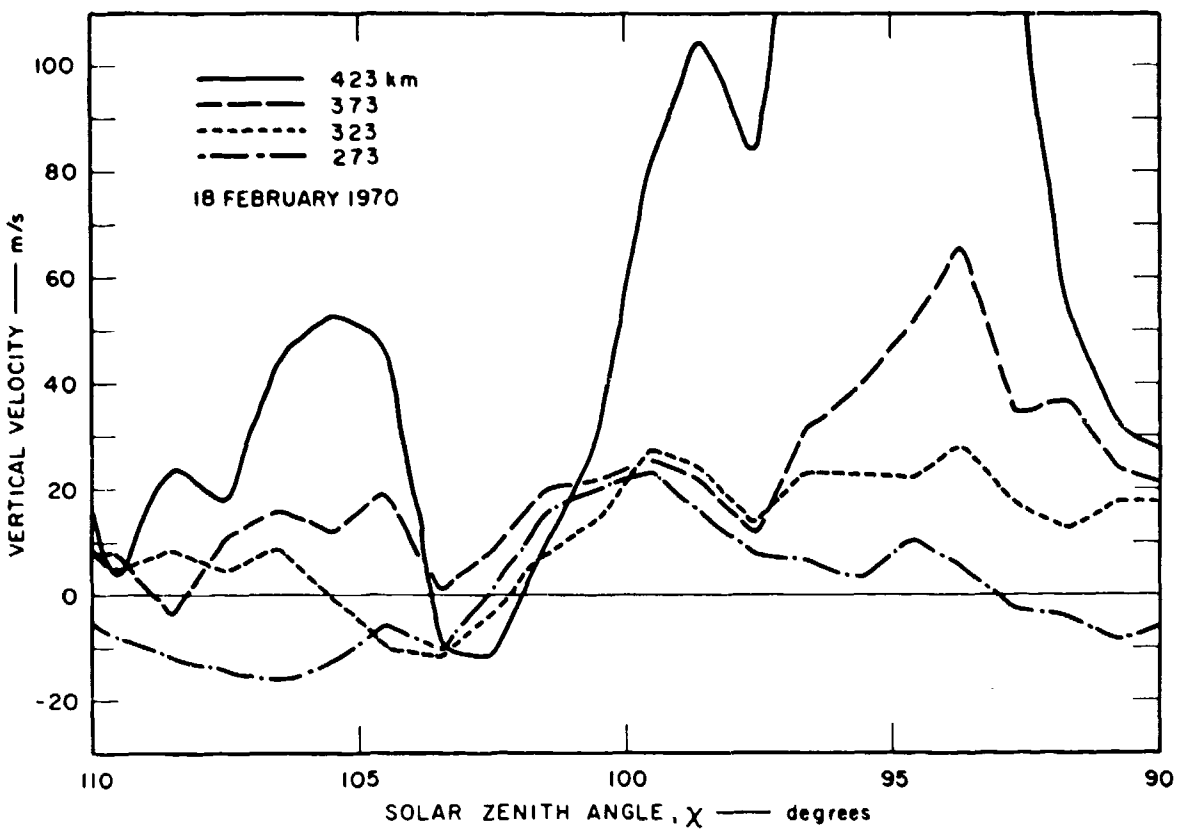

FIGURE 40 VERTICAL DRIFT VELOCITY vs. SOLAR ZENITH ANGLE FOR THE 18 FEBRUARY 1970 SUNRISE

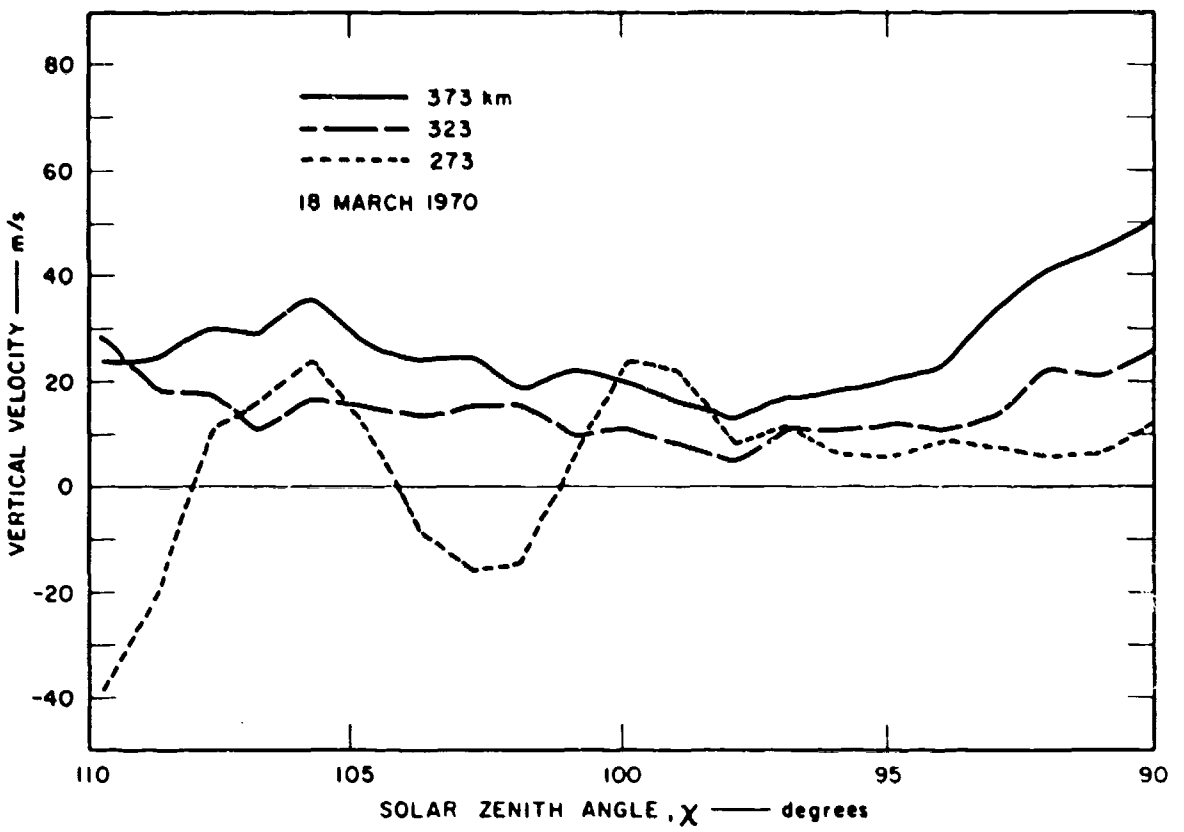

FIGURE 41 VERTICAL DRIFT VELOCITY vs. SOLAR ZENITH ANGLE FOR THE 18 MARCH 1970 SUNRISE

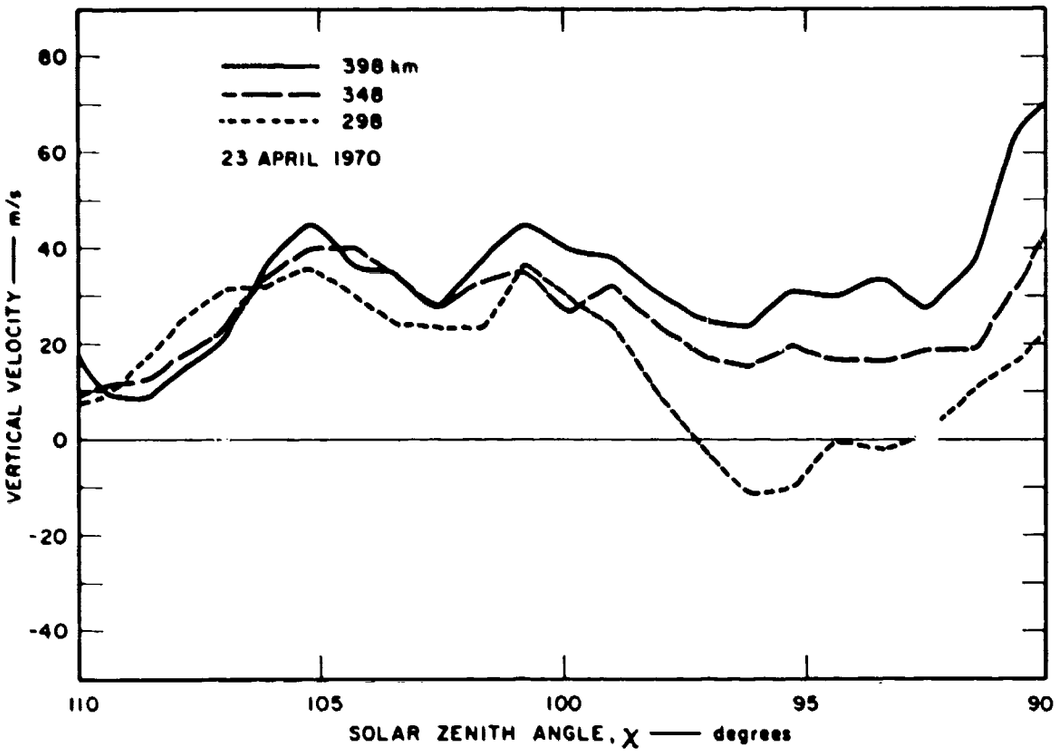

FIGURE 42 VERTICAL DRIFT VELOCITY vs. SOLAR ZENITH ANGLE FOR THE 23 APRIL 1970 SUNRISE

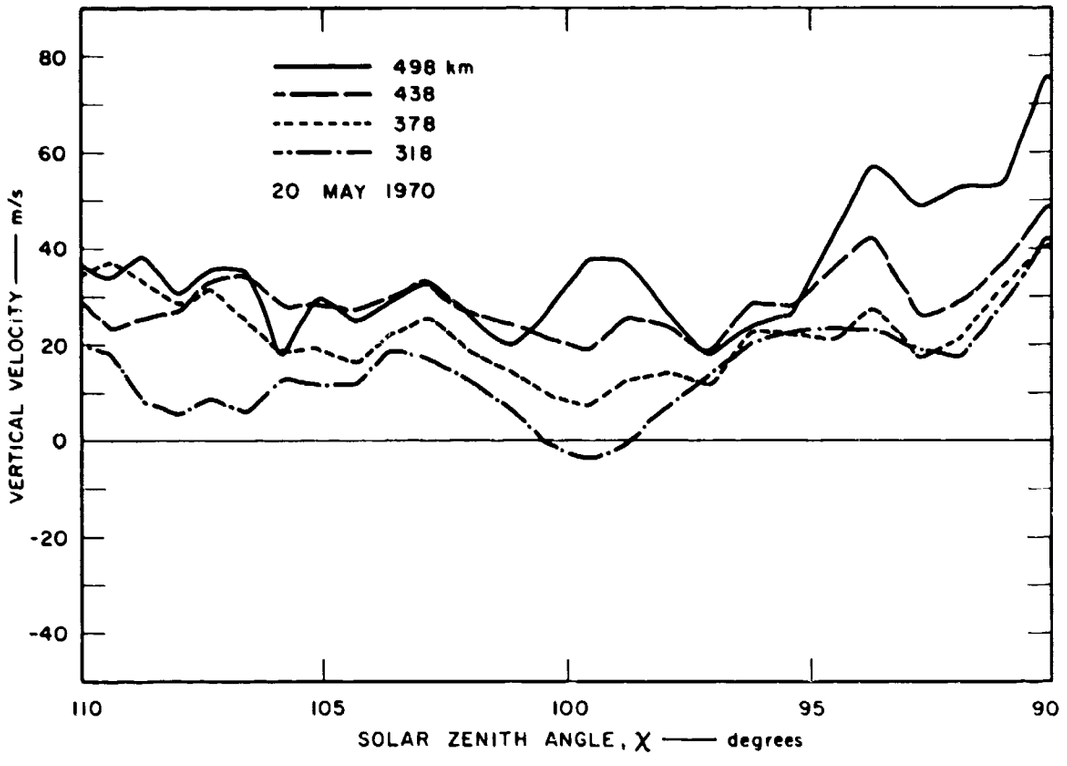

FIGURE 43 VERTICAL DRIFT VELOCITY vs. SOLAR ZENITH ANGLE FOR THE 20 MAY 1970 SUNRISE

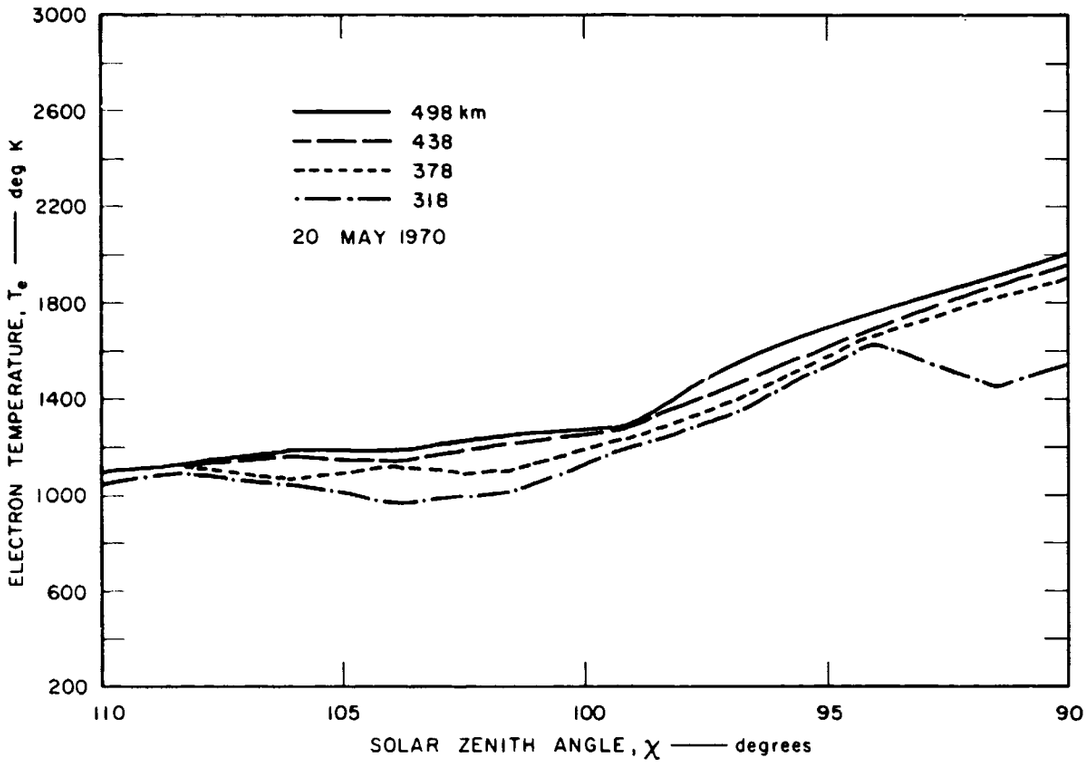

FIGURE 44 ELECTRON TEMPERATURE vs. SOLAR ZENITH ANGLE FOR THE 20 MAY 1970 SUNRISE

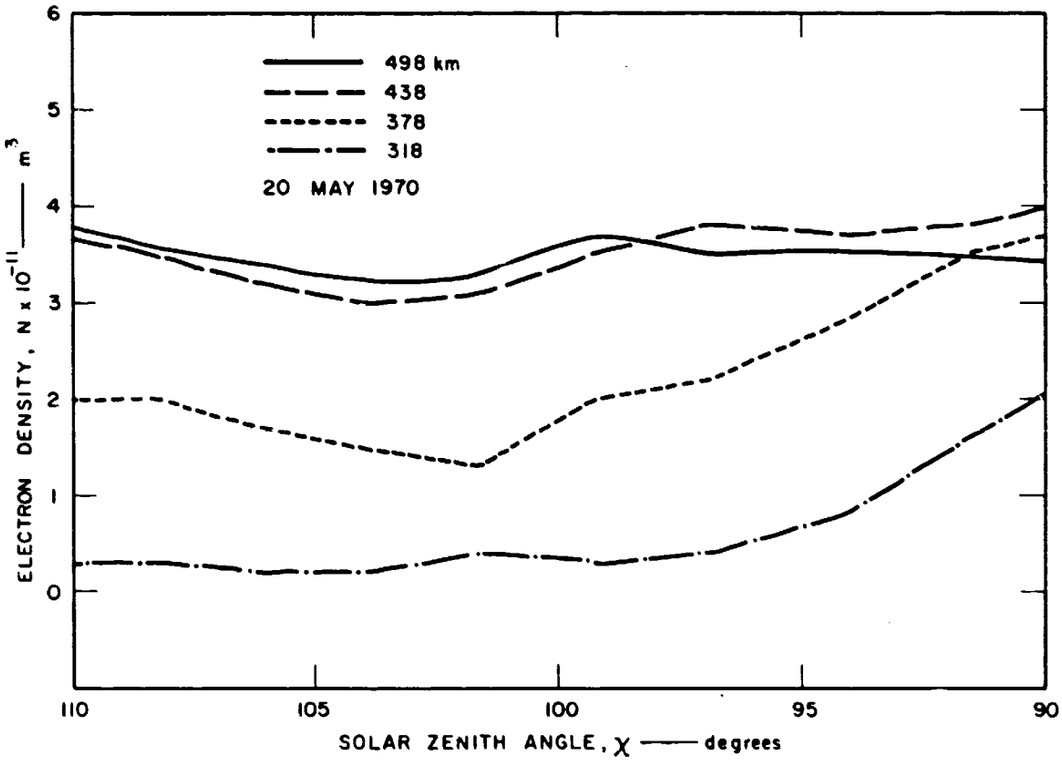

FIGURE 45 ELECTRON DENSITY vs. SOLAR ZENITH ANGLE FOR THE 20 MAY 1970 SUNRISE

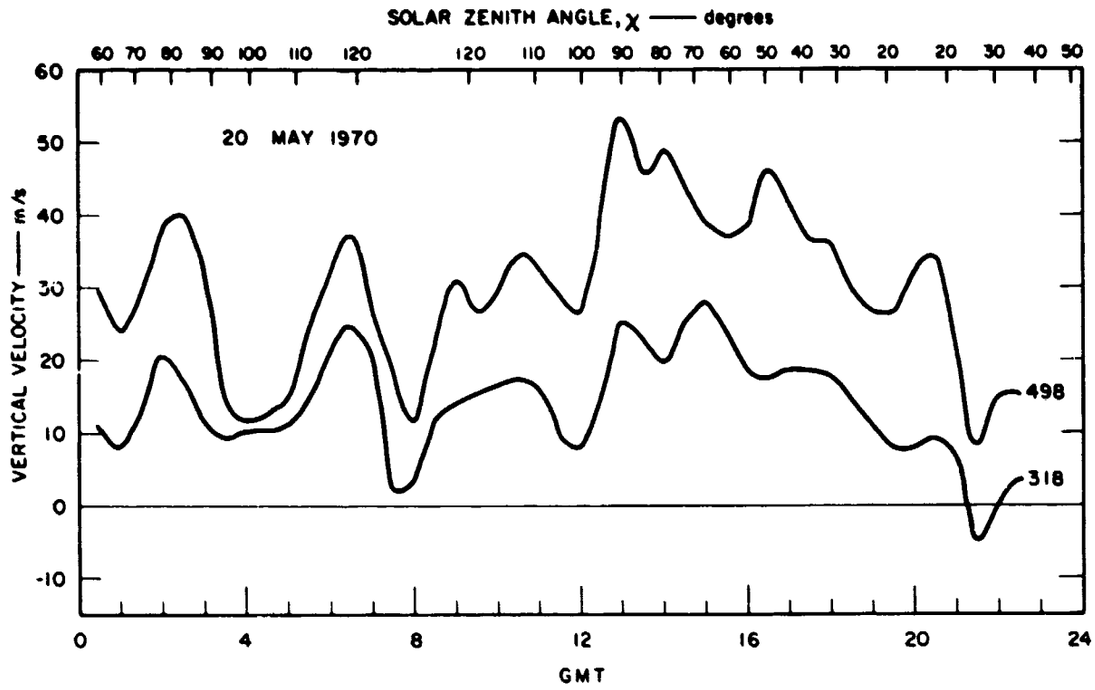

FIGURE 46 VERTICAL DRIFT VELOCITY ENVELOPE LIMITS vs. TIME FOR THE PERIOD 0030-2230 GMT, 20 MAY 1970

The results illustrate wide variations in ionospheric behavior from day to day, and also reveal some consistent systematic behavior.

A characteristic of ionospheric vertical velocities during the sunrise period, as illustrated by Figures 40 through 43, is that upward velocity generally increases with increasing altitude. Although local or short-term disturbances cause some exceptions to this, the trend is unmistakable.

There appear to be two types of responses to sunrise, as shown in the velocity curves. The results obtained for March, April, and May indicate a slow but definite upward flux beginning between about $\chi = 95^\circ$ and $\chi = 97^\circ$, and occurring slightly earlier at the higher altitudes. In contrast to this behavior, the response on February 18 was substantially

different. On this day, the ionization above about 350 km altitude exhibited strong upward flow of short duration, beginning at about $\chi = 101^\circ$ and ending about $\chi = 91^\circ$.

Figures 44 and 45 illustrate, respectively, plots of electron temperature and number density for sunrise conditions on May 20, 1970. It can be seen that electron temperatures at all observed altitudes begin to increase at about $\chi = 102^\circ$. Electron number densities show very little increase at the highest altitudes and a much more pronounced increase at the lower altitudes. In addition, the approximate time of electron-density buildup becomes later with decreasing altitude. The characteristics of observed electron densities during this period are entirely consistent with both other experimental evidence and ionospheric photochemical theory.[23]

A close examination of Figures 43, 44, and 45 suggests that the point of increase of upward velocity ($\chi \approx 97^\circ - 99^\circ$) occurs later than the point of electron-temperature increase ($\chi \approx 101^\circ - 104^\circ$), and approximately coincident with the point of electron-density increase ($\chi \approx 97^\circ - 101^\circ$).

Figure 46 illustrates a 24-hour envelope of velocities for May 20, 1970 between the altitudes 318 km and 498 km. Although not shown explicitly, detailed examination of the data confirms that upward velocities increase consistently with increasing altitude; thus the lower bound of the envelope is the velocity profile at 318 km, and the upper bound is the velocity profile at 498 km. Solar zenith angle is scaled along the abscissa in correspondence with universal time, and even with the diminished detail of the 24-hour plot, the sudden increase in upward velocity is seen to take place at sunrise. An interesting consequence of the results illustrated by Figure 46 is that the vertical flux appears to have a net upward value when averaged over a 24-hour period.

At present, these effects have only been observed and no attempt has been made to explain the observations in terms of ion production, plasma heating, etc. Both Watt[21] and Evans[20] have considered predawn thermal expansion effects at higher altitudes, and Evans[20] has also observed a large-velocity effect at 450-km altitude similar to our February 18 observations. The notion of an apparent non-zero average flux has been considered only recently, and some speculation about it exists although a satisfactory explanation has not yet been given for this effect.

V PARTIAL SOLAR ECLIPSE MEASUREMENTS

A. General

This section reports observations of electron density, and electron and ion temperatures, made during the 11 September 1969 and 7 March 1970 partial solar eclipses at Stanford, California. Vertical drift velocities and gravity-wave effects are also considered for the 7 March eclipse. The technique used for these measurements was the incoherent-backscatter method. Electron-density profiles were obtained over a 300-to-400 km altitude range at 15-minute intervals for at least an hour preceding each eclipse and for several hours following the eclipse. Profiles over the same altitude range with the same time resolution were also taken on the day before each eclipse and on the day after the eclipse for use as background control data.

An exception to this procedure was necessary on 8 March 1970. An unusually large magnetic storm occurred on this date, and the resulting disturbed ionosphere was not useful as a background comparison for eclipse measurements A synoptic study of magnetic storm effects would, of course, be interesting in its own right. Unfortunately, a failure in the transmitter's intermediate power amplifier occurred at 1721 GMT on 8 March and no data are available after that time. As far as the 7 March eclipse is concerned, the only useful control day for background data was 6 March.

Electron and ion temperatures were deduced from the backscattered spectra for all six days at 50-km intervals. For many of the measurements, ground clutter was apparent in both the power profiles and spectra at heights below about 200 km, thus making it impossible to scale these

measurements. Also, at times and altitudes when the density was low, the spectra were too noisy to scale temperatures accurately. However, for most of the F-region, usable measurements were obtained and the main eclipse effects--namely, reduced electron densities and reduced electron temperatures--were evident at almost all altitudes above 200 km for two to three hours following the eclipse.

Eclipse effects have been reported before.[5] The main effects of an eclipse as reported earlier are as follows:

(1) Electron densities tend to decrease at all altitudes, or if the eclipse occurs during sunrise when electron density is normally increasing the rate of increase is substantially slowed down during the period of the eclipse.

(2) Electron temperatures decrease during the period of the eclipse.

(3) The height of the maximum of the electron-density profile decreases during the period of the eclipse.

(4) Recovery time of the ionosphere following an eclipse appears to be of the order of two to three hours.

In the present report two eclipses are considered and for each the same general trends seem to appear. Because these observations have been reported before, they will not be dealt with in detail here but simply presented and pointed out. Three new aspects will be considered here, however. The first aspect is that of the possibility of gravity waves directly associated with the eclipse. Chimonas and Hines[24] have predicted that gravity waves might be caused by an eclipse, and an attempt has been made here to verify their prediction. The second aspect is the consideration of vertical drift velocities for the eclipse of 7 March 1970. Recent improvements in the radar equipment and processing techniques have made it possible to determine drift velocities associated with the plasma along the range vector of the radar. For most cases, and in the particular case of the eclipse observations, the radar vector

was vertical and thus information has been obtained about vertical drift velocities for both the eclipse day and the control day (6 March). The third aspect associated with these eclipse observations is that the period of the 7 March eclipse was one of very high magnetic activity. The day of 8 March was considered a period of a magnetic storm, but, in fact, the three-hour K_p index experienced a substantial increase during the last six hours of 6 March and remained high through the first six hours of 9 March. The data for these three days, because of the overlapping phenomena, are therefore very difficult to interpret. Nevertheless the observations will be presented and discussed.

B. Electron Densities, Electron Temperatures, and Ion Temperatures

Figures 47 through 53 illustrate percent obscuration and contours of electron density, electron temperature, and ion temperature taken directly from the data for the two eclipse days and the four control days. Generally electron densities and electron temperatures behave in a predictable manner, as described above. Electron-density variations for the September eclipse are rather mild in comparison to those during the March eclipse, but the September eclipse effects can be easily seen in the electron-temperature contours as shown in Figure 50.

It is well known that ion-temperature variations tend to be very sluggish in comparison with electron temperature variations. This is seen regularly under sunrise conditions. Under eclipse conditions the same trend is apparent. There appears to be some variation in ion temperatures that is caused by the eclipse, but the variations are far less pronounced than the variations of electron temperatures during the same period.

Figures 54 and 55 summarize electron-density effects associated with the eclipses. It can be seen, for instance, that during the eclipse, electron densities at the peak of the layer are depressed from normal

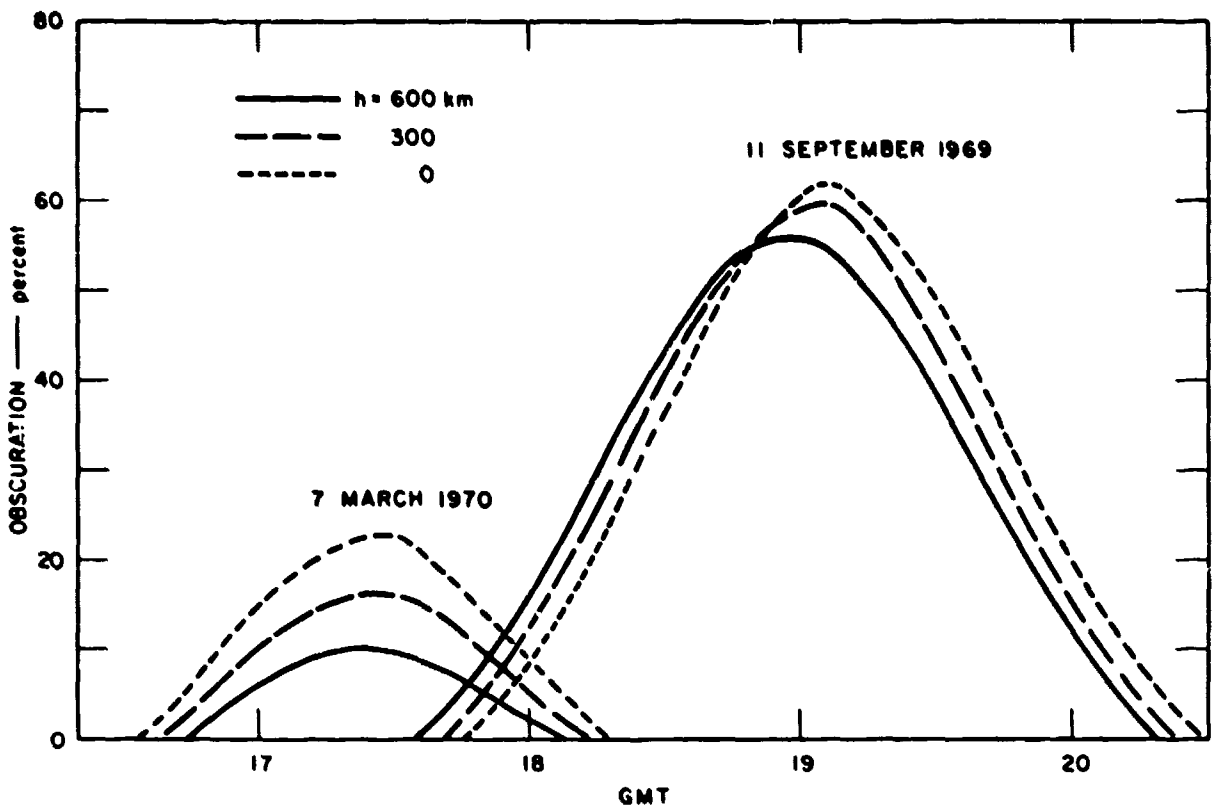

FIGURE 47 PERCENT OBSCURATION AS A FUNCTION OF TIME FOR THE ECLIPSES OF 11 SEPTEMBER 1969 AND 7 MARCH 1970 AND FOR ALTITUDES OF 0, 300, AND 600 km

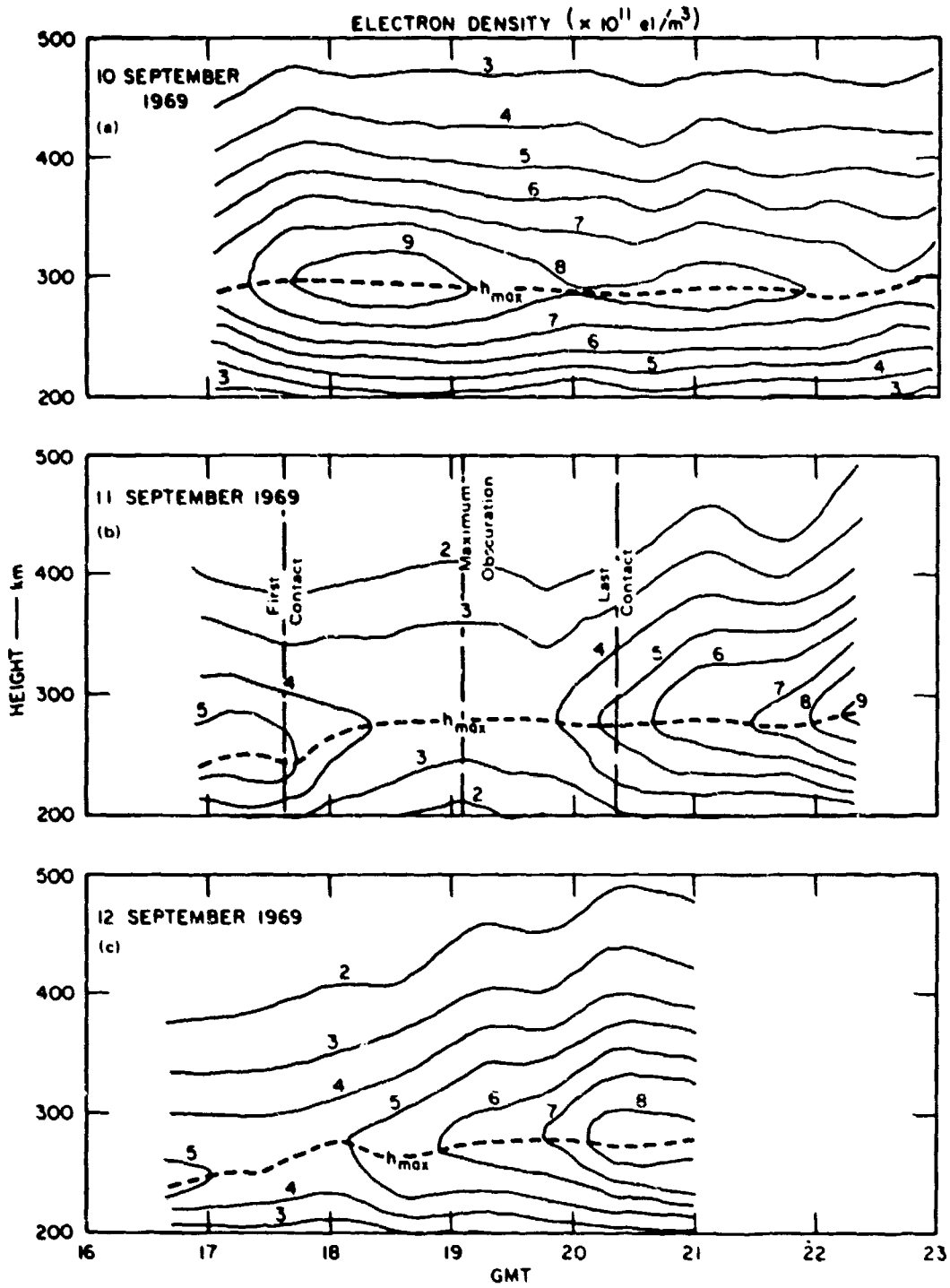

FIGURE 48 ELECTRON DENSITY CONTOURS AS FUNCTIONS OF ALTITUDE AND TIME FOR (a) 10 September; (b) 11 September; (c) 12 September 1969

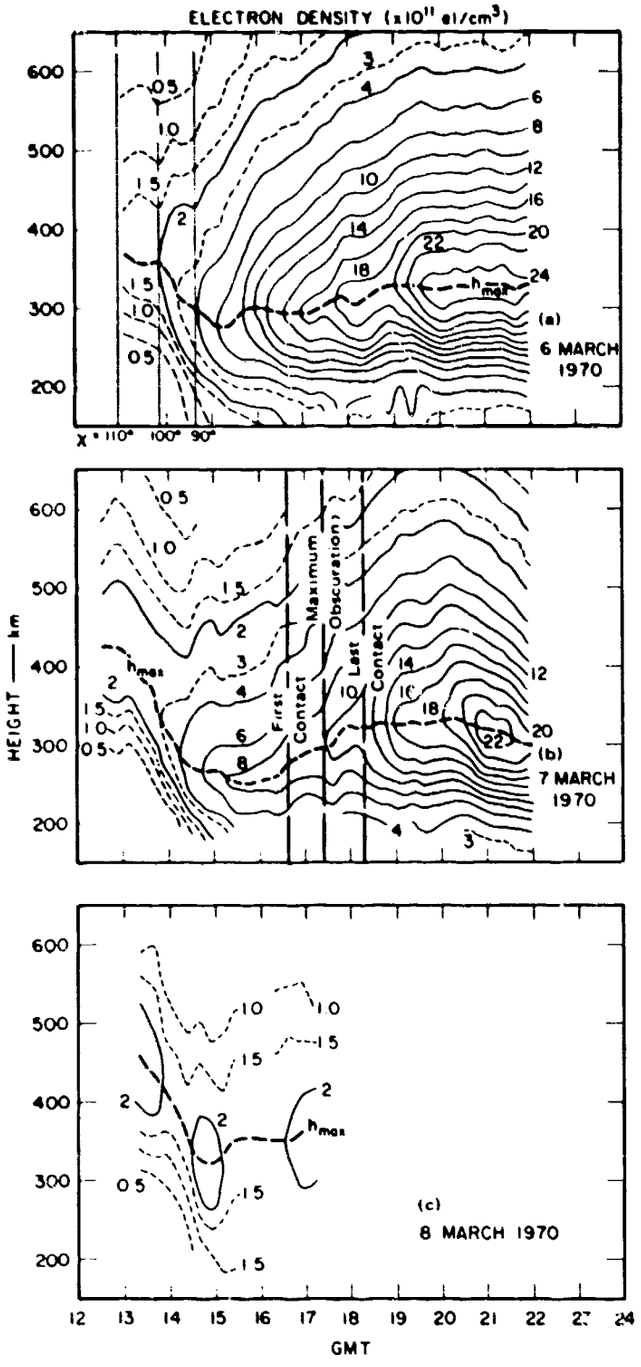

FIGURE 49 ELECTRON DENSITY CONTOURS AS FUNCTIONS OF ALTITUDE AND TIME FOR (a) 6 March; (b) 7 March; (c) 8 March 1970

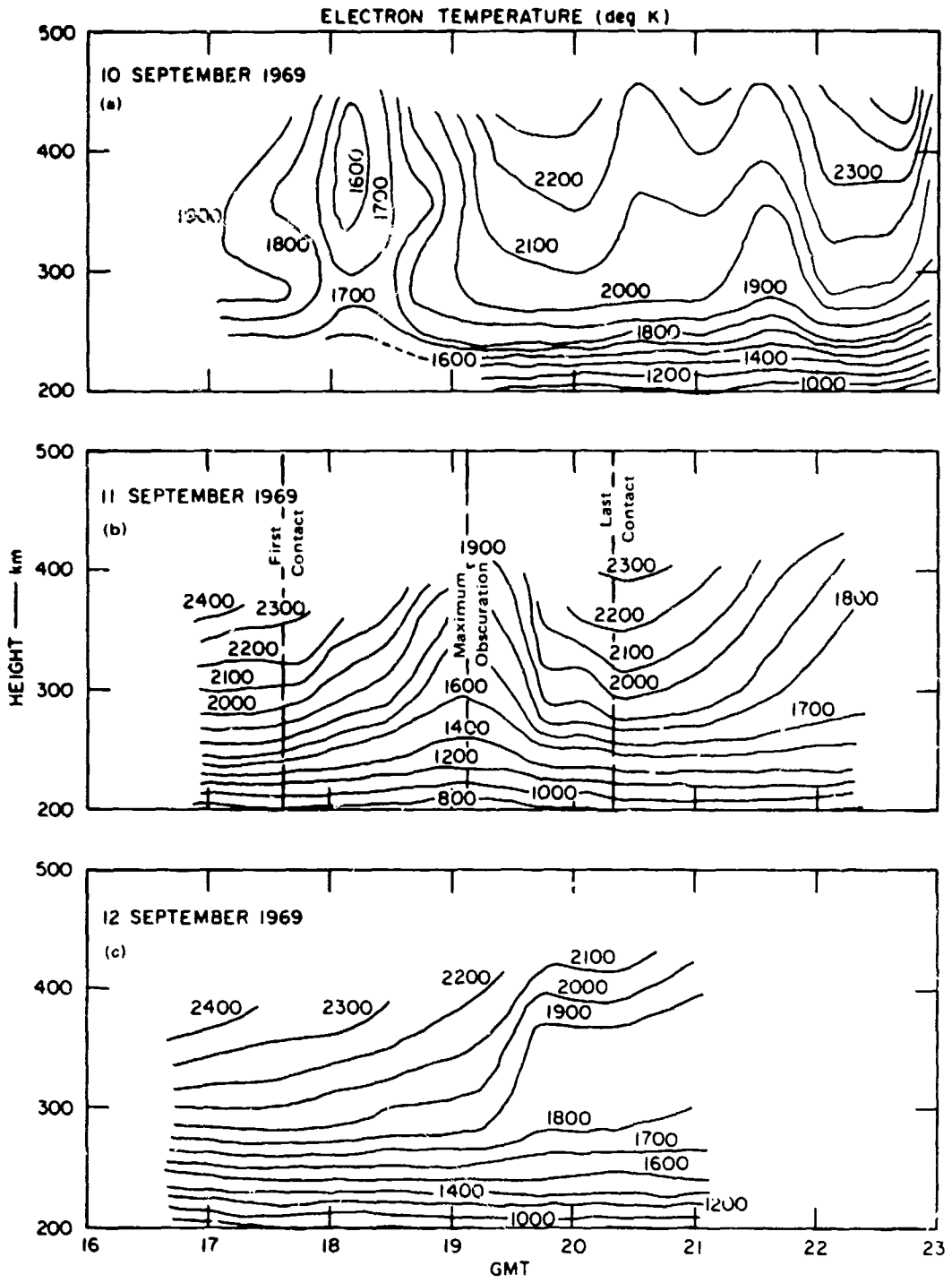

FIGURE 50 ELECTRON TEMPERATURE CONTOURS AS FUNCTIONS OF ALTITUDE AND TIME FOR (a) 10 September; (b) 11 September; (c) 12 September 1969

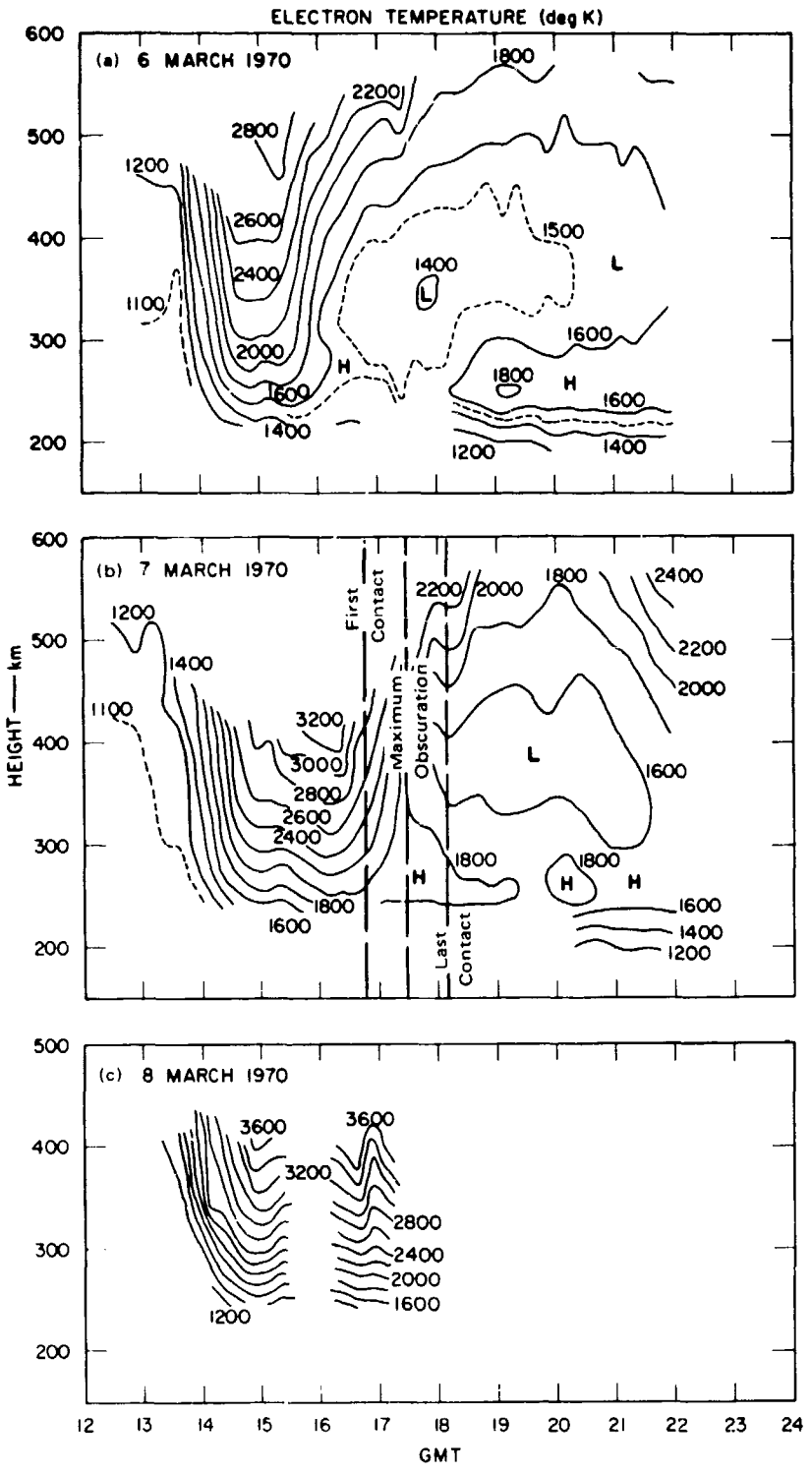

FIGURE 51 ELECTRON TEMPERATURE CONTOURS AS FUNCTIONS OF ALTITUDE AND TIME FOR (a) 6 March; (b) 7 March; (c) 8 March 1970

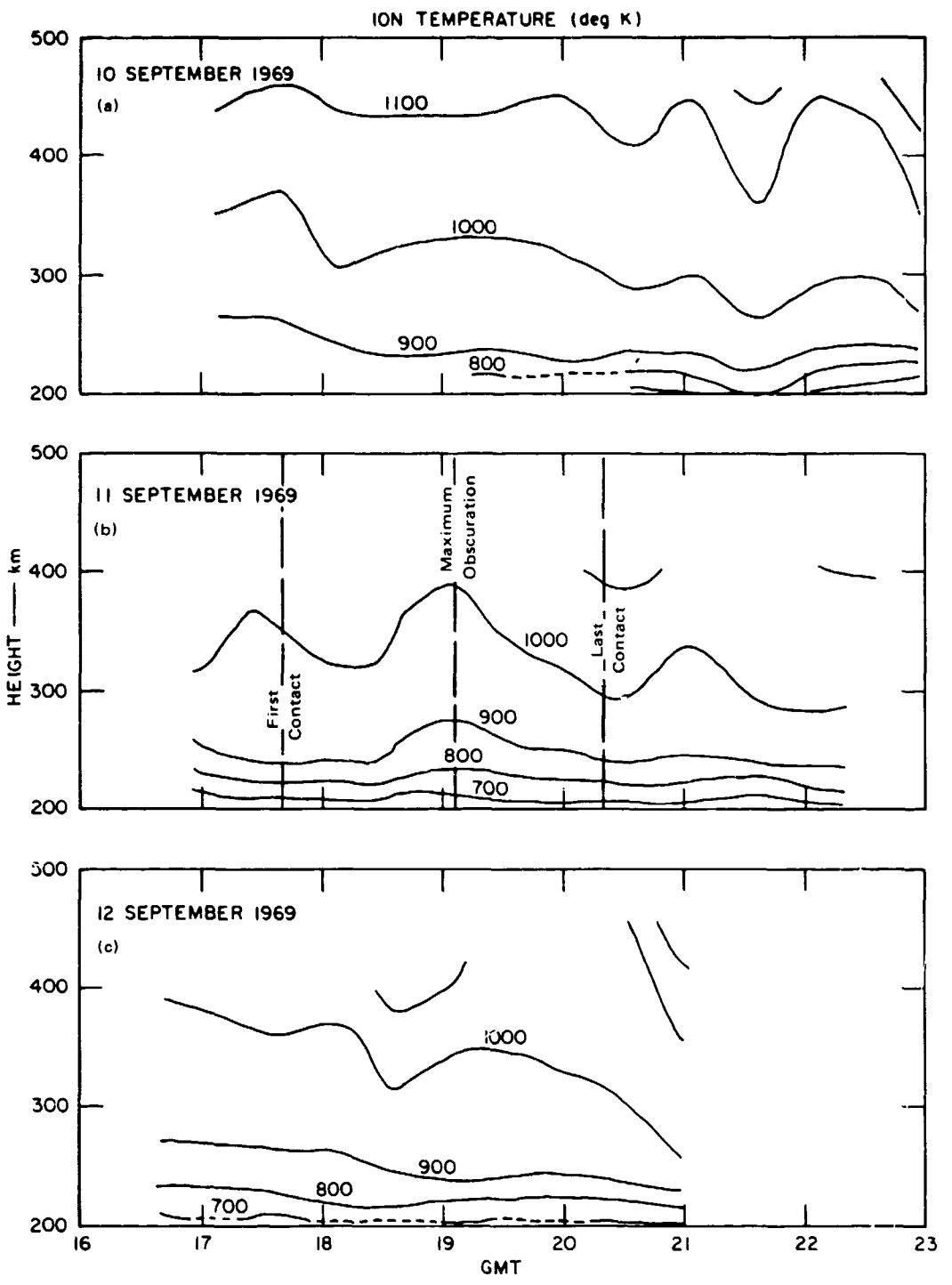

FIGURE 52 ION TEMPERATURE CONTOURS AS FUNCTIONS OF ALTITUDE AND TIME FOR (a) 10 September; (b) 11 September; (c) 12 September 1969

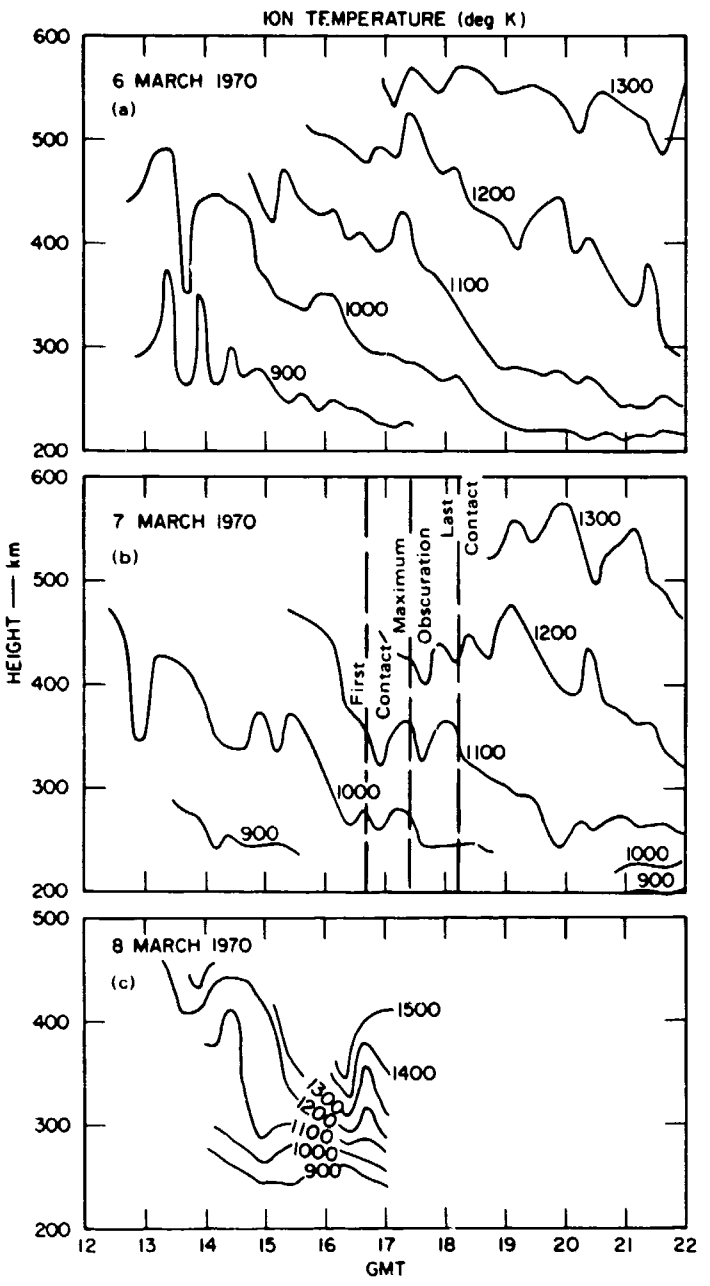

FIGURE 53 ION TEMPERATURE CONTOURS AS FUNCTIONS OF ALTITUDE AND TIME FOR (a) 6 March; (b) 7 March; (c) 8 March 1970

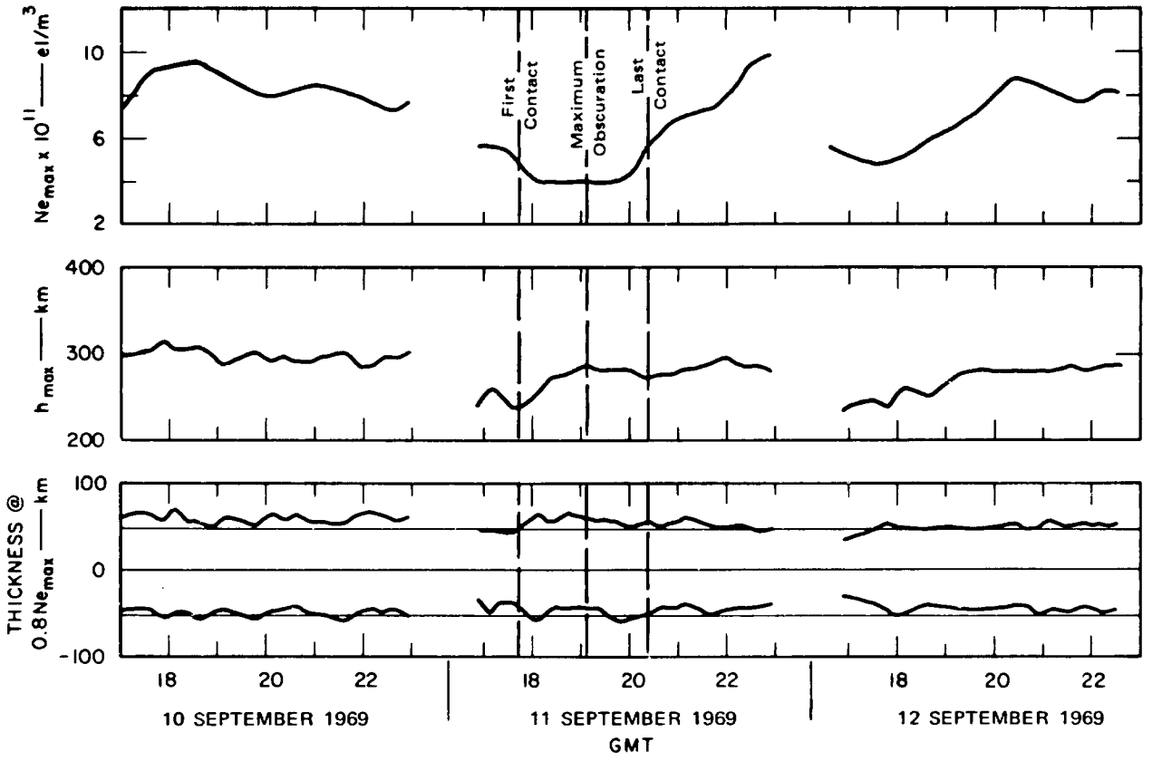

FIGURE 54 F-LAYER PARAMETERS Ne_{max}, h_{max}, AND THICKNESS vs. TIME FOR 10, 11, AND 12 SEPTEMBER 1969

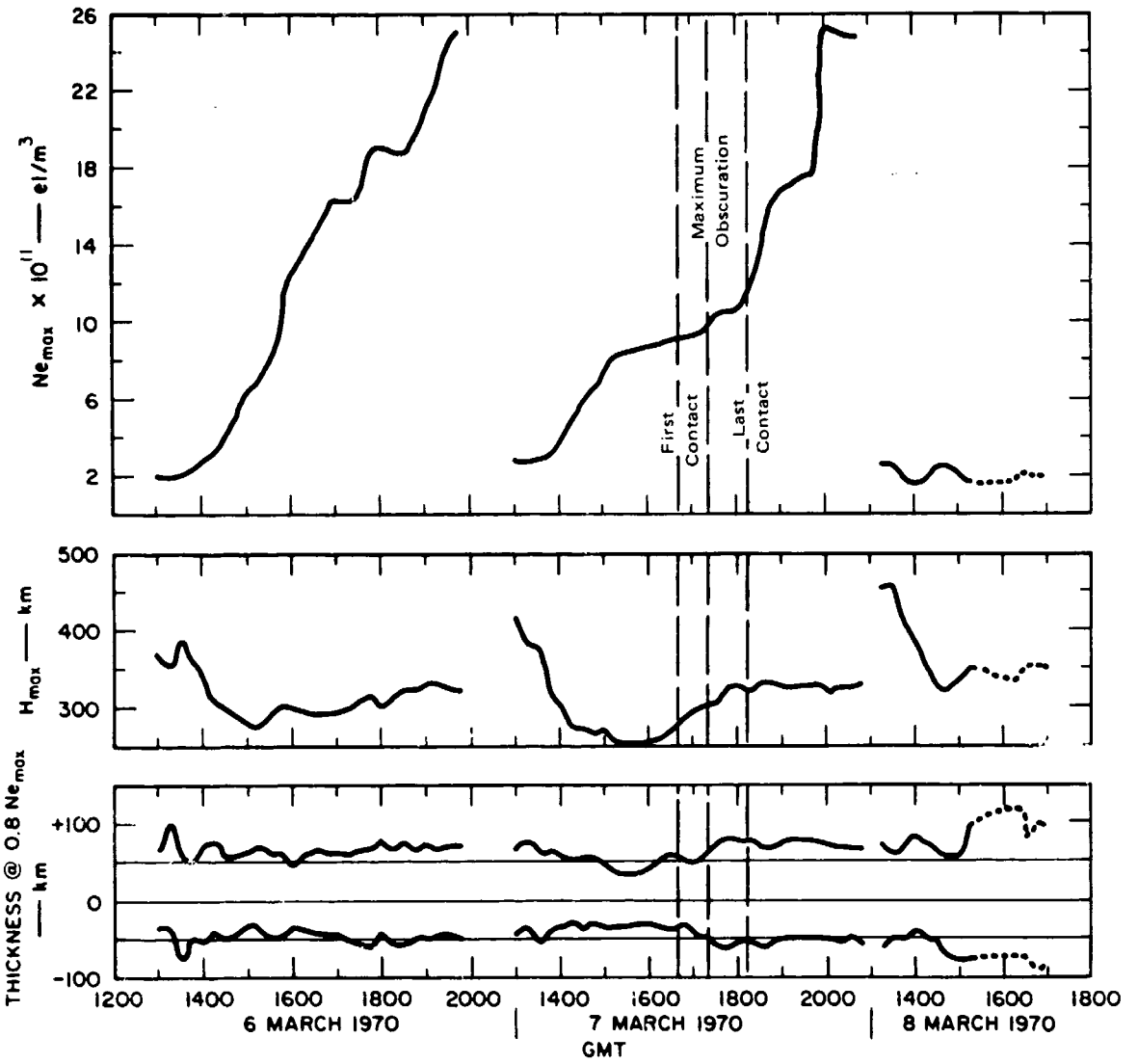

FIGURE 55 F-LAYER PARAMETERS Ne_{max}, h_{max}, AND THICKNESS vs. TIME FOR 6, 7, AND 8 MARCH 1970

conditions, the height of the maximum decreases, and the thickness of the layer (as illustrated here, the distance between the 80 percent of maximum density altitudes) decreases slightly. For the March eclipse, the control day of 8 March is seen to be useless as a "normal" day. As mentioned earlier, the data are incomplete and even where data are taken they appear to be very unusual, most probably due to the presence of the magnetic storm.

C. Eclipse-Induced Gravity Waves

In a previous report[5] consideration was given to the possibility that the presence of gravity waves could be detected through Thomson scatter techniques, and observations seemed to indicate the presence of some wave-like structure propagating downward. Chimonas and Hines[24] predicted that gravity waves should be induced by an eclipse. We therefore have considered this possibility for the March eclipse using the same technique discussed in the previous report.[5] Figures 56 and 57 illustrate the results obtained for 6 March and 7 March 1970. Plotted are profiles representing constant percentage of maximum density. Such a plot tends to normalize all density values to the value of maximum density in the layer and thus eliminate the effect of the variations that tend to affect all of the layer equally. A careful plot of these profiles reveals that certain deviations appear at all altitudes. Some of the deviations considered are identified by the dashed lines, and it can be seen that the deviations do occur later at lower altitudes, suggesting a downward propagation of wave energy. However, in order to verify the prediction it would be necessary to show significantly more evidence for gravity waves on the day of the eclipse than on the control day, and this is not observed. If the deviations observed and identified by the dashed lines do indeed signify gravity waves, then it would appear

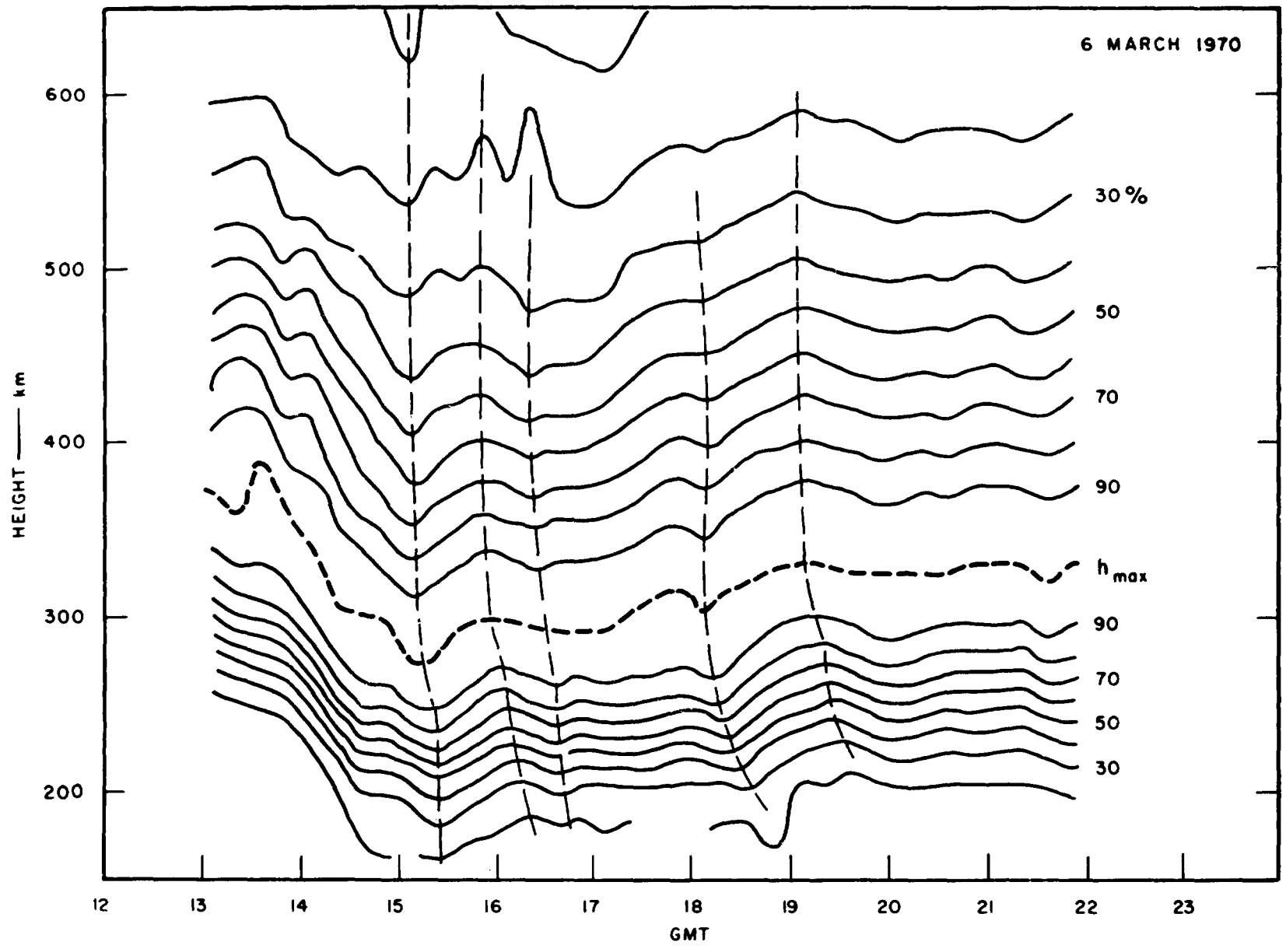

FIGURE 56 CONTOURS OF CONSTANT PERCENTAGE OF Ne_{max} AS FUNCTIONS OF ALTITUDE AND TIME FOR 6 MARCH 1970

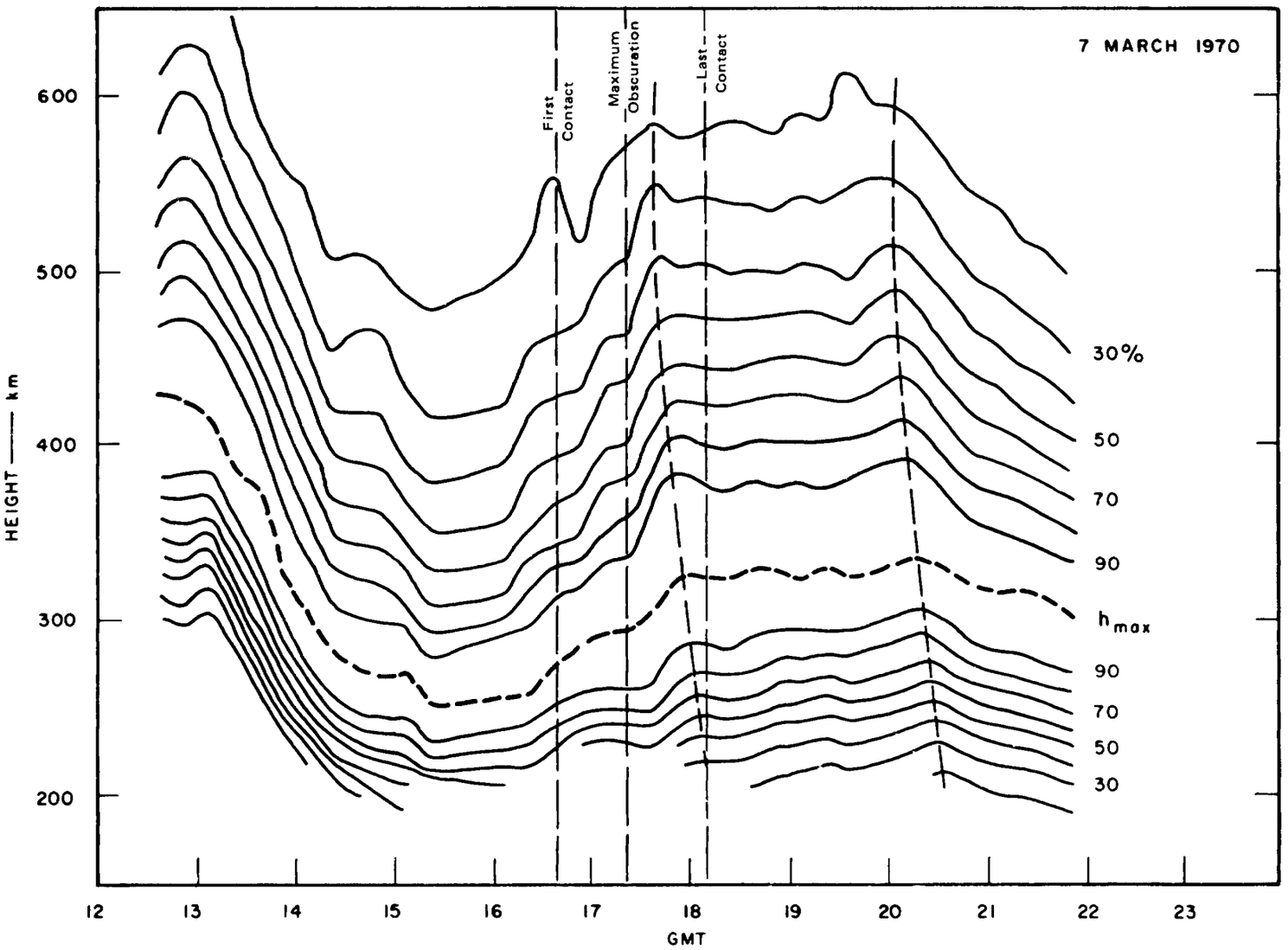

FIGURE 57 CONTOURS OF CONSTANT PERCENTAGE OF Ne_{max} AS FUNCTIONS OF ALTITUDE AND TIME FOR 7 MARCH 1970

either that gravity waves are not more likely to appear as a result of a solar eclipse or that the particular eclipse of 7 March was not complete enough to produce the predicted effects.

D. Eclipse-Induced Drift Velocities

As part of the study of phenomena associated with a partial solar eclipse, an attempt was made to determine whether or not variations in vertical drift velocity of the plasma could be attributed to the eclipse of 7 March 1970.

Determination of vertical plasma drifts was discussed in Section IV, where it was shown that in the upper F-region and upward drift of the plasma can be associated with sunrise. It was also shown that a wide day-to-day variation exists in observed drift velocities.

Figures 58 and 59 illustrate envelopes of observed vertical drift velocity for periods of interest during 6 March and 7 March 1970. The envelopes illustrate maximum and minimum vertical velocity limits observed during the periods of interest. As discussed in Section IV, observed velocities tend to increase monotonically with increasing altitude so that the upper and lower curves might be said to represent observed velocities at altitudes of 448 km and 298 km respectively.

Because of the wide day-to-day variations in drift velocity known to exist in the upper F-region, it is difficult to attribute observed differences in the 6 March and 7 March results to the 7 March eclipse.

There are two features of the velocity profiles on 7 March that are interesting and deserve comment, however. Firstly it can be seen that the upward velocity present at all altitudes just prior to the beginning of the eclipse is generally increasing with time until just after obscuration begins, when a sudden decrease takes place. It appears

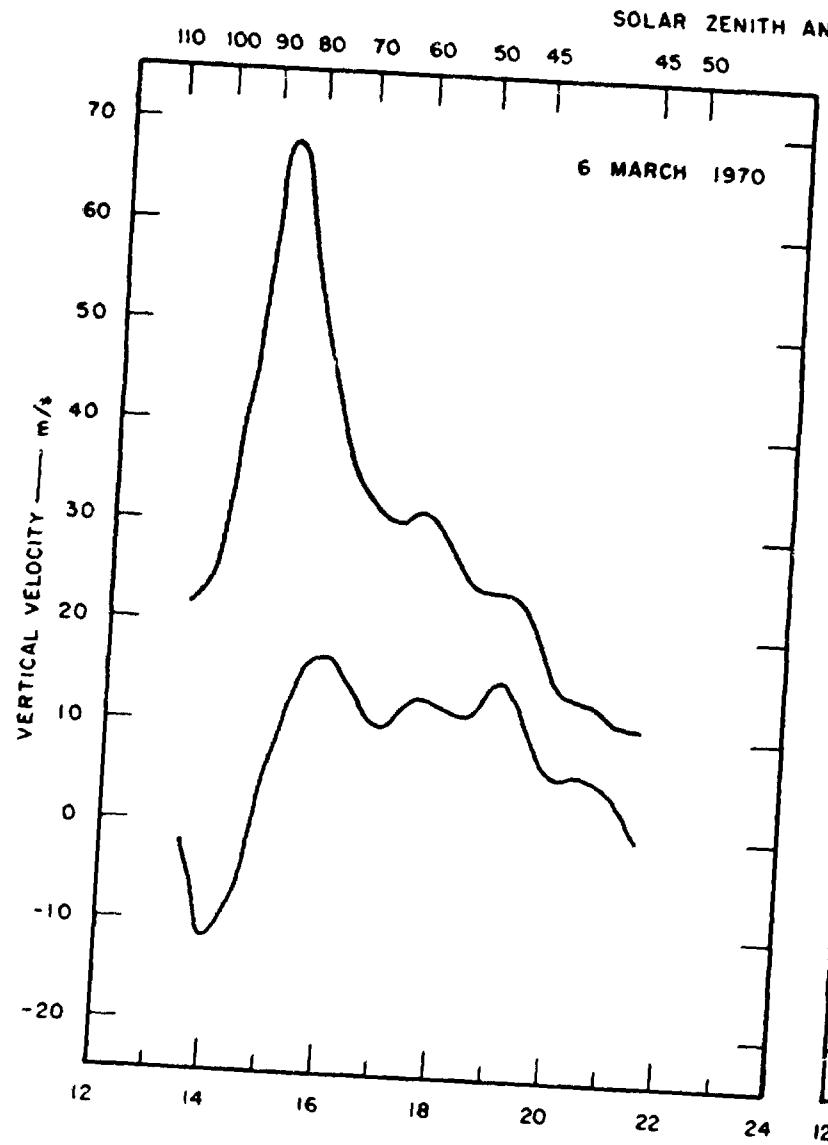

FIGURE 58 VERTICAL-DRIFT-VELOCITY-ENVELOPE LIMITS vs. TIME FOR THE PERIOD 1330-2130, 6 MARCH 1970

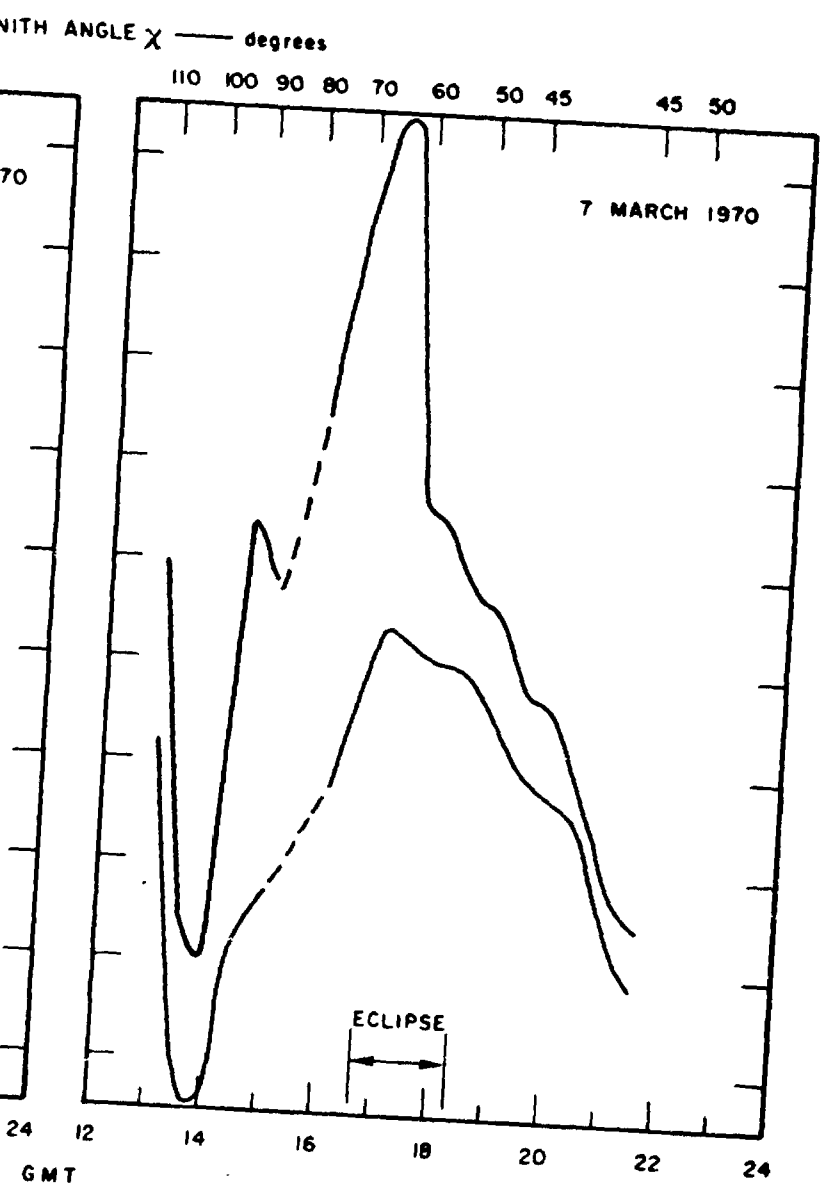

FIGURE 59 VERTICAL-DRIFT-VELOCITY-ENVELOPE LIMITS vs. TIME FOR THE PERIOD 1300-2130, 7 MARCH 1970

from this that the ambient velocity profile has been affected by the eclipse-associated cooling of the ionosphere, resulting in a thermal contraction and a subsequent tendency toward diminishing the upward flow.

The second curiosity associated with the 7 March observations is that, following the period of obscuration, upward velocities continue to decrease steadily until finally, by 2100 GMT, a net downward flux begins at all observed altitudes more than two hours after the eclipse. This velocity trend is interesting because it differs from the other observed trends occurring at the same time of day. This observed velocity trend may or may not be significant in terms of eclipse effects, since, as was pointed out, the entire period of observation was one of high geomagnetic activity.

VI CONCLUSIONS AND RECOMMENDATIONS

This report has described the results of several ionospheric studies carried out over the past year. A large amount of data, collected over a three-year period, has been collated and analyzed to provide a description of the ionosphere's diurnal and seasonal behavior. During this time period, a number of improvements to the radar system and data-processing system have been made, resulting in an order-of-magnitude reduction in data-processing time and a two-to-three-fold improvement in measurement accuracy.

Section II reviews the behavior of the daytime electron and ion temperatures in the F-layer. These ionospheric parameters are correlated with various solar-geophysical disturbance indices. No significant correlations were found. Large day-to-day variations in height, electron density, and electron temperature appear to be typical of F-layer behavior over Palo Alto.

The behavior of the ionosphere at sunrise and sunset has been studied and described. Typically, sunrise is characterized by an increase in the electron temperature, followed by a decrease in h_{max}, followed by an increase in N_{max}. Seasonal variations of these parameters are shown. Sunset behavior is characterized by a decrease in both electron density and temperature. During the winter, these effects are coincident. However, in the summer the temperature decrease occurs significantly earlier than the density decrease.

The maximum density of the F-layer is typically greatest in winter, and smallest in summer. During the winter, N_{max} varies by an order of magnitude from day to night, while during the summer the day-to-night variation may be only a factor of two or three.

Seasonal variations of the height of maximum density have been studied. The F-layer is generally highest in summer and lowest in winter. During the course of a 24-hour period, h_{max} undergoes the greatest excursions at the equinoxes, and the least at the solstices.

The behavior of the ionosphere during the course of two partial solar eclipses has been studied and reported. In general, the eclipse effects are characterized by decreases in electron density and temperature.

Vertical velocity measurements, made for the first time in 1970, are reported here. A general upward motion of the ionospheric plasma at sunrise was found to exist. Vertical velocity measurements also made during the 7 March 1970 eclipse indicate that an eclipse occurring near sunrise may cause a diminution of the normal upward flux associated with sunrise.

For the past several years the ionosphere over Palo Alto has been studied, using the incoherent-scatter techniques. Other incoherent-scatter radars (Millstone, Arecibo, St. Santin) are located, as is ours, so as to study the midlatitude ionosphere. The radar at Jicamarca, Peru has been used to study the equatorial ionosphere. No incoherent-scatter facility has yet been geographically located so that it can study the very interesting auroral ionosphere. DASA has recently initiated moving the Project 617 radar to the vicinity of College, Alaska; a location beneath the region of maximum visual auroral occurrence. The relocation f the radar to the auroral zone will allow the radar to be operated at a geographic location where the natural ionosphere more closely approximates the disturbed ionosphere caused by

and following a high-altitude nuclear detonation. In addition, many scientifically new and interesting studies can be made on the unique auroral ionosphere. Among the studies that can be envisioned for the radar are:

(1) F-region behavior during an auroral disturbance when conventional HF measurement techniques cannot be made due to absorption, blanketing, sporadic E, etc.

(2) Morphology of auroral ionosphere.

(3) Electron-loss processes and loss coefficients in the E region.

(4) Electron-density increases in the ionosphere produced by the aurora.

(5) Auroral sporadic-E ionization measurements.

(6) Electron density and collision frequency in the D region during auroral and polar cap events.

(7) Transition from normal incoherent scatter to scatter from field-aligned irregularities.

(8) Non-equilibrium electron-velocity-distribution measurements using observation of the plasma lines.

However, as with the application of any new technique in a complicated environment for the first time, the most exciting studies will probably be discovered during the operation of the radar. We recommend that the radar relocation be carried out and completed as soon as possible.

REFERENCES

1. J. Fejer, "Scattering of Radio Waves by an Ionized Gas in Thermal Equilibrium," Can. J. Phys., Vol. 38, pp. 1114-1133 (1960).

2. J. P. Dougherty and D. T. Farley, "A Theory of Incoherent Scattering of Radio Waves by a Plasma," Proc. Roy. Soc. (London), Vol. A259, pp. 79-99 (1960).

3. T. Hagfors, "Density Fluctuations in a Plasma in a Magnetic Field with Applications to the Ionosphere," J. Geophys. Res., Vol. 66, pp. 1699-1712 (1961).

4. R. I. Presnell, ed., "Electron Backscatter Radar," Final Report, Contract DA-49-146-XZ-259, DASA Report 1823, SRI Project 4740, Stanford Research Institute, Menlo Park, California (1966).

5. M. J. Baron, H. F. Bates, E. J. Fremouw, and J. Petriceks, "Electron Backscatter Research," Final Report, Contract 01-67-C-0019, DASA Report 2088, SRI Project 6291, Stanford Research Institute, Menlo Park, California (1968).

6. M. J. Baron, ed., "Electron Scatter Research Using the Project 617 Radar," Final Report, Contract 01-67-C-0019, DASA 2088-II, SRI Project 6291, Stanford Research Institute, Menlo Park, California (1969).

7. M. J. Baron, et al., "Project 617 Radar--Readiness Achievement Program, Part A--Data Processing and Analysis," Final Report Part A, Contract 01-67-C-0019, SRI Project 6291, Stanford Research Institute, Menlo Park, California (1970).

8. H. F. Bates, and M. J. Baron, "F-Region Temperatures Over Palo Alto in 1967 and 1968," J. Geophys. Res., Vol. 74, p. 6497 (1969).

9. L. H. Brace, and N. W. Spencer, "Detailed Behavior of the Midlatitude Ionosphere from the Explorer XVII Satellite," Planet. Space Sci., Vol. 13, p. 647 (1965),

Preceding page blank

10. H. Carru, M. Petit, and P. Waldteufel, "Measures de températures électroniques et ioniques par diffusion incoherente," J. Atmos. Terrest. Phys., Vol. 29, p. 351 (1967).

11. A. Dalgarno, M. B. McElroy, and J.C.G. Walker, "The Diurnal Variation of Ionospheric Temperatures," Planet. Space Sci., Vol. 15, p. 331 (1967).

12. P. B. Rao, "Electron Concentrations and Electron and Ion Temperatures in the F-Region for Magnetically Quiet and Disturbed Conditions," J. Geophys. Res., Vol. 73, p. 1661 (1968).

13. J. E. Geisler, and S. A. Bowhill, "Ionospheric Temperatures at Sunspot Minimum," J. Atmos. Terrest. Phys., Vol. 27, p. 457 (1965).

14. J. V. Evans, "Electron Temperature and Composition in the F1 Region," J. Geophys. Res., Vol. 72, p. 3343 (1967).

15. K. K. Mahajan, "10.7-cm Solar Radio Flux and Ionospheric Temperatures," J. Atmos. Terrest. Phys., Vol. 29, p. 1153 (1967).

16. K. Davies, Ionospheric Radio Propagation (U.S. Dept. of Commerce, NBS, 1965).

17. H. C. Carlson, Ionospheric Heating by Magnetic Conjugate-Point Photoelectrons," J. Geophys. Res., Vol. 71, pp. 195-199 (1966).

18. J. V. Evans, "Sunrise Behavior of the F-Layer at Midlatitudes," J. Geophys. Res., Vol. 73, pp. 3489-3504 (1968).

19. A. V. Da Rosa, "The Theoretical Time-Dependent Thermal Behavior of the Ionospheric Electron Gas," J. Geophys. Res., Vol. 71, pp. 4107-4120 (1966).

20. J. V. Evans, R. A. Brockelman, R. F. Julian, W. A. Reid, and L. A. Carpenter, "Determination of F-Region Vertical Drifts at Millstone Hill," Radio Science, Vol. 5, pp. 27-38 (1970).

21. T. M. Watt, "The Topside Ionosphere at Sunrise," J. Geophys. Res. (1970); in press.

22. J. V. Evans, "Theory and Practice of Ionosphere Study by Thomson Scatter Radar," Proc. IEE, Vol. 57, No. 4, pp. 496-530 (1969).

23. F. L. Smith, III, "Electron Production and Loss Rates in the F-Region," J. Geophys. Res., Vol. 73, pp. 7385-7398 (1968).

24. G. Chimonas, and C. O. Hines, "Atmospheric Gravity Waves Induced by a Solar Eclipse," J. Geophys. Res., Vol. 75, p. 875 (1970).

UNCLASSIFIED
Security Classification

DOCUMENT CONTROL DATA - R & D

Security classification of title, body of abstract and indexing annotation must be entered when the overall report is classified

1. ORIGINATING ACTIVITY (Corporate author) Stanford Research Institute Menlo Park, California	2a. REPORT SECURITY CLASSIFICATION UNCLASSIFIED 2b. GROUP N/A

3. REPORT TITLE

PROJECT 617 RADAR--READINESS ACHIEVEMENT PROGRAM
Part B--IONOSPHERIC MEASUREMENTS

4. DESCRIPTIVE NOTES (Type of report and inclusive dates)

Final Report--Part B Covering the period May 1969 through June 1970

5. AUTHOR(S) (First name, middle initial, last name)

Murray J. Baron Theodore M. Watt Howard F. Bates

6. REPORT DATE June 1970	7a. TOTAL NO. OF PAGES 120	7b. NO. OF REFS 24
8a. CONTRACT OR GRANT NO Contract DASA 01-67-C-0019 b. PROJECT NO NWER XAXH Task and Subtask A048 c. Work Unit 01 d.	9a. ORIGINATOR'S REPORT NUMBER(S) Final Report--Part B SRI Project 6291 9b. OTHER REPORT NO(S) (Any other numbers that may be assigned this report) DASA 2519-2	

10. DISTRIBUTION STATEMENT

This document is subject to special export controls and each transmittal to foreign governments or foreign nationals may be made only with prior approval of Director, Defense Atomic Support Agency, Washington, D.C. 20305

11. SUPPLEMENTARY NOTES	12. SPONSORING MILITARY ACTIVITY Defense Atomic Support Agency Washington, D.C.

13. ABSTRACT

This report describes the ionospheric studies performed between June 1969 and May 1970 using the DASA Project 617 incoherent-scatter radar. During this time period, significant improvements were made in the radar system to allow nearly real-time processing of the data and to increase the accuracy, time resolution, and altitude extent of the measurements. The 1970 measurements presented here are the first to be made using the new system.

The daytime F-layer over Palo Alto between 1967 and 1969 was studied to determine (1) its seasonal behavior, (2) its day-to-day variations, and (3) its correlation with solar geophysical indices. Continuous 48-hour data runs were made in 1969-1970 and were used to study the ionosphere's diurnal behavior as well as its seasonal behavior during the sunrise and sunset periods. A new type of measurement, the determination of ionospheric vertical velocities, was made for the first time in 1970. Increased upward velocities during the sunrise period were found to exist. Observations of the F-layer during two partial solar eclipses were made and are reported.

DD FORM 1 NOV 65 1473 (PAGE 1)
S/N 0101-807-6801

UNCLASSIFIED
Security Classification

UNCLASSIFIED
Security Classification

14 KEY WORDS	LINK A ROLE	LINK A WT	LINK B ROLE	LINK B WT	LINK C ROLE	LINK C WT
Ionospheric measurements						
F-layer						
F-region						
Electron density						
Electron temperature						
Ion temperature						
Solar eclipse measurements						
Ionospheric vertical velocity						

DD FORM 1 NOV 65 1473 (BACK)
(PAGE 2)

UNCLASSIFIED
Security Classification

Defense Threat Reduction Agency
45045 Aviation Drive
Dulles, VA 20166-7517

CPWC/TRC November 3, 1999

MEMORANDUM FOR DEFENSE TECHNICAL INFORMATION CENTER
ATTN: OCQ/MR WILLIAM BUSH

SUBJECT: DOCUMENT CHANGES

The Defense Threat Reduction Agency Security Office has performed a classification/distribution statement review for the following documents:

DASA-2519-1, AD-873313, STATEMENT A
DASA-2536, AD-876697, STATEMENT A
DASA-2519-2, AD-874891, STATEMENT A
DASA-2156, AD-844800, STATEMENT A
DASA-2083, AD-834874, STATEMENT A
DASA-1801, AD-487455, STATEMENT A
POR-4067, AD-488079, STATEMENT C, ADMINISTRATIVE/OPERATIONAL USE
~~DASA-2228-1, AD-851256, STATEMENT C,~~ No Target only chged from ST A to adm/oper. ADMINISTRATIVE/OPERATIONAL USE
RAND-RM-2076, AD-150693, STATEMENT D, ADMINISTRATIVE/OPERATIONAL USE
AD-089546, STATEMENT A, ADMINISTRATIVE/OPERATIONAL USE * ST-A Jun 65
DASA-1847, AD-379061, UNCLASSIFIED, STATEMENT C, ADMINISTRATIVE/OPERATIONAL USE ~~NOT IN DTIC~~
~~RAND-RM-4812-PR~~, ELEMENTS OF A FUTURE BALLISTIC MISSILE TEST PROGRAM, UNCLASSIFIED, STATEMENT C, ADMINISTRATIVE/OPERATIONAL USE * 370168 Conf
Authority to Declassify

If you have any questions, please call me at 703-325-1034.

Leave ST-A
Gen A. Jarrett 23 Nov 99

Ardith Jarrett
ARDITH JARRETT
Chief, Technical Resource Center